

DA
340
1985
① C:454.7

寄贈	昭和
辻本英和氏	年月日

DYNAMIC CONDITIONS FOR SHORE PLATFORM INITIATION

by

Hidekazu TSUJIMOTO

A dissertation
submitted to the Institute of Geoscience
University of Tsukuba
in partial satisfaction of the
requirements for the degree of Doctor of Science

1986

86318823

TABLE OF CONTENTS

	PAGE
TABLE OF CONTENTS	i
LIST OF FIGURES	iii
LIST OF TABLES	v
ACKNOWLEDGEMENTS	vi
ABSTRACT	vii
CHAPTER 1 INTRODUCTION	1
CHAPTER 2 PREVIOUS STUDIES OF SHORE PLATFORM FORMATION AND RELATED PROBLEMS	4
CHAPTER 3 STUDY PURPOSE	16
CHAPTER 4 STUDY AREA	18
4.1. Reasons for selecting study areas	18
4.2. Morphology and geology of study areas	19
CHAPTER 5 PHYSICO-MECHANICAL PROPERTIES OF COASTAL ROCKS	50
5.1. Basic properties of rocks	51
5.2. Mechanical properties of rocks	53
CHAPTER 6 OCEANOGRAPHICAL CONDITIONS	59
6.1. Tidal conditions of study areas	59
6.2. Wave climate	60

CHAPTER 7	DYNAMIC CONDITIONS FOR SHORE PLATFORM	
	INITIATION (1): DEMARCATION BETWEEN	
	SHORE PLATFORMS AND PLUNGING CLIFFS	65
7.1.	Basic concept for shore platform	
	initiation	65
7.2.	Quantification of assailing force	
	of waves	66
7.3.	Quantification of resisting force	
	of rocks	75
7.4.	Dynamic condition for demarcating	
	shore platforms and plunging cliffs	78
CHAPTER 8	DYNAMIC CONDITIONS FOR SHORE PLATFORM	
	INITIATION (2): DEMARCATION BETWEEN	
	TYPE A AND TYPE B PLATFORMS	81
8.1.	Basic concept for Types A and B	
	shore platform initiation	81
8.2.	Quantification of assailing force	
	of waves	82
8.3.	Quantification of resisting force	
	of rocks	86
8.4.	Dynamic condition for demarcating	
	Types A and B shore platforms	87
CHAPTER 9	SUMMARY AND CONCLUSIONS	89
REFERENCES		92

LIST OF FIGURES

FIGURE		PAGE
1	Three types of rocky coasts.	105
2	Factors affecting wave induced cliff erosion.	106
3	Profile change caused by breaking waves (after Sunamura, 1976).	107
4	Profile change caused by breaking waves (after Tsujimoto and Sunamura, 1984).	108
5	Profile change caused by breaking waves (after Sanders, 1968).	109
6	Location of study areas.	110
7	Coastal profiles of each study sites.	111
8	Study site of Notsuka.	112
9	Study site of Shichiri-Nagahama.	113
10	Study site of Odosezaki.	114
11	Study site of Oga-Kitaura.	115
12	Study site of Unosaki.	116
13	Study site of Kuji.	117
14	Study site of Rikuchu-Noda.	118
15	Study site of Okuma.	119
16	Study site of Byobugaura.	120
17	Study site of Taito.	121
18	Study sites of Ubara and Kominato.	122

FIGURE	PAGE
19 Study sites of Kamogawa-Bentenjima and Shinyashiki.	123
20 Study sites of Shimoda-Ebisujima, Kakizaki, Akanejima, and Tatado.	124
21 Study site of Tsushi-Tsunokawa.	125
22 Study site of Nagao-Bana.	126
23 Study site of Iwami-Tatamigaura.	127
24 Study sites of Yadakemen and Nagakushimen.	128
25 Study site of Hario.	129
26 Study site of Oyano-Kodomari.	130
27 Definition of shear strength.	131
28 Seven coastal areas and representative stations.	132
29 Wave climate (1): relationship between deep-water wave height, H_0 , and wave period, T .	133
30 Wave climate (2): occurrence frequency of wave height.	134
31 Wave refraction diagram at Kakizaki site.	135
32 Wave types in front of the cliff.	136
33 Vertical distribution of dynamic pressure caused by standing waves.	137

FIGURE	PAGE
34 Vertical distribution of dynamic pressure caused by breaking waves.	138
35 Vertical distribution of dynamic pressure caused by broken waves.	139
36 Determination of initial front depth.	140
37 Result of wave pressure estimation.	141
38 Relationship between compressive strength and other indices.	142
39 Demarcation between shore platforms and plunging cliffs.	143
40 Demarcation between Type A and Type B shore platforms.	144

LIST OF TABLES

TABLE	PAGE
1 Landform types.	145
2 Basic properties of rocks.	146
3 Mechanical properties of rocks.	147
4 Oceanographical conditions of study areas.	148
5 Estimation of p and S_{ξ}^*	149
6 Estimation of τ and S_{ξ}^*	150
7 Conditions for shore platform initiation.	151

ACKNOWLEDGEMENTS

The present study was conducted under the supervision of Associate Professor T. Sunamura. His support and guidance were essential for the completion of this dissertation. I am also indebted to Professor M. Inokuchi for his encouragement and valuable advice during the course of this research program. Suggestions by Professors H. Igo and S. Shindo are very helpful. The field survey could not have been accomplished without the resourceful assistance given by Drs. I. Takeda and Y. Katsura, and Mr. K. Mizuno, and without encouragement by H. Tsujimoto (nee Sakurai).

ABSTRACT

Shore platforms are composed of a nearly horizontal or a slightly seaward-sloping rock surface which is located in the vicinity of sea level. Shore platforms are largely classified into two types: one is a gently seaward-sloping platform which is extending from the sea level to the shallow-water region without any topographic breaks (Type A); the other is a nearly horizontal platform which has a steep descent at the seaward margin (Type B). In contrast to these landforms, plunging cliffs are found which continue beneath sea level with no platform development.

Field investigations were conducted at twenty-five study sites which were selected from various parts of Japanese coast. This study aims to examine the following two conditions for shore platform initiation in connection with wave dynamics and rock mechanics: (1) condition for demarcating shore platforms and plunging cliffs; (2) condition for discriminating Type A and Type B shore platforms.

A formative condition for shore platforms and plunging cliffs should be equivalent to a critical condition whether cliff erosion occurs or not, and this condition is given by $f_w = f_r$ where f_w is the assailing force of waves and f_r is the resisting force of rocks. By representing these two forces by wave pressure, p ,

and compressive strength of the rock body, S_C^* , respectively, a dynamic condition for delimiting shore platforms and plunging cliffs is found to be given by

$$p = 0.081S_C^*$$

Shore platforms develop when $p > 0.081S_C^*$; whereas plunging cliffs form when $p < 0.081S_C^*$.

A formative condition for Types A and B shore platforms should be equivalent to a critical condition whether surface lowering of the platform once formed occurs or not, i.e., $f_{ws} = f_{rs}$ where f_{ws} is the wave assailing force which causes the surface lowering and f_{rs} is the rock resisting force against the lowering. By representing these two forces by shear force, τ , and shear strength of the rock body, S_S^* , respectively, a dynamic condition for demarcating Type A and Type B platforms can be described by

$$\tau = 0.005 S_S^*$$

Type A platforms develop when the lefthand side of this equation is greater than the righthand side; otherwise Type B platforms form.

CHAPTER 1

INTRODUCTION

Shore platforms are composed of a nearly horizontal or a gently seaward-sloping rock surface which is located in the vicinity of sea level. Shore platforms are largely classified into two types (Fig. 1): Type A is a gently sloping platform which is extending from the sea cliff to the shallow water region without any topographic break; and Type B is a nearly horizontal platform which has a steep descent at the seaward margin. Beside these two types of landforms, plunging cliffs (Fig. 1) develop in some places on rocky coasts.

It is clear that shore platforms are typical erosional landforms which are produced by the recession of sea cliffs. The sea-cliff recession is caused by erosion due to waves. Many factors are involved in the wave erosion as illustrated in Fig. 2 showing possible interrelationships among them. The relative intensity of wave assailing force, f_w , and rock resisting force, f_r , determines whether erosion occurs or not (Sunamura, 1983). Offshore wave energy has a direct relation to f_w , while topography in shallow water indirectly

influences f_w . The shallow water topography determine the wave type just in front of the cliff. There are three types of waves: standing, breaking, and broken waves. Standing waves occur when the depth in front of the cliff (front depth) is large, broken waves occur when the front depth is small, and breaking waves occur when the front depth is suitable for wave breaking. Thus the topography in shallow water is also the important factor affecting f_w .

The resisting force of rocks, f_r , is closely related to lithology. The mechanical strength of rocks is directly related to f_r , while the geologic structures such as jointings, faultings, and stratifications act to reduce f_r (Fig. 2). Chemical and mechanical weathering plays a significant role in some cases, i.e., (1) solution on lithology which has a significant carbonate content (Wentworth, 1939; Emery and Foster, 1956) and (2) frost action in high latitudes (Hudson, 1983). Importance of bio-chemical activity has been recognized: boring shells encroach the rock in some cases (Neumann, 1966; Ricketts and Calvin, 1968, p.332-334; Trudgill, 1976); encrusting organisms facilitate the lithification of rock surface in other cases (Focke, 1978).

Dynamic conditions demarcating the above-mentioned

three types of rocky coasts should be obtained from quantitatively evaluating f_w and f_r . Actually f_w and f_r have a pronounced vertical distribution. The rock resisting force f_r is strongly affected by the effect of weathering, generally showing the reduction in f_r -value in the subaerial part. The wave assailing force f_w shows the maximum value at around Still Water Level (S.W.L), and decreases abruptly toward the sea bottom. In order to investigate the rocky coast evolution, it is insufficient to evaluate f_w and f_r only at a certain elevation, and the vertical distribution of the two should be always taken into account. From this viewpoint, the previous studies on shore platforms will be critically reviewed in the following chapter.

CHAPTER 2

PREVIOUS STUDIES OF SHORE PLATFORM FORMATION AND RELATED PROBLEMS

Shore platforms have been studied for the last one hundred and fifty years since Dana (1849) first described the formative process of shore platforms (Gill, 1972a). Until the early 1960s, Type B shore platforms had been studied by Australasian workers as stated by Trenhaile (1980). Johnson (1919, p. 221) considered this type of shore platforms as a transient feature appeared in younger stages of his concept in normal shore profile of equilibrium.

In contrast to Johnson's normal shore profile concept, Bartrum (1926) has stated that "the abnormal shore platform, which is in truth by no means abnormal, but must be regarded as an expectable consequence of shore-line erosion wherever local conditions comply with certain requirements". He has also stated that there are two types in shore platforms ; the well-known "Old Hat" type at Russell and the storm wave type at North Auckland, New Zealand. He considered that the "Old Hat" type is formed by subaerial erosion down to the level of permanent saturation (Mean High Water

Level), whereas the storm wave type is formed by wave action under storm conditions.

After the study of Bartrum (1926), it has been centered in the shore platform studies whether wave action or weathering plays more important role in the formation of shore platforms. Wentworth (1939), Hills (1949), Tricart (1959), Cotton (1963), Bird and Dent (1966), Toyoshima (1968), Johannessen and Feiereisen (1982), and Hudson (1983) have emphasized the role of weathering. After reviewing the previous studies, Hills (1949) has stated that storm waves act only to remove the product of weathering. Bird and Dent (1966), who studied the shore platforms on the south coast of New South Wales, have reported that shore platforms are well developed on fine-grained rock formations subject to rock decomposition by weathering processes. Thus, a factor of weathering especially wet-dry weathering was emphasized. Toyoshima (1968) has also emphasized the role of wet-dry weathering in the development of Tertiary mudstone platforms at Kushimoto, Wakayama, Japan.

Recently, intensive studies on wet-dry weathering has been performed in Japan on rock mechanics basis by Suzuki et al (1970) and Takahashi (1975, 1976); the former study was conducted at Arasaki, Miura Peninsula,

and the latter was made at Aoshima, Miyazaki. On these locations marked washboard-like relief is found on the surface of shore platforms. In these studies, various kinds of mechanical strength parameters were examined in order to explain quantitatively the relationship between the washboard morphology and lithology. It is found that the lithological difference appeared in the wet-dry slaking process plays the most important role in the washboard-like relief formation. Some researchers layed stress on the weathering processes other than wet-dry slaking. Wentworth (1939), who studied the shore platforms developed on calcarenite in Hawaii, emphasized the solution process in the subaerial part of the platforms, because this rock is soluble in fresh water and insoluble in sea water. Hudson (1983) in his study of shore platforms in high latitudes has stressed the role of frost action and reported that the width of the shore platform reaches 800m in maximum in Shetland Island, Antarctica. Cotton's (1963) study of shore platforms on the tropical coast of Brazil indicates that the effect of salt crystallization is important. Tricart (1959) has also stressed the importance of crystallization. Work of Johannessen and Feiereisen (1982), conducted on shore platforms of Oregon coast, indicates that sunny,

south-facing sea cliff retreat is many times more rapid than the shady-side cliff retreat. Thus, these weathering processes become a significant factor on specific lithology or in very limited environment.

Edwards (1941, 1951) has examined shore platforms which are actively developing. The upper part of sea cliffs shows weathering occurred for a considerable depth, but in the lower part, i.e., the section rising up from shore platforms, weathering is not pronounced. He has emphasized the role of storm wave action in the primary development of shore platforms and the subsequent planation. The importance of the weathering factor which gradually increases as the platform develops is also described in his work. With increasing width of platform, the degree of weathering in the cliff increases facilitating wave erosion, and thus balancing the weaker attack of waves which advance against the cliff.

The processes which are dominant in the shore platform development has not yet been thoroughly investigated. However, most researchers agree that wave erosion is essential in the shore platform initiation and weathering processes are limited to the secondary modification (e.g., Bartrum, 1938; Trenhaile, 1980).

Bartrum (1938) has payed attention to the existence of a rampart, a rise on the outer margin of the platform, and has emphasized the role of wave erosion in platform initiation. At the stage of platform initiation, the cliff surface is always wet and unweathered. With the development of shore platforms, the cliff surface becomes dry on a calm condition and the weathering process operates on the cliff surface. However, the seaward margin is always kept wet and is not weathered, so that it becomes pronounced to form a rampart which stands slightly above the platform surface. The height of the rampart shows the height etched by waves.

Sunamura (1978a) has also stressed the role of wave erosion in his study on the shore platform formation. Shore platforms are found not only at the headlands but also along the sheltered waters on the southeastern coast of the Izu Peninsula, Japan. He has introduced wave dynamics and has concluded that the shore platforms of headlands are formed by the breaking waves and those of sheltered area are formed by the interaction of broken waves and weathering. His study constitutes a valuable contribution to the study of shore platform formation. In his study, however, the wave assailing force and the rock resisting force have

not yet been quantitatively evaluated.

Geological influence in shore platform development has caught the attention of shore platform workers. Gill (1972a) has described shore platforms in southeastern Australia. Gently seaward-sloping platforms (Type A) are developed on the soft rocks such as clay, sand, claystone, siltstone, decomposed basalt, and decomposed granite. Horizontal type (Type B) are well developed on the soluble rocks such as aeolianite and calcarenites. On hard rocks such as fresh granite, shore platforms are not developed and plunging cliffs are common. His study seems significant; unfortunately his description on geology and topography is not quantitative. Takahashi (1974) conducted a similar study in southwestern Japan in an attempt to examine the relationship between coastal landforms and geology. Dividing coastal rocks into four categories such as Neogene, Mesozoic-Paleogene, Paleozoic, and igneous rocks, he mentioned that shore platforms are well developed on the coasts of Neogene and Mesozoic-paleogene rocks, but scarcely on the coasts of Paleozoic and igneous rocks. He examined coastal geology based on geological maps and coastal features using topographic maps. Because he recognized shore platforms as "reefs exposed at low tide", shore-

platform typification is not possible in his study.

Bird and Dent (1966) has stated that lithological and structural factors are of prime importance in the development of high-tide shore platforms and shore platforms are best developed on fine-grained rock formations subject to decomposition by weathering processes. In their study, it is worth noticing that (1) high-tide platforms (Type B) are best developed in the area which is sheltered by headlands and islands from waves and swell, and on the more exposed shores they are narrower or more dissected, and (2) at a place where the waves are armed with shingle a sloping, intertidal platform (Type A) develops. In discussing the influence of lithology in a dynamic study of shore platform formation, it is necessary to properly assess the kind and degree of processes operating on a coast under consideration, and to make an effort to describe them as quantitatively as possible.

The first attempt to clarify the dynamic condition for platform formation was performed by Tsujimoto (1985) on the eastern coast of Chiba Prefecture. He has investigated the quantitative relationship between types of rocky coast and the lithological condition (resisting force of rocks against wave erosion). It is found that with increasing rock resisting force, Type A

platforms, Type B platforms, and plunging cliffs appear in this order in his study area. However, a generalized condition which is applicable to other regions with different wave climate has not been established in his study, because the regional differences in input wave condition were not taken into account.

Type A shore platforms attract civil engineer's attention because sea cliffs located landward are eroding rapidly and the need of protection works has been widely recognized. Erosion rates of sea cliffs have been recorded in many countries in the world (Sunamura, 1983). The erosion rates are mainly obtained by comparing the position of the cliff line on different editions of maps or old and new aerial photographs. There have also been some studies which attempt to directly measure cliff erosion rates. A micro-erosion meter (MEM) technique originally developed for the measurement of the change on bare rock surfaces (High and Hanna, 1970) was modified for coastal studies, and the technique has been applied to studies of morphological changes of rocky coasts (Kirk, 1977; Robinson, 1977,a.b; Gill and Lang, 1983). An MEM is an instrument with three legs which has an accuracy

of $\pm 0.025\text{mm}$. The amount of rock surface erosion can be measured by use of the MEM. Erosion rates are obtained through repeatitive measurements. Robinson (1977b) has measured the lowering rate of Type A shore platforms at Whitby in northeastern Yorkshire, England. He has revealed that erosion rates are 15 - 18.5 times higher in places where there is a beach at the cliff foot compared with those where there is no beach. The erosion rate is also measured on the coast of Type B shore platforms (Kirk, 1977; Gill and Lang, 1983). Kirk (1977) has measured the surface lowering rate and cliff recession rate of Type B shore platforms at Kaikoura Peninsula, New Zealand. The mean lowering rate measured by use of MEM from 1973 to 1975 was 1.53 mm/year, and the mean cliff recession rate which is obtained from analysis of air photographs over the period of thirty-two years from 1942 to 1974 was 0.3 m/year. The erosion rates were generally higher on mudstone than on limestone. Gill and Lang (1983) has measured the surface lowering rate of Type B shore platforms on the Otway coast, Australia. The rate measured from 1978 to 1980 ranged from 0.02 to 1.8 mm/year according to rock type and the degree of exposure to waves. From these studies, it is clear that the surface of shore platforms is now eroded and

the erosion rates are affected by lithology and wave intensity. It is difficult to investigate the shore platform formation (initiation) by this manner, because these studies only examine the modification of the surface of shore platforms once formed.

Apart from these field studies, some theoretical approaches have been taken. Flemming (1965) has mathematically treat Type A shore platform evolution with a static sea level. The rate of cliff recession in his model decreases with time, but does not reach zero. It is reasonable to consider that with a static sea level, there exists an equilibrium state. A model in which cliff recession rate reaches zero is proposed by Sunamura (1978b).

Without making distinctions between Types A and B, Trenhaile (1983) treated shore platform development considering the erosion rates at the high and low tide levels. In his model, the difference between the rates at the high and low tide levels reaches zero, and a dynamic equilibrium state is attained.

For the case of Type B, a model for shore platform development was proposed by Jutson (1939). There exist two cliffs in the longitudinal profile, namely, the landward cliff and seaward bluff. Shore platforms develop as a result of the differences in the

retreating rates of these two cliffs. As the width of platform increases, the difference in recession rates of two cliffs reaches zero. His model has been accepted by some researchers (Cotton, 1942, p.416; Edwards, 1951; Toyoshima, 1967; Trenhaile, 1978). However, this model contains a serious defect, that is, the retreat of seaward bluff. It is difficult to assume the parallel retreat of this cliff because the force of waves acting on the bluff has a marked vertical distribution: the maximum force exerts at or slightly above sea level and the force decreases abruptly toward the sea bottom.

From the existing field studies on the formation of shore platforms, it is extremely difficult to envisage the origin of shore platforms. It is difficult to discriminate in the field between contemporary platforms and raised ones with ancient origin, because of complicated natural phenomena such as varieties of lithological factor, sea level fluctuations, wave and tidal conditions, and local tectonic influences. To overcome these difficulties, laboratory approaches using a wave tank have been taken (Sunamura, 1975, 1976, 1977, 1982; Tsujimoto and Sunamura, 1984). In these studies, a mixture of portland cement, well-sorted fine quartz sand, and

water is used as a cliff material. Waves which break just in front of the cliff operate on a model cliff. Figures 3 and 4 show the profile change of cliff made of such material. It is found that erosion first occurs in the vicinity of S.W.L., and a notch is formed. The notch is deepened with time, but no erosion does occur below a certain level; the seaward bluff is kept as an initial profile of a steep drowned coast as Cotton (1963) has stated from his field observations. Similar wave-tank experiment has been performed using plaster as a cementing material (Sanders, 1968). Plaster is soluble in water and the strength of the plaster-mixed cliff placed in water decreases with time. Therefore the erosion first occurred in the vicinity of S.W.L. extends to the cliff base in time (Fig. 5). His experiment is helpful for an understanding of the erosion process occurring in the area made of soluble rocks such as limestone. Gill's (1972b) discussion for Sander's experiment includes a topic of great interest. On the coast east of Warranbool, Victoria, Australia, narrow Type B shore platforms are cut by present-day processes into huge blocks made of aeolianite, which have fallen from adjacent high cliffs. Such contemporary platforms are a good example of proto-type experiments in which natural waves have operated.

CHAPTER 3

STUDY PURPOSE

As shown in the preceding chapter, the previous studies have some basic problems unsolved:

(1) Many researchers have emphasized the importance of wave factor in the platform initiation. However, the effort for quantitatively evaluating the wave assailing force is entirely absent.

(2) Cliff-forming rocks are described qualitatively, and it is widely recognized that there exists some suitable rock type for shore platform formation. Quantification of the resisting force of rocks against wave erosion has not yet been fully conducted.

(3) Shallow-water topography which is essential to evaluate the wave assailing force just in front of the cliff is scarcely investigated. The presence of the seaward bluff is the most important point with which one can discriminate between Types A and B shore platforms. Most of the existing literatures have not described the seaward bluff in longitudinal profiles.

In order to solve the problem of shore platform development, it is essential to first investigate the

following conditions for shore platform initiation: (1) condition demarcating shore platforms and plunging cliffs; (2) condition discriminating Type A and Type B shore platforms. This study therefore attempts to examine these two conditions on a dynamic basis.

With this purpose, twenty-five study sites are chosen from Japanese coast and field investigations were conducted. In the field, profile levelling was performed to obtain precise information on the subaerial and subaqueous topographic features. In an attempt to quantify the rock resisting force, various mechanical properties of rocks were examined. The wave assailing force was estimated from existing wave data.

CHAPTER 4

STUDY AREA

4.1 Reasons for selecting study areas

Study areas were selected from various parts of Japanese coast. In choosing them, were used such criteria that (1) the influence of crustal movement has been small in the recent several thousands years, (2) characteristic landforms shown in Fig. 1 are found at or near the present sea level. Moreover, to avoid the difficulties in quantifying rock resisting force, the following limitations were set up: (1) beddings are thick and the differences in lithology (rock strength) are small; (2) rock mass does not contain the soluble rocks such as limestone and dolomite to remove the influences of solution and bio-erosion.

Based on aerial photographs and existing field studies, reconnaissances were first made and preliminary field investigations were performed. Finally twenty-five study areas shown in Fig. 6 were selected. In these areas, Type A shore platforms are developed at seven areas, Type B shore platforms are found at eleven areas, and the remaining seven areas

are of plunging cliffs (Table 1). These study areas are in wide range of wave climate and lithological condition.

4.2 Morphology and geology of study areas

In the above-mentioned twenty-five study areas, longitudinal profiles were measured at low water of spring tide (Fig. 7). The measurement line was set up in the area where characteristic landforms most typically develop. The line was perpendicular to the general trend of the landward cliff line in the case of Types A and B shore platforms. Levelling of subaerial parts was conducted using an auto-level and surveyor's staff. Subaqueous topography was examined by soundings. The underwater profiles of Taito, Ubara, Kominato, Bentenjima, and Shinyashiki were measured using a range finder and lead.

On coasts with Type A shore platforms, a beach usually develops at the cliff foot on a calm sea condition and the platform surface is covered by a veneer of beach sediment. Under such circumstances, levelling could not be performed and only a concise profile sketch was made.

(1) Notsuka

The study area is located at the southern part of the Tokachi Plain, Hokkaido (Fig. 8). The Tokachi Plain consists of a large alluvial fan extending from the foot of the Hidaka Mountains. The margin of this large fan is eroded by wave action, and is backed by a series of cliffs. This fan is regarded to be formed at the time of lower sea level of Wurm glacial stage (Kaizuka, 1956). Several rivers originated from the Hidaka Mountains cut down the fan and flow from northwest to southeast. The general trend of the coastline is perpendicular to these rivers. In this area, Type A shore platforms are present. The coastline is almost straight and the heights of sea cliffs range from 10 to 20 m. Unconsolidated fan deposits are made of poor-sorted gravel, the size of which is varied from cobble to boulder. Matrix of this gravel layer is moderately-sorted coarse sand (Matsui, 1973). The study site is located at northeast of the Hiroo City (Fig. 8). At this site, the alluvial fan is cut down by the Notsuka and Rakko Rivers. Sea cliffs of this site have heights of 10 to 15 m. The cliffs consist of a poorly sorted gravel layer with a thickness of about 15 m. Gravel of this layer is 5 to 30 cm in diameter and mainly made of sandstone. The

gravel is relatively fresh, hard and sub-rounded. Matrix of this layer consists of fine to medium sand. On a cliff face, this matrix is eroded and the gravel makes protrusion. Weathered volcanic ash with a thickness of about 50 cm, covered by a thin humus layer, overlays the gravel layer. Sandy gravel layer with a thickness of 0.5 to 1 m is exposed to the sea cliff base against which waves attack. This sand layer is the most sand-rich part in the gravel layer. Samples for strength tests are taken from this sand-rich layer because of the difficulties in the strength measurement of gravel-rich layer. At the cliff foot, a gravel beach which has a width of 5 to 10 m develops. Beach forming gravel and cliff forming gravel are of the same kind. The cliff-platform junction is just located at L.W.L.(Low Water Level). From this point, a gently sloping shore platform continuously extends seaward without any topographic breaks. On this coast, the sea cliff has receded approximately 25 m during the period of ten years from 1964 to 1974 (Toyoshima, 1974). Long-term recession rate obtained from different editions of maps (1920 and 1975) is 1.3 m/year on an average. This result coincides with the recession rate of the last 6000 years, i.e., 1.25 m/year; this value was obtained by the author based on

the diagram which Yoshikawa et al. (1973, Fig. (3)-17) plotted.

(2) Shichiri-Nagahama

The study area is located at the western side of the Tsugaru Peninsula (Fig. 9). In the eastern part of this area, the Iwaki River flows from south to north. Fluvial terraces along this river are classified into four surfaces. The coastline of this area has been severely eroded eastward. The first terrace (the highest terrace) of the Iwaki River is now exposed to the sea forming a coastal cliff. The bedrock of this terrace is mainly composed of Quaternary clayey fine tuff, and peat and peaty clay are interbedded in the clayey tuff. The terrace is 10 m in height at the eastern end and the altitude progressively increases toward the western margin where it is 20 m high. There are many lakes and marshes such as Otaki-numa and Hiranuma on the terrace surface. On the north of the study area, several sand dunes develop parallel to the coastline. At the foot of the sea cliff, Type A shore platforms are found in the marshy area. A cliff does not form in the dune area. A study site is installed in the marshy area (Fig. 9). The cliff 6 to 7 m high develops at the study site. Long-term recession rate

of the cliff can be obtained from different editions of maps. In this area, the sea cliff has recede approximately 63m during the period of sixty-eight years from 1911 to 1979. An average recession rate is about 0.9 m/year. The base of the cliff is composed of a peaty clay layer on which peat with a thickness of 2 to 3 m is overlaid; a sand layer 2 to 3 m thick is placed on the peat. On the top of this geological sequences, dune sand is deposited with a thickness of 0.5 m. Notable discontinuities such as faults and joints are not present at the study site. The clay and peat layers are always wet, but the upper sand layer is dry when the weather is fine. A notch forms in the clayey layer at the base of the sea cliff. The depth of the notch reaches 1 m, and the deepest part of the notch is located about 1.5 m above M.S.L.(Mean Sea Level). At the foot of the sea cliff, there is a beach with a thickness of about 2 m and 20 to 30 m in width. Beneath the beach, the Type A platform exists.

(3) Odosezaki

The study area is located in the southwestern part of Aomori Prefecture (Fig. 10). The green-tuff formation of Neogene is widely distributed in this area. Marine terraces with five to six surfaces well

develop in the study area. The altitude of the highest terrace is about 150 m above sea level. The lowest terrace was formed at the earthquake occurred in 1793. The amount of upheaval by the 1793 earthquake was 0.5 to 1 m in this area (Nakata et al., 1976). Pyroclastic rocks of andesite which belong to the Odose Formation of Miocene (Moritani, 1968) are exposed to the coast. These rocks have been eroded by waves and Type B shore platforms well develop (Fig. 7). The landward part of the shore platform is located about 1 m high above M.S.L. In the seaward part, the altitude of the platform surface corresponds approximately to the present sea level. The lower platform is always washed by waves. The higher platform has a width of 120 m, and the lower platform is 12 m. At the seaward end of the lower platform, there is a steep cliff with a height of about 4 m. The surface of the higher shore platform is nearly horizontal and the platform slightly increases its height toward the seaward margin to form a rampart.

(4) Oga-Kitaura

The study area is located on the northern coast of the Oga Peninsula (Fig. 11). The root of the Oga Peninsula is considered to be a raised sand bar

connecting Oga Island with Honshu. The altitude of this area ranges from 50 to 100 m above sea level. This area is of arcing coastline fringed by a steep sea cliff with a height of 10 to 30 m.

A study site is selected about 1 km southwest of Anden (Fig. 11). The slope of the sea cliff is about 50m. The surface of the cliff is vegetated to some extent. At the foot of the sea cliff, a beach with a width of 20 to 30 m develops. The width of the beach increases progressively toward the east. On a calm sea condition, a narrow beach develops, but waves directly attack the cliff foot under violent sea conditions. This is supported by a fact that sea cliffs of this area has receded approximately 40 m during the period of sixty-seven years from 1911 to 1978. A shore platform of Type A develops at this site. The cliff/platform junction is slightly below L.W.L. Cliff-forming material is the Shibikawa sandstone of Pliocene (Kitazato, 1975). At the cliff foot, a coarse sand layer which contains many shell fossils is exposed. The strike and dip of this layer are N 10-20°W and 10°N, respectively. There are few joints and faults on the cliff face. The surface of the cliff face is generally smooth.

(5) Unosaki

The study area is located on the southern coast of the Oga Peninsula (Fig. 12). Marine terraces which are classified into four surfaces well develop in this area (Katsurahara, 1968). The altitude of the highest terrace is 170 to 180 m above sea level. This area is composed of Tertiary sedimentary rocks such as the Monzen Group of Early Miocene and the Wakimoto Formation of Pliocene (Fujioka, 1958). These sedimentary rocks outcrop on the coast. The coastline shows some irregularity and Type B shore platforms develop in this area. A study site (Fig. 12) is located about 3 km southwest of Funakawa. The third terrace and the lowest terrace (the fourth terrace) well develop at this site. The lowest terrace is exposed to the sea, bordered by a sea cliff 1 to 2 m high. The cliff is now covered with concrete blocks to protect a road which runs parallel to the cliff line at the seaward margin on the terrace. A typical profile of the Type B shore platform at the study site is shown in Fig. 7. Note that there exists a marked seaward bluff. Shale of the Miocene Onagawa Formation outcrops at this site. On the shore platform surface, hard part of shale makes a slight protrusion with a relative height of 0.5 to 1 m. Most part of the shore platform

surface is situated at about L.W.L. There is a rampart at the seaward margin where waves always break. The water depth in front of the seaward bluff could not be measured because of rough sea conditions. The front depth, 4 m, was known from a hydrographic chart published by the Japan Maritime Safety Agency (No.148).

(6) Kuji

The study area is located in the northern part of Iwate Prefecture, including the Bay of Kuji (Fig. 13). The southern coast of Iwate Prefecture, well-known as a typical Rias coast, is of highly irregular shoreline. On the northern coast, on the other hand, a relatively monotonous shoreline is stretched. In this area, Tertiary and Late Cretaceous sedimentary rocks make embayments, while igneous rocks and Early Cretaceous sedimentary rocks form promontories. A study site is located in the northern part of Kuji Bay (Fig. 13). Sedimentary rocks of the Kuji Group (Late Cretaceous) are found at the study site (Miki, 1977). A shore platform of Type B (Fig. 7) with a landward steep cliff 5 m high juts out into the sea; a wide beach develops in the adjacent area. The platform is composed of sandstone. The mean width of shore platform is 80 m. The landward half of the shore platform is covered with

sandy deposits. The platform is of a very smooth surface which is situated about L.W.L. There is a bluff with an average relative height of 2 m at the seaward margin. The landward cliff is usually wet.

(7) Rikuchu-Noda

The study area is located 10 km south of the Kuji study area (Fig. 14). Tertiary Noda Group and Late Cretaceous Kuji Group of sedimentary rocks are widely distributed, forming embayments. Igneous rocks, on the other hand, make promontories. Type B shore platforms well develop at Minato and its adjacent region. Oligocene sedimentary rocks of the Minato Formation (Noda Group) are exposed to the coast (Shimazu and Teraoka, 1960). Coastal cliffs of this area are mainly composed of conglomerates and tuffaceous rocks of Minato Formation. Type B shore platforms well develop on a coast where greenish sandy tuff is exposed. A study site is located about 1km northeast of Minato (Fig. 14). The Type B shore platform at this site is formed at or slightly below M.S.L. with an average width of 100 m (Fig. 7). The seaward portion of about 10 m width is approximately 0.5 m below the general level of shore platform surface. Both the lower and higher surfaces are horizontal and almost smooth.

There is a steep cliff with a relative height of 3.5 m at the seaward margin of the platform. The height of a landward cliff, which is mainly composed of sandy tuff, is about 20 m. Lenticular gravel layers with a thickness of 1 to 2 m are interbedded in the sandy tuff. Cobble supplied from the layers is accumulated by waves at the cliff foot with a thickness of 2.5 m.

(8) Okuma

The study area is located in the central part of Fukushima Prefecture (Fig. 15). A marine terrace well develops in this area. The margin of the terrace is fringed by a series of sea cliffs with a height of about 30 m. Type A shore platforms are extending from the feet of these cliffs. These cliffs suffer severe wave erosion. Some previous studies have reported the erosion rate of this area and its surroundings (Horikawa and Sunamura, 1968; Aramaki, 1978). Mean annual recession rates are found in a range from 0.13 to 2.1 m/year. Tertiary sedimentary rocks are exposed to the sea cliffs. At the study site, the coastal cliff is made of Pliocene sandstone and mudstone. At the top of the cliff, there are terrace deposits mainly composed of gravel (Horikawa and Sunamura, 1967). A narrow beach develops at the cliff foot. The thickness

of the beach deposits is about 2 m at the cliff foot, and diminishes seaward. The bedrock (Pliocene sedimentary rocks) are exposed to the submarine slope at a depth of 10 m. The cliff/platform junction is located at L.W.L. (Horikawa and Sunamura, 1968).

(9) Byobugaura

Byobugaura, located in the northeastern part of Chiba Prefecture, consists of an upland with a height of approximately 50 m (Fig. 16). The south end of the upland is terminated with sea cliffs. The sea cliffs with a height of 10 to 60 m extend alongshore about 9 km. A coastline in the study area is nearly straight. Type A shore platforms well develop in this area. Pliocene mudstone named Iioka Formation (Ozaki, 1958) is exposed at the cliff foot, and Quaternary deposits which are composed of sand and gravel are found in the upper part of the cliff. The volcanic ash called "Kanto Loam" lies on the Quaternary deposits. The upper part of the cliff face is dry on a fine weather, and major cracks with a spacing of 30 to 50 cm and minor ones with 2 to 3 cm are found on the surface of Kanto Loam. The surface of mudstone exposed at the cliff foot is always wet. Mudstone exfoliation with a depth of 10 to 30 cm occurs parallel to the cliff face,

and vertical joints develop with a spacing of 1 to 2 m. Pliocene Naarai Formation is slightly exposed at the eastern end of Byobugaura. A study site is selected at the western part of Byobugaura area (Fig. 16). The sea cliff has a height of about 50 m and a slope angle of 70° in the lower section of the cliff. A Type A shore platform with a slope of 1° to 2° develops at this site. The platform is also made of mudstone of Iioka Formation. On a calm condition, the surface of the shore platform near the cliff base is covered by a thin layer of beach sand. The cliff/platform junction coincides with L.W.L. In this area, cliff erosion studies have been performed. Horikawa and Sunamura (1969) obtained, as a short-term recession rate, the value of 0.91 m/year using large scale topographic maps drawn based on two aerial photographs taken in 1960 and 1967. Long-term recession rate from 1884 to 1969 is found 0.73 m/year on an average (Horikawa and Sunamura, 1970). Such severe erosion makes small rivers hanging valleys except the Isomi River.

(10) Taito

The study area is located in the eastern part of Chiba Prefecture (Fig.17). The rocky coast of this area forms an approximately north to south oriented

coastline of 2 km length. The height of sea cliffs ranges from 10 to 70 m. The cliff height is in minimum at the north end and increases toward the south. The coastline is somewhat irregular. The Plio-Pleistocene Kiwada Formation is exposed to the cliff. A study site is situated at the northern end of the area. The sea cliff at this site is about 10 m in height. A Type A shore platform develops. The cliff/platform junction is located at about L.W.L. The platform is inclined seaward at 1° to 2° without any topographic breaks. A narrow beach develops at the cliff foot on a calm sea condition. The beach sediment at the cliff foot is about 1m in thickness diminishes seaward. The cliff face is composed mainly of nearly horizontal mudstone layer of the Kiwada Formation intercalated with a thin sandstone layer. The upper part of sea cliff is dry on a fine weather. Joints in this part is of primary origin with a spacing of 30 to 40 cm and weathering cracks develop with a narrow spacing of 1 to 2 cm. On the cliff foot, the cliff material is always in wet state with only primary joints. The irregularity of coastline is, in most cases, controlled by the spacing of fault systems; the fracture zone with an average width of a few meters makes an embayment. This study area has been severely eroded and the cliff recession

has continued. Short-term recession rate for the cliff has been obtained from air photographs (Sunamura, 1973): the mean value is about 1 m/year during the period of ten years from 1960 to 1970. On the same area, long-term recession rate has been examined based on topographic maps (Sunamura and Tsujimoto, 1982): the mean value is about 0.6 m/year during the period of eighty-five years from 1883 to 1968.

(11) Ubara

The study area is located on the south coast of Chiba Prefecture (Fig. 18). The Boso Hills which form the southern part of Chiba Prefecture are 200 to 350 m in height above sea level. The main divide of the hills is located near the coast. The height of the hills gradually decreases toward the north from this divide, but abruptly decreases toward the south. Especially in the area south of Kamogawa, the distance between the divide and the coastline is only 0.5 to 2.5 km. The southern edge of the hills is fringed by a series of sea cliffs. The Mio-Pliocene sedimentary rocks called the Kiyosumi, Anno, Kurotaki, and Katsuura Formations (Nakajima et al., 1981) are exposed to the sea cliffs. The coastline is fairly irregular. Type B shore platforms well develop especially at the

promontories. A study site is located at about 3 km west of Katsuura (Fig. 18). Sedimentary rocks of Kiyosumi Formation, mainly composed of sandstone, are exposed to the coast. This site is composed of alternating layers of sandstone (1 to 5 m in thickness) and mudstone (30 to 40 cm), which strike N 60-70°W and dip 10-20° N. Some scoriaceous sandstone beds are interbedded with the alternating layers. The alternation of sandstone and mudstone crops out to the surface of the cliff and the shore platform. The shore platform is generally flat and the above-mentioned scoriaceous sandstone makes a protrusion with a height of 20 to 30 cm from the general level of the platform surface (Fig. 7). The shore platform, located at about M.S.L., is 250 m in average width and has a seaward bluff of about 4 m in relative height. The shore platform is indented due to the furrows developed along fault lines.

(12) Kominato

The study area is located about 6 km west of Ubara area (Fig. 18). The Boso Hills are close to the sea. The divide is located only 500 m away from the coastline. The Boso Hills in this area are made of the Miocene Amatsu Formation (Nakajima et al., 1981). The

Amatsu Formation is mainly composed of massive mudstone interbedded with a scoriaceous thin layer, forming sea cliffs. The coastline, i.e., a landward cliff line, of about 4 km long is nearly straight and in front of the cliff, Type B shore platforms well develop. The height of sea cliff ranges from 20 to 40 m and the shore platforms are 100 to 200 m in width. A study site is selected at about 2 km southwest of Kominato. A shore platform of this site is horizontal and about 200 m in width (Fig. 7). The surface of shore platform is smooth and located at slightly below M.S.L. There is a rampart at the seaward end of the platform and waves break here. The seaward bluff with a relative height of about 4 m exists at the seaward of this rampart. The mudstone of the Amatsu Formation outcrops on the surface of landward sea cliff and shore platform. The protrusion (less than 30 cm in relative height) on the platform surface is mainly composed of the scoriaceous layers. No significant correlation is found between the rampart and its forming rocks. The surface of shore platform is wet and ditches in the seaward part of the platform in Fig. 7. Faults and joints strike N 20-30°E and the axis of indentation of platform outline shows a similar direction (Fig. 18).

(13) Kamogawa-Bentenjima

A small island about 150 m long and 100 m wide located in the west of Kamogawa City is selected as a study site (Fig. 19). The eastern end of Mineoka Mountains, which stretch from east to west, faces the sea. The Mineoka Mountains are composed of the Paleogene Mineoka Group which is mainly made of shale (Nakajima et al., 1981). The mountains are 100 to 400 m high above sea level. Northern and southern sides of the mountains are fringed by lowlands made of alluvial deposits of the Kamo and Soro Rivers. Basaltic rocks intruded into the Mineoka Group form dome-like protrusions on the Mineoka Mountains (Nakajima et al., 1981). The small island, Bentenjima, is one of these dome-like protrusions. The rock exposed to the island is dolerite, the rock-forming grains of which are generally coarser than basalt. No platforms develop and plunging cliffs are found at this site. As shown in the longitudinal profile, plunging cliff continues beneath sea level to a water depth of about 7 m, where it is connected to a slightly seaward inclined sea bottom (Fig. 7). The sea bottom consists of the bare rock with a thin layer of sediment. At the cliff foot, there is some gravel of 20 to 100 cm in diameter. Little weathering occurs on the cliff surface and

primary joints of several tens centimeters in spacing are found.

(14) Shinyashiki

The study area is located at about 1 km south of the Bentenjima site (Fig. 19). This area is also placed at the eastern end of the Mineoka Mountains. Basalt, which intruded into the Mineoka Group, is exposed to the coast. The rock is of finer grain-size than that of Bentenjima. In this area, basalt makes a dome-like protrusion which is about 700 m long in east-west direction and about 300m in north-south. Basalt occurs in the form of pillow lavas (Nakajima et al., 1981). Plunging cliff develops at this site. Nearly vertical cliff plunges beneath sea level and is connected to the sea bottom which is gently sloping seaward (Fig. 7). At the underwater cliff foot, gravel with diameters of 30 to 50 cm is present. The sea bottom is composed of the bedrock and overlain with scarce sediment.

(15) Shimoda-Ebisujima

The study area is located at the southeastern end of the Izu Peninsula (Fig. 20). This area mainly consists of hilly mountains. The crests of the

mountains often show similar height. Significant marine terrace formation has not been taken place in this area during Holocene age (Sawamura et al., 1969). This area is mainly composed of Miocene to Pliocene volcanic rocks (Sumi, 1958), which are named the Shirahama Group (Matsumoto et al., 1985). A study site is located at the southern tip of the Suzaki Peninsula (Fig. 20). The Suzaki Peninsula consists of hills of 60 to 80 m in height and is fringed by sea cliffs of 30 to 40 m in height. Andesite lava and pyroclastic rocks of andesite form this peninsula. At the study site of Ebisu Island, a Type B shore platform well develops. This island is about 150 m long and about 100 m wide. At the open sea side of this island, the shore platform has a width of about 50 m. At the sheltered side, the platform width is narrow with a width of 5 to 10 m. The study site is located at the open sea side. The shore platform is generally horizontal with its surface being at an elevation of about 1 m above M.S.L. The platform has a seaward bluff of about 6 m in relative height (Fig. 7). The eastern half of the shore platform in Ebisu Island is composed of tuffaceous sandstone and the western half is composed of andesitic volcanic breccia, all of which belong to the Suzaki Formation of Shirahama Group. There is little

difference in shore platform profiles between the eastern and western halves. Although there are primary joints with a spacing of about 1m, the platform surface is smooth and irregularity in surface configuration due to the joints is scarcely found. The surface of rocks forming shore platform are wet even on a calm sea condition. On the upper part of sea cliff where waves do not reach, the rocks are dry and the honey comb structures are observed.

(16) Shimoda-Kakizaki

The study area is located, slightly eastward of the head of Shimoda Bay, at the base of the Suzaki Peninsula (Fig. 20). This area is sheltered from swell due to the presence of the Suzaki Peninsula. This area consists of a hill which is 30 to 50 m in height and sea cliffs are 5 to 10 m in height. A plunging cliff coast develops in this area. The cliff selected as a study site plunges into the sea and is connected to the sea bottom at a place where water depth is about 1 m. The sea bottom is a slightly seaward slope and overlain with little veneer of sediments. Rock exposed to this site is whity tuff of the Harada Formation of the Shirahama Group (Matsumoto et al., 1985). The Harada Formation of this area is made of the tuffaceous

sandstone of Early Pliocene. This tuff is vesicular and soft. There is little evidence of weathering on the rock surface.

(17) Shimoda-Akanejima

Akanejima is a small island, about 300 m both in length and width, is located at about 1km southeast of Shimoda (Fig. 20). The highest part of this island is about 80 m above sea level. This island is fringed by a plunging cliff with a height of 30 to 40 m. The study site is located on the side of open sea. The steep cliff plunges into the sea. The inclination of the cliff is 40° to 50° in the subaerial part and is steeper in the subaqueous part. This cliff is connected to the sea bottom which is gently sloping seaward. The water depth of the cliff/sea-bottom junction is about 14 m. A cliff is composed of andesite lavas. The andesite of this site is hard and has primary joints with a spacing of several tens centimeters. Mini-sized furrows develop along these joints.

(18) Tatado

Tatado area (Fig. 20) is composed of the hills of 100 m high on an average. The hills consist mainly of

andesite lavas and pyroclastic rocks of the Suzaki Formation, Shirahama Group. Type B shore platforms develop on the area where pyroclastic rocks outcrop. The study site is selected at the center of this area (Fig. 20). A shore platform at this site is nearly horizontal and about 25 m in width (Fig. 7). The shore platform/cliff junction is located at about 2 m above M.S.L. There is a steep cliff at the seaward margin of the platform. The water depth in front of the bluff is about 4 m. This nearly vertical cliff is connected with the sea bottom gently sloping seaward. The sea cliff and shore platform are composed of volcanic breccia of the Suzaki Formation. The breccia includes many hard angular blocks made of andesite which are 10 to 30 cm in maximum length. The matrix of the breccia is of sandy ash. On the surface of cliff and shore platform, the matrix is eroded away and the andesite blocks make protrusions.

(19) Tsushi-Tsunokawa

This area is located on the western coast of Awaji Island (Fig. 21). This area consists of the Tsuna Hills with a height of 100 to 200 m. The hills are composed of Quaternary deposits belonging to the Awaji Formation which is correlated to the Osaka Group

(Ikebe, 1959). The upper Awaji Formation is mainly composed of sand and gravel, and the lower part is made of silty clay. The lower Awaji Formation outcrops to the coastal area from Ei to Tsushi. The promontories of Tsushi and Hotokezaki (Fig. 21) are made of granitic rocks (Ikebe, 1959). The coastline of about 3-km length runs nearly straight with sea cliff having a relative height of 10 to 30 m. Type A shore platforms develop in front of the cliff. The study site is located in the northern part of the area and is about 1km south of Tsushi. The sea cliff here is about 10 m in height and the shore platform extends shallow-water zone without any topographic change. A beach about 1 m in thickness and 5 m in width develops at the cliff foot. The sea cliff is made of greenish silty clay. Cliff forming material is wet at the cliff foot, whereas in the upper part of the cliff, it is dry and has weathering cracks with a spacing of 1 to 2 cm. Long-term recession rate is obtained using topographic maps with different editions. The mean annual recession rate of this area is found approximately 0.15 m/year during the period of fifty-three years from 1928 to 1981.

(20) Nagao-Bana

The study area is located in the central part of Tottori Prefecture. This area consists of a lava plateau jutting out 2 km in north-south direction into the Sea of Japan (Fig. 22). The height of the plateau decreases gradually toward north and it attains 80 m near the coast. In this area, a precise survey has been accomplished (Toyoshima, 1967). Figure 7 shows one of his survey results. Plunging cliffs develop in the area. The plateau of several tens meters make a steep descent with 50° inclination. This descent extends to below sea level. The water depth in front of the cliff ranges from 8 to 11 m depending on locations. The water depth at the promontory is about 11 m. Andesite lava which forms the cliff is very hard and has primary joints with a spacing of several tens centimeters. The lava is wet and fresh in the vicinity of sea level. In the upper part of the cliff, the lava is dry and broken to thin plates due to weathering.

(21) Iwami-Tatamigaura

This area is located in the central part of Shimane Prefecture (Fig. 23). The Miocene Togane Formation (sandstone, conglomerate, and shale) and the Kou Group (tuffaceous sandstone) are exposed to the coast

(Murakami, 1960). Coastal hills have a height of 50 to 200 m. The coastline is rather irregular. The study site is selected about 6 km north of Hamada City (Fig. 23). "Tatamigaura" is a place name termed to refer to the flat surface. Type B shore platforms well develop at this site. There are hills of about 50 m high on the back of the site. The hills are fringed by sea cliffs 20 to 40 m in height and 60° in slope angle. At this site, conglomerate and tuffaceous sandstone outcrop on the coast. These rocks belong to the Togane Formation. Shore platforms well develop in the area composed of tuffaceous sandstone, but poorly develop on conglomerate coasts. No beach develops at the cliff foot, from which horizontal shore platforms of about 200 m width jut out into the sea. There are bluffs at the seaward end (Fig. 7). The water depth in front of this seaward bluff is about 4 m. The most part of these shore platform is located about 50 cm high above M.S.L. and the most seaward part about 15 m wide is located at about L.W.L. The platform of this seaward zone is probably having created under the present sea level condition, because this area was uplifted about 1 m at the time of earthquake occurred in 1872. On a calm condition, waves wash the surface of shore platform including the foot of landward cliff.

Therefore, weathering joints do not exist on the platform surface. The shore platform is generally flat, but many protrusions with relative height of several tens centimeters are found. These protrusions are made of hard nodules which are 30 to 70 cm in diameter. The nodules are of coarser material than the other part of the platform and sometimes contain fossil snails in their center. Toyoshima (1973) stated that the top of these nodules indicates the height of surface of shore platform before the 1872 earthquake. The upper part of these nodules is now weathered with cracks having a spacing of a few centimeters.

(22) Yadakemen

Yadakemen is located in the northern part of Nagasaki Prefecture (Fig. 24). This area is called "Tsukumo-jima", which literally means ninety-nine islands, referring to many islands. The coastline is extremely irregular. The study area is sheltered by the islands, so that the energy of waves coming from the open sea diminishes. Plunging cliffs exist in the study area. Cliff-forming material is sedimentary rocks of the Oligocene Sasebo Group and the Miocene Nojima Group (Yamamoto and Minoda, 1973). A study site is selected about 5 km northwest of Sasebo City. This

site is sheltered by Maejima Island (Fig. 24). A plunging cliff is connected to the sea bottom at a water depth of about 2 m (Fig. 7). Well-sorted coarse-grained sandstone is exposed to the cliff face. This sandstone belongs to the Sasebo Group. There are few joints and cracks on the surface. The upper part of the cliff is dry, and the lower part is always wet and covered with algae. Many holes with a diameter of 1 to 5 cm, probably made by boring shells, are present on the cliff face of the intertidal zone.

(23) Nagakushimen

The study area is located in the northern part of Nagasaki Prefecture (Fig. 24). Hills with a height of 50 to 100 m face the sea, and rocky coasts develop with an extremely irregular shoreline. A study site is located about 3 km north of the Yadakemen site (Fig. 24). This site is sheltered by many islets and plunging cliffs develop. The cliff of this site which inclines about 30° plunges into the sea with almost same inclination (Fig. 7), and connects with the sea bottom at 2-m water depth. The cliff inclination coincides with the dip of cliff forming rock of tuffaceous sandstone of the Miocene Nojima Group striking N 60° E and dipping about 30° N. The cliff face

is dry in the upper part of the cliff without any weathering cracks being present. No noticeable joints and faults develop on the cliff face. The cliff forming material is easily broken along the bedding plane to platy blocks with a thickness of 10 to 15 cm.

(24) Hario

Hario is an island located in the northernmost part of Omura Bay (Fig. 25), which is about 15 km in east-west direction and 20 km in north-south. The water depth of the bay is about 30 m in maximum and 20 m on an average. The bay is connected with the East China Sea through narrow straits of Hario and Haiki (Fig. 25). The energy of swell entering from the open sea is negligible in the bay area. The core of Hario Island consists of igneous rocks such as andesite and basalt. The marginal part is made of the Miocene Sasebo Group (mainly of sandstone) and the Oligocene Kishima Group (mainly of sandstone). Type B shore platforms develop on the coast where the sedimentary rocks are exposed. A study site is situated at the head of Egami-ura cove located in the southwestern part of Hario Island. This site is made of sedimentary rocks of the Kishima Group (Magarikawa Formation), which is mainly composed of very fine-grained sandstone

(Nagahama and Matsui, 1982). A shore platform (Type B) is flat and has a bluff at the seaward end (Fig. 7). The relative height of this seaward bluff is about 1 m. The platform made of fine-grained sandstone is located at about M.S.L. Joints with a spacing of 0.5 to 1 m are found on the cliff and platform surfaces. The rock forming the platform is separated into blocks by these joints and the onion structure develops on these blocks. The spacing of cracks developing in the onion structure is 1 to 5 cm. Such joints and cracks make no significant irregularity on the shore platform profile.

(25) Oyano-Kodomari

The study area is located in the southwestern part of Oyano Island, Kumamoto Prefecture (Fig. 26). This island is situated between the Ariake Sea and the Yatsushiro Sea. The study area, facing the Ariake Sea, is made of sedimentary rocks of the Eocene Kyoragi Formation (Inoue, 1962). A study site is selected at the southwestern corner of Oyano Island (Fig. 26) and consists of the Kyoragi Formation, an alternation of sandstone and mudstone. A shore platform of Type B well develops in the area of sandstone where the study site is located. The mudstone area makes an embayment, where a bay-head beach develops. The shore platform is

about 250 m in width. The active sea cliff (landward) is not found because of the shore protection works. Although the shore platform is located slightly above M.S.L., the platform surface is always wet due to large tidal range of this area (about 4 m). At the seaward end of the shore platform, a steep cliff with a height of about 1 m exists (Fig. 7). There is little sediment on the shore platform surface.

CHAPTER 5

PHYSICO-MECHANICAL PROPERTIES OF COASTAL ROCKS

In order to quantitatively estimate the resisting force of rocks forming shore platforms and/or sea cliffs against wave erosion, multiple measurements have been done in the laboratory and the field. Compressive strength, tensile strength, shear strength, and longitudinal wave velocity were measured for each study site. Samples for these measurements were taken from the bedrock which is always wet even at the low water of spring tide; the size of samples was approximately 50 cm high, 40 cm wide, and 20 cm deep. In the case of the samples which were fragile by a shock, much care was taken in the transportation and handling. All the samples were kept saturated during the transportation. The tests for the mechanical properties were performed in saturated state. In addition to these mechanical properties, specific gravity, density, water content, and porosity were measured for basic physical properties.

5.1. Basic properties of rocks

(1) Specific gravity

Specific gravity is the ratio of the mass of a body to the mass of an equal volume of water at a specific temperature. The specific gravity is an index which shows the kind and composition of rock forming materials. Quartz and feldspar have a specific gravity of about 2.65, and colored minerals generally show a larger value. Rock samples were broken into fragments of 1 to 2 mm in diameter and the specific gravity was measured by using a pycnometer. Measured values of specific gravity, G_s , ranges from 2.6 to 2.7 (Table 2). The specific gravity of Bentenjima and Shinyashiki samples show the largest value, which is over 2.9. The reason for this is that basaltic rocks contain a large amount of colored minerals such as pyroxene and magnetite. The smallest value of Shichiri-Nagahama sample, 2.3, is probably due to the presence of many plant remains.

(2) Density

Density is the mass of a substance (usually expressed in grams per cubic centimeter). There is a general trend that the larger the value of density, the

firmer the rocks. Wet density, ρ_w , was obtained from the measurement of the mass and volume of cylindrical specimen in saturated state (Table 2). Cylindrical specimen was also used for the measurements of dry density, ρ_d ; the mass of the specimen was measured after 48-hour oven drying (Table 2). The igneous rocks of Bentenjima, Shinyashiki, Akanejima, and Nagaobana show larger values and the sedimentary rocks of other study sites generally have smaller values. Young sedimentary rocks forming Kakizaki, Byobugaura, and Taito are of the smallest values.

(3) Porosity

Porosity is the ratio of the aggregate volume of interstices in a rock to its total volume. It is usually stated as a percentage. Measured values of porosity vary according to locations from 5 to 60 % (Table 2).

(4) Water content

Water content is water contained in porous sediment or sedimentary rock, and generally expressed as a ratio of water weight to dry sediment weight. This value shows the ratio of the void in rocks similar to porosity. The data shown in Table 2 are the water

content in saturated condition, w_{max} . Measured values widely range from 1.9 to 67 % (Table 2).

5.2. Mechanical properties of rocks

In order to evaluate the resisting force of rocks against wave erosion, the measurements of mechanical strengths are of crucial importance. Waves exert stress in coastal rocks in various modes of forces such as compression, tension, and shear. As indices for the resistance against these forces, compressive, tensile, and shear strengths were measured (Table 3). Besides these mechanical strengths, the longitudinal wave velocity, a frequently used index for rock strength, was also measured (Table 3). Saturated samples were employed in all the measurements because these indices will be adopted to evaluate the resisting force of rocks against erosion of waves.

(1) Compressive strength

Compressive strength is the load per unit of area under which a block fails by shear or splitting. The compressive strength, S_c , is therefore given by

$$S_c = P_c/A \quad (5.1)$$

where P_c is the load under which a specimen fails and A is the cross-sectional area of the specimen. The cylindrical specimen which is 3 cm in diameter and 6 cm in height was used for this test in which a strain-controlled testing machine with the maximum load of 20 tf was used. Top and base of the specimen were finished within the accuracy of 1/300. The rate of strain for this test was 0.2 to 0.5 mm/min. For sedimentary rock samples, all specimens were cored and the load was acted perpendicular to bedding planes. The number of test specimens is not sufficient. Averaged values were obtained (Table 3) because there is a small degree of scatter in the measured values. The results widely range from 10 to 20000 tf/m² (Table 3).

(2) Tensile strength

Tensile strength is the ability of a material to resist a stress tending to stretch it or to pull it apart, and is given by

$$S_t = P_t/A \quad (5.2)$$

where P_t is the tensile load under which the specimen

fails and A is the cross-sectional area of the specimen. The test which meets requirement of this definition is called a uniaxial tensile test. The disadvantage of this test are difficulties in making specimen and in equally loading. Because of these difficulties, the results of measurements is not always fully trusted (Yamaguchi and Nishimatsu, 1977, p.123). In place of this test, a radial compression is generally conducted in the field of rock mechanics. This test has the following advantages: (1) specimens required for the test are core sample which can be also used for the compression test, (2) precise specimens are easy to make, and (3) equal loading is possible. Although this test is not performed under purely tensile condition, the strengths measured in this way are in reasonable agreement with values obtained in uniaxial tension tests (Jaeger and Cook, 1969, p.162). The radial compression test has therefore been standardized in the Japan Industrial Standard as a tension test (JIS M0301). This test consists of applying diametral compression between the plates of a compression testing machine to a rock cylinder which, for convenience, is usually shorter than its diameter (Jaeger, 1972, p.42). The tensile strength, S_t , is obtained from

$$S_t = 2P/\pi dl \quad (5.3)$$

where P is the load under which the specimen fails, d is the diameter of specimen and l is the thickness of specimen. Specimens which are 3 cm in diameter and 1.5 to 3 cm in thickness were used in this study. The same testing machine as used in the compression test was employed here. The strain rate was 0.1 to 0.3 mm/min. The measured value widely range: $S_t = 1 - 1500 \text{ tf/m}^2$ (Table 3).

At the study sites of Notsuka, Shichiri-Nagahama, and Kitaura, samples are too weak to be able to measure through this test. Tensile strength for these locations was therefore estimated from the compressive strength measured already, assuming that the brittleness index, a ratio of compressive strength to tensile strength (Yamaguchi and Nishimatsu, 1977, p. 108), to be 10.

(3) Shear strength

Shear strength is the internal resistance offered to shear stress. It is measured by the maximum shear stress, based on original area of cross-section, that can be sustained without failure. Because of

difficulties in direct shear tests of rocks, in this study, shear strength was obtained through calculation using the values of compressive and tensile strengths. Shear strength is generally defined as the value at which the Mohr's envelope intersects the y-axis as shown in Fig. 27 (Yamaguchi and Nishimatsu, 1977, p. 130). Some methods are proposed to calculate this value. The Mohr's envelope is assumed to be a straight line in the simplest method (Fig. 27) and shear strength, S_s , for this case is expressed by

$$S_s = S_c S_t / 2 \quad (5.4)$$

where S_c is the compressive strength and S_t is the tensile strength. The Mohr's envelope is in practice a curve which is plotted by a bold line (Fig. 27). It is found that the real shear strength is larger than the strength which is calculated by using equation (5.4). The following equation which is proposed by Kobayashi and Okumura (1971) gives a more accurate value :

$$S_s = S_c S_t / 2 \sqrt{S_t (S_c - 3S_t)} \quad (5.5)$$

The result obtained using this equation (Table 3) shows a wide variety in S_s -value : 2 to 3100 tf/m².

(4) Longitudinal wave velocity

Longitudinal wave velocity of rocks was measured both on bedrocks in situ and on the cylindrical specimen in the laboratory (Table 3). The wave velocity propagating through the bedrock in situ, V_{pf} , was measured at the study site by using an instrument named "Pocket Seis"(OYO Co. Ltd., Model PS-1). The velocity was calculated from the average time which is required for the longitudinal wave to transmit a distance of 0.5 to 2 m. The value of V_{pf} ranges from 0.4 to 2.5 km/sec (Table 3). Wave velocity measurements for the cylindrical specimen were made in the laboratory by using an instrument, "Sonic Viewer" (OYO Co. Ltd., Model 5210). The specimen which is 3 cm in diameter and 6 cm in height was taken from the most fresh part of the bedrocks which does not include visible cracks. This wave velocity, V_{pc} , is found to vary from 0.9 to 4.3 km/sec according to study sites (Table 3). The value of V_{pc} is closely related to characteristic properties of rocks such as Young's modulus, density, poisson ratio, and shear modulus (Yamaguchi and Nishimatsu, 1977, p. 187). The value of V_{pf} decreases with increase in the degree of (1) weathering and (2) discontinuities such as faults, joints, and stratifications. This value is, therefore, smaller in general than that of V_{pc} .

CHAPTER 6

OCEANOGRAPHICAL CONDITIONS

6.1. Tidal conditions of the study areas

The mean tidal range of each study site is shown in Table 4. The mean tidal range is defined as the yearly averaged value of the difference in height between consecutive high and low waters. This is measured during five days before and after full moon and new moon. This value ranges from 0.4 to 4 m in places. On the Japan Sea coast, the tidal range is generally smaller with a range from 0.4 to 0.6 m, as compared with the Pacific coast where the tidal range is about 1.5 m. In the embayment areas, the tidal range becomes larger : approximately 2.5 m in the areas of Nagakushimen and Yadakemen, and 4 m at Oyano-Kodomari. Although the Hario site is situated in the embayment, the tidal range shows a small value, 1.0 m. The reason for the small value is that the strait which connects the embayment to the East China Sea is so narrow that the tidal waves can not be sufficiently transmitted.

6.2. Wave climate

Due to the location characteristics of study sites, it is difficult to estimate the wave climate by a unified method. Study sites are therefore classified into three categories: (1) the sites facing on the open sea, (2) the site situated in the embayment, and (3) the sites situated in the sheltered area. The wave climate of each category is described in the following section.

The larger the wave height is, the larger the wave energy in deep water becomes. In order to evaluate the magnitude of wave energy, the largest height of waves, $(H_0)_{\max}$, is estimated in each area.

(1) Open coast areas

Wave climate at the sites facing on the open sea is estimated from wave records which have been measured at seven representative stations by Ports and Harbors Bureau, Ministry of Transport, Japan. According to Tanaka (1980), Japanese coastal waters are divided into seven areas (Fig. 28).

The wave climate of these areas is shown in Figs. 29 and 30. Figure 29 shows the relationship between wave height and wave period. The wave climate is

characterized by that the larger the wave height, the larger the wave period. This tendency is pronounced on the coast facing the Sea of Japan as shown by Hamada, Kanazawa, and Sakata data (Fig. 29).

Figure 30 shows the occurrence frequency of wave height for the representative stations. A general trend shown in this figure is that the occurrence frequency of waves with a height of less than 1m is about 60 % (Fig. 30). Waves with more than 3 m high occur 3 to 5 % in frequency, and waves larger than 5 m in height is only 0.3 to 0.5 %. At Kashima, Habu, and Aburatsu, all located on the Pacific coast, the frequency of waves smaller than 1 m in height shows a smaller value, 20 to 40 %, than the general tendency mentioned above. In these coastal areas, waves with a height of more than 1m are dominant. At Sakata, located in the Japanese coast, waves larger than 5 m in height occur with the largest frequency, 1 %. Heights of waves occurring with a probability of 20 years are listed in Table 4 for each coastal area (Takahashi et al., 1982). These values, ranging from 7 to 10 m in places, are regarded as the largest height of waves in each area.

(2) Embayment area

Refraction is the process by which the direction of a wave moving in shallow water at an angle to the contours is changed. The part of the wave advancing in shallower water moves more slowly than that part still advancing in deep water, causing the wave crest to bend toward alignment with the underwater contours (CERC, 1977, p. (A)-28). The study site of Shimoda-Kakizaki is located in the shadow area at the head of Shimoda Bay. In order to estimate the degree of wave height reduction for this site, refraction diagrams are constructed by using the orthogonal method.

The incident direction of waves having the highest possibility to exert significant force on the study site is selected as southwest (Fig. 31). Waves entering into the bay from other directions are of negligibly small energy due to the presence of the Suzaki Peninsula and Akane Island. The waves coming from southwest pass through a shoal with an approximate water depth of 3 m which is located off Toji. Using the well-known breaking criterion : $H/h = 0.78$ where h is the water depth at which waves with a height of H breaks, H becomes 2.3 m when $h = 3$ m. All waves with $H > 2.3$ m will break at this shoal and dissipate their energy to act insignificant force at the study site.

The waves with $H = 2.3$ m are probably most important and these are equivalent to deep-water waves having a height of 1.9 m (Table 4).

(3) Sheltered areas

The study sites which are located in sheltered areas such as inland sea areas are not affected by swell transmitting from the ocean. At such study sites, waves generated within the confined waters are of much importance. Satoh and Goda (1972, p. 94) states that it is difficult to theoretically estimate the wave generation and its growth for such environments; some empirical methods therefore have been proposed for the wave prediction.

The Svedrup-Munk-Bretschneider [SMB] method is the most convenient system to predict waves in deep water when a limited amount of data and time are available (CERC, 1977, p. (3)-34). When a wind blows for a long time, the wave height at any place is determined by (1) horizontal distance over which a wind blows, fetch, and (2) wind velocity. In addition to these factors, wave reduction due to the bottom friction and the wave breaking limits the wave growth in the shallow water region. Bretschneider (1954) applied the SMB method to shallow water region and proposed a method to estimate

the wave height using (1) average water depth, (2) fetch, and (3) averaged wind velocity. Because the study sites under consideration are all located in a shallow water region, the Bretschneider method would be reasonable to apply to this study. The water depth and the fetch of each study site are obtained from hydrographic charts. The average wind velocity is obtained from meteorological data. Wind velocity at an observatory which is located in the vicinity of the study site is measured once per hour and averaged over a day. This daily-averaged value during ten years from 1970 to 1979 does not exceed 10 m/sec in maximum. The value of 10 m/sec is therefore adopted as the maximum wind velocity to predict the maximum wave height. The results of the prediction are shown in Table 4. The wave height ranges from 0.3 to 1.3 m (Table 4).

CHAPTER 7

DYNAMIC CONDITIONS FOR SHORE PLATFORM INITIATION(1): DEMARCATIION BETWEEN SHORE PLATFORMS AND PLUNGING CLIFFS

7.1. Basic concept for shore platform initiation

This chapter attempts to establish a critical condition under which shore platforms (Types A and B) are formed. It is considered that wave-induced cliff recession results in shore platforms at the foot of the cliff. In order to resolve the problem on shore platform initiation, it is therefore essential to elucidate a threshold for cliff erosion. The most important factors affecting cliff erosion, namely, shore platform initiation, are the resisting force of coastal rocks and the assailing force of waves. A fundamental relation of cliff erosion by waves can be expressed as (Sunamura, 1983)

$$X = \phi (F,t), \quad F = f_w/f_r \quad (7.1)$$

where X is the eroded distance of the cliff, F is the relative intensity of the wave assailing force, f_w , to

the rock resisting force, f_r , and t is the time. No erosion occurs if $F < 1$ ($f_w < f_r$), while erosion takes place if $F > 1$ ($f_w > f_r$). It is easily found that a critical condition for shore platform initiation is given by

$$f_w = f_r \quad (7.2)$$

The quantification of these two forces will be made in the following sections.

7.2. Quantification of assailing force of waves

7.2.1. Index of wave assailing force

By physical intuition the assailing force of waves, f_w , is assumed:

$$f_w \sim m(du/dt) \quad (7.3)$$

where m and u are the mass and the horizontal velocity of water particle, respectively, and t is the time. The right-hand side of equation (7.3) can be rewritten as follows:

$$m(du/dt) = d(mu)/dt \quad (7.4)$$

because the mass m is time-independent. When waves hit the cliff face, water particle velocity u is brought to zero in time dt and wave pressure exerts on the cliff. The right-hand side of equation (7.4), i.e., the rate of the change of momentum is equal to wave pressure, p :

$$d(mu)/dt = p \quad (7.5)$$

From equations (7.3), (7.4), and (7.5), the assailing force of waves is in proportion to the wave pressure:

$$f_w = Ap \quad (7.6)$$

where A is a nondimensional constant. The assailing force of waves actually consists not only of compressive force, wave pressure, but also of shear and tensile forces. After a wave breaks on a cliff, the water mass climbs the cliff face exerting shear force. At wave recession, the water mass exert tensile force on the cliff. It is easily assumed, however, that the larger the value of du/dt , the larger the degree of both shearing and tensile forces. It is possible to quantify the wave assailing force synthetically by knowing the value of the wave pressure, p , although the constant A is unknown.

7.2.2. Estimation of wave pressure

It is obvious that wave energy in deep water directly affects the wave pressure, p , which is adopted here for the index of wave assailing force. However, this deep water wave energy is diminished by the friction in shallow water region, and energy of waves approaching to the coast is influenced by nearshore submarine topography. Topography in shallow water and wave characteristics in deep water determine the type of waves just in front of the cliff. There are three types of waves: standing, breaking, and broken waves. Standing waves occur when the water depth in front of the cliff, called the front depth, d , is larger than the wave breaking depth, d_b ; breaking waves occur when $d = d_b$; and broken waves occur when $d < d_b$ (Fig. 32). The wave pressures of these three types are obtained in the following manners, respectively.

Figure 33 shows the vertical distribution of wave pressure (dynamic pressure) due to standing waves. This distribution, originally obtained from a theoretical consideration, is simplified by Sainflou (1928). The maximum value appears at S.W.L. and is given by

$$p = \left\{ \frac{w_0 H}{\cosh(2\pi d/L)} + w_0 d \right\} \left(\frac{H + h_0}{d + H + h_0} \right) \quad (7.7)$$

where H is the wave height in front of the cliff, L is the wavelength, d is the water depth, $h_0 = (\pi H^2/L) \coth(2\pi h/L)$, and w_0 is the weight of water per unit volume.

Figure 34 indicates the vertical distribution of dynamic pressure caused by breaking waves. The result is experimentally measured by Ross (1955). The maximum wave pressure, p , appears at slightly above S.W.L. It should be noted that the wave pressure abruptly diminishes below this level. The maximum pressure value of breaking waves is obtained from (Ross, 1955)

$$p = 35w_0(H_0)_b \quad (7.8)$$

where $(H_0)_b$ is the height of deep water waves which break just in front of the cliff.

Figure 35 shows the distribution of dynamic pressure resulting from broken waves. It is found that the pressure is uniformly distributed from S.W.L. to a height h_c above this level. The height h_c is given by $h_c = 0.78H_b$, where H_b is the breaking wave height. The dynamic pressure exerted by broken waves is obtained from (CERC, 1977, p. (7)-169):

$$p = 0.5w_0h_b \quad (7.9)$$

where h_b is the wave breaking depth. As shown in equations (7.7), (7.8), and (7.9), calculation methods for the wave pressure differs with different wave types: standing, breaking, and broken waves. The maximum value among wave pressure values for these wave types is adopted as an index for the assailing force of waves. The maximum value at the study site is obtained in the following way.

To elucidate the wave pressure at the study site, it is necessary to know the deep-water wave parameters and the characteristics of nearshore submarine topography. The parameters of maximum waves which are considered to occur at each study site are already estimated (Table 5). Concerning the shallow-water topography, knowledge of the water depth in front of the cliff, i.e., the front depth, is indispensable. The front depth can be estimated on the basis of an initial profile which is reconstructed in the following manners:

(1) For Type A shore platforms, it is difficult to reconstruct the initial profile because no topographic features of the initial profile do not remain in the present profile due to incessant severe erosion. It

would be valid to assume that cliff recession has taken place maintaining the profile similar to the present one (Fig. 36). The front depth known from the present profile is regarded as the same as the initial front depth.

(2) For the profile of Type B platforms, there always exists a steep cliff at the seaward end. Cotton (1963) suggested that this seaward bluff would be the initial profile of a steep drowned coast and the erosion of this bluff is negligible. The initial profile of Type B platforms is assumed to be the plunging cliff which was located at the seaward end of the present platform (Fig. 36). Wave tank experiments (Sunamura, 1975; Tsujimoto and Sunamura, 1984), in which a model cliff is made of a mixture of portland cement, well-sorted fine sand, and water, have shown the validity of this assumption; that is to say, the platform cutting does not extend to the cliff base, so that the underwater seaward cliff does remain unchanged.

(3) In the case of plunging cliff, it is assumed that an initial profile has been scarcely modified (Fig. 36).

Based on these assumptions, the water depths in front of the initial cliff are obtained at each study site (Table 5). The depths shown in Table 5 are

measured from H.W.L., because the values thus obtained produce for most cases the maximum value in the calculation of wave pressure.

With knowledge of wave parameters in deep water and the shallow-water topography, it is possible to obtain the height of deep-water waves which will break just in front of the cliff. The relation between the deep-water wave characteristics and the front depth at which waves break, d_b , is obtained from (Mitsuyasu, 1962):

$$d_b/H_0 = C_m(H_0/L_0)^{-0.25} \quad (7.10)$$

where H_0 and L_0 are the wave height and wavelength in deep water, respectively, and C_m is a constant which depends on the shallow-water bottom gradient, $\tan \beta$. The constant, C_m , is formulated from Mitsuyasu (1962, Fig. 14-6) as:

$$C_m = 0.034/(0.038 + \tan \beta) \quad (7.11)$$

The height of waves which break in front of the cliff is obtained from solving equation (7.10) for H_0 :

$$(H_0)_b = (d/C_m)^{1.33}/L_0^{0.33} \quad (7.12)$$

where $(H_0)_b$ is the height of deep-water waves which break in front of the cliff. In equation (7.12), d is already known as the front depth (Table 5) and C_m is given by equation (7.11) where $\tan \beta$ is obtained from a hydrographic chart. Two variables, H_0 and L_0 , remain unknown. Because the relation between H_0 and T has been already obtained in Fig.29, the H_0 vs. L_0 relation is easily obtained using the well-known equation: $L_0 = gT^2 / 2\pi$. Using this H_0 - L_0 relation and equation (7.12), the value of (H_0) is determined through a trial and error method.

When the value of $(H_0)_b$ thus obtained is larger than that of $(H_0)_{max}$, the largest height of waves occurring in each area, waves do not break at H.W.L. In such cases, the value of d which induces breaking of the waves having $(H_0)_{max}$ just in front of the cliff is obtained from equation (7.10), by changing the sea level within a mean tidal range. The value of $(H_0)_{max}$ is adopted here instead of $(H_0)_b$ in equation (7.8). The relative height of H to $(H_0)_b$ determines the types of waves which occur in front of the cliff: (1) if $(H_0)_b > H_0$, then standing waves are created by reflection from the cliff; (2) if $(H_0)_b = H_0$, then breaking waves are produced; and (3) if $(H_0)_b < H_0$,

then broken waves are formed. The wave pressure of these three types can be calculated by using equations (7.7), (7.8), and (7.9), respectively.

As an example, Fig. 37 shows the result of calculation at the Kominato site. The value of wave pressure is outstandingly large when $(H_0)_b = H_0$, namely, breaking waves are produced (Fig. 37). Pressure caused by both standing and broken waves is very small. Such a characteristic pattern of wave pressure distribution is found at other study sites except the Akane site. At this study site, due to the large front depth, all waves do not break to form standing waves, and the pressure of which is extremely small.

At the Kakizaki site, the effect of refraction should be taken into account. In the refraction analysis, it is assumed that energy of waves advancing toward shore does not flow laterally along the wave crest; that is to say, the energy remains constant between orthogonals (CERC, 1977, p. (2)-66). From this assumption, wave height in shallow water, H , is given by (e.g., Komar, 1976, p. 110)

$$H = K_S \sqrt{b_0/b} H_0 \quad (7.13)$$

where H_0 is the wave height in deep water, K_S is the shoaling coefficient, and b_0 and b are the spacing between the selected orthogonals in deep water and shallow water, respectively. At the study site, $\sqrt{b_0/b} = 1/6.2$ and $K_S = 0.94$. It is found from equation (7.13) that the waves which are 1.9 m high in deep water (Table 5) reduces their height in shallow water, with only 0.29 m in height. The waves with this height in shallow water are equivalent to deep-water waves having a height of 0.28 m without considering the effect of wave refraction. This value ($H_0 = 0.28$ m) was used for the evaluation of $(H_0)_b$ in equation (7.8).

7.3. Quantification of resisting force of rocks

One should employ an appropriate index which can represent the resisting force of rocks against the wave assault. Because waves exert stresses in various modes such as compression, tension, and shear, it is actually difficult to represent the rock resisting force by only one index. However, it is assumed that indices such as compressive, tensile, and shearing strength of rocks are closely related and not independent of one another (Sunamura, 1975). In order to examine this point, correlations of these indices are examined in Fig. 38,

which shows tensile strength, shear strength, and longitudinal wave velocity plotted against compressive strength. This figure suggests that it is possible to use one of them as representative of the resisting force. Of these indices, compressive strength, S_c , is a widely used index in the fields of soil sciences and rock mechanics, and the testing criteria for this index is well established. Compressive strength has been therefore employed for the recent studies which attempt to dynamically describe topographic changes (Horikawa and Sunamura, 1967, 1969, 1970; Sunamura, 1973, 1977, 1982; Takahashi, 1975; Suzuki, 1982). In the study of shore platforms, S_c has been employed and its validity is recognized (Tsujiimoto, 1985). For the above reasons, compressive strength is employed as representative of the resisting force of rocks in the present study.

Various indices expressing the resisting force of rocks such as compressive, tensile, and shear strengths are mostly obtained from specimens without visible cracks. These indices show the strength in the most resistant part of a rock body. In actual field situations, a rock body has discontinuities of joints and faults with spacing of several tens centimeters to a few meters. It is clear that such discontinuities

reduce the resisting force of the rock body. It is therefore inappropriate to represent the rock resisting force by compressive force only. By knowing the fact that the propagation of longitudinal wave velocity through a rock body decreases when discontinuities exist in the rock (Tanaka, 1970), Suzuki (1982) has introduced a discontinuity index, V_{pf}/V_{pc} , in which V_{pf} and V_{pc} are the longitudinal wave velocity measured in the rock body in situ and measured for cylindrical specimen without visible cracks in the laboratory, respectively. The total resisting force of rocks, f_r , is represented here by multiplying this index by compressive strength:

$$f_r = BS_c(V_{pf}/V_{pc}) = BS_c^* \quad (7.14)$$

where

$$S_c^* = S_c(V_{pf}/V_{pc}) \quad (7.15)$$

and B is a nondimensional constant. The quantity S_c^* is an index for the magnitude of the rock resisting force. The value of S_c^* widely ranges from 13 to 5600 tf/m^2 depending on the study sites (Table 5).

At the sites of Notsuka, Shichiri-nagahama,

Kitaura, and Okuma, samples are so weak that the longitudinal wave velocity in the laboratory could not be measured. If the measurement could have been possible, then one would obtain $V_{pf} < V_{pc}$. It is clear that the actual value of S_C^* is smaller than S_C (Table 5).

7.4. Dynamic condition for demarcating shore platforms and plunging cliffs

A formative condition of shore platforms and plunging cliffs should be equivalent to a critical condition between erosion and no erosion. This is given by equation (7.2):

$$f_w = f_r$$

The resisting force of rocks, f_r , can be represented, as shown in equation (7-14), by an index which is obtained from multiplying the compressive strength, S_C , by the discontinuity index, V_{pf}/V_{pc} :

$$f_r = BS_C^x$$

The assailing force of waves, f_w , can be directly

related to wave pressure, p , i.e., from equation (7.6):

$$f_w = Ap$$

A dynamic condition for delimiting shore platforms and plunging cliffs is obtained from equations (7.2), (7.6), and (7.14):

$$p = cS_C^* , \quad c = b/a \quad (7.16)$$

where c is an unknown dimensionless constant. Equation (7.16) indicates that the demarcation should be expressed by a straight line with an inclination of 45° on the logarithmic graph paper.

The data of S_C^* and p obtained at each site (Table 5) are plotted in Fig. 39. In this figure, the open circle shows the site where shore platforms are formed and the closed square denotes the site of plunging cliffs. The subscript means the location number shown in Fig. 6. At the sites of 1, 2, 4, and 8, longitudinal wave velocity of rocks could not be measured, therefore the possibility of lower S_C^* -value is expressed by an arrow.

Figure 39 indicates that the two types of landforms are clearly demarcated by a solid line, which is given

by

$$p = 0.081S_C^* \quad (7.17)$$

In the left-hand side area of this line, f_w is in excess of f_r and shore platforms are formed. In the right-hand side area, no erosion occurs because of $f_w < f_r$ and plunging cliffs are found. Figure 39 shows that only one data point of plunging cliff case (the Kakizaki site) is plotted in the area of shore platform formation. A possible reason for this is that maximum wave height, $(H_o)_{max}$, was overestimated because the effect of shoal off Toji (Fig. 31) was not properly incorporated in the wave estimation.

CHAPTER 8

DYNAMIC CONDITIONS FOR SHORE PLATFORM INITIATION(2): DEMARICATION BETWEEN TYPE A AND TYPE B PLATFORMS

8.1 Basic concept for Types A and B shore platform initiation

This chapter attempts to establish a critical condition for the initiation of Type A or Type B shore platform. Both types of platforms are the results of cliff recession. The most marked difference between the two is the existence or non-existence of a seaward bluff: Type B platforms have, whereas Type A do not. As is clear from the result of the wave tank experiment (Figs. 3 and 4), the seaward bluff is the initial profile of a steep drowned coast. The critical condition between Type A and Type B can be determined by whether the initial underwater bluff disappears or exists. Disappearance of the seaward bluff is not brought about by destruction due to the direct wave assault on the bluff face, but by surface lowering of the platform once formed. Because the force of waves exponentially decreases downward as the water depth increases below S.W.L. (Figs. 33, 34, and 35). If the

seaward bluff is eroded away due to continuous surface lowering, then Type A platforms are created. In Type B platforms, the surface lowering does not progress; so that the seaward bluff is maintained. The critical formative condition between Type A and Type B is therefore determined by the occurrence or non-occurrence of the surface lowering, and this is expressed by

$$f_{ws} = f_{rs} \quad (8.1)$$

where f_{rs} is the rock resisting force against the lowering of the platform surface and f_{ws} is the wave assailing force which causes the surface lowering. The quantification of these two forces will be made.

8.2. Quantification of assailing force of waves

8.2.1. Index of wave assailing force

When the condition for platform initiation which is described by equation (7.16), is satisfied, a notch is formed, at the initial stage of platform development, at or near S.W.L. where the assailing force of waves has its maximum value; this is clear from the profile change shown in Figs. 3 and 4. It is

considered that the critical condition for demarcating Type A and Type B shore platforms is ultimately determined by whether the lowering of the notch bottom occurs or not.

The wave assailing force on the notch bottom consists mainly of compressive, tensile, and shear forces. It is clear that the most effective agent in the notch lowering is the shear force. Then the shear force, τ , is adopted as an index for representing the wave assailing force acting on the notch bottom, f_{ws} :

$$f_{ws} = a\tau \quad (8.2)$$

where a is a nondimensional unknown constant.

8.2.2. Estimation of shear force

It is extremely difficult to directly measure wave-induced shear force in the field. The shear force is therefore estimated here by the following way. The shear force τ , which is caused by the movement of water particles along the surface of sea bottom, is related to the velocity of water particle, U , by (e.g., Komar, 1976, p. 186):

$$\tau = C_f \rho U^2 \quad (8.3)$$

where C_f is a nondimensional coefficient of friction and ρ is the density of water. The velocity U is obtained by using solitary wave theory which can be applied in a very shallow water region. The wave velocity of solitary wave, C , is approximately expressed by (Komar, 1976, p. 55)

$$C = \sqrt{g(H+h)} \quad (8.4)$$

where H is the wave height and h is the water depth. Because the h is approximately zero in the situation under consideration, C becomes

$$C = \sqrt{gH} \quad (8.5)$$

In the very shallow water region, water particles move only horizontally and the velocity distribution is uniform. Because the velocity of water particles seems equivalent to wave velocity, the velocity of water particles near the bottom U is written as

$$U = \sqrt{gH} \quad (8.6)$$

From this equations (8.3) and (8.6), the shear force is

obtained:

$$\tau = C_f \rho g H \quad (8.7)$$

In the actual calculation for the value of τ , it is necessary to evaluate the friction coefficient C_f . The value of 0.01 is often used in a shallow water region. However, in a very shallow water region, the effect of friction is supposed to be more marked. Kohno et al. (1978) have measured the reduction of wave height on a coral reef where the water depth is very small, and have obtained the value of 0.15 as the friction coefficient. Based on this result, $C_f = 0.15$ is adopted in this study. In equation (8.7), the wave height H remains unknown. It is necessary to evaluate the value of H which gives rise to the maximum shear force. When waves produce the maximum pressure on the cliff face, the horizontal velocity component also attains the maximum. This in turn would produce the maximum shear force on the bottom.

When breaking waves occur just in front of the cliff, the wave pressure shows the maximum value as compared with other types of waves such as standing and broken waves, as mentioned in Chapter 7. The height of breaking waves is therefore adopted to estimate the

maximum shear force, τ_{\max} :

$$\tau_{\max} = 0.15\rho g H_D \quad (8.8)$$

This result of calculation by use of this equation show that the value of τ_{\max} ranges from 0.1 to 1.0 tf/m^2 depending on study site (Table 6).

8.3. Quantification of resisting force of rocks

It is reasonable to take shear strength as the most appropriate index for rock resisting force, because the assailing force mainly consists of shear force. The shear strength shown in Table 3 was obtained through calculation using equation (5.5) because of difficulty in conducting direct shear tests on rocks. The resisting force of rocks, f_{rs} , is represented here by multiplying the discontinuity index V_{pf}/V_{pc} by shear strength, S_s :

$$f_{rs} = b(V_{pf}/V_{pc})S_s = bS_s^* \quad (8.9)$$

where $S_s^* = (V_{pf}/V_{pc})S_s$ and b is a nondimensional unknown constant. The quantity S_s^* is a quantity showing the shear strength including the effect of

discontinuities in the rock body. The value of S_S^* widely ranges from 2 to 300 tf/m^2 depending on study site (Table 6). At the study sites of Notsuka, Shichiri-Nagahama, Kitaura, and Okuma, only the value of upper limit is calculated assuming that $V_{pf}/V_{pc} = 1$, because the measurements of V_{pc} were not possible.

8.4. Dynamic condition for demarcating Type A and Type B shore platforms

A dynamic condition for delimitating Types A and B shore platforms is obtained from equations (8.1), (8.2), and (8.9):

$$\tau = c'S_S^* , \quad c' = b/a \quad (8.10)$$

where c' is a dimensionless unknown constant. Equation (8.10) indicates that demarcation should be expressed by a straight line with an inclination of 45° on the logarithmic graph paper.

The data of S_S^* and τ obtained at each site are plotted in Fig. 40. In this figure, the open triangle shows the site where Type A shore platforms are formed and the closed circle denotes the site of Type B shore platforms. The subscript indicates the location number

shown in Fig. 6. Arrows at the sites of 1, 2, 4, and 8 show the possibility of lower S_S^* -value. Figure 40 indicates that two types of shore platforms are clearly demarcated by the solid straight line, which is given by

$$\tau = 0.005S_S^* \quad (8.11)$$

In the left-hand side area of this line, f_{ws} is in excess of f_{rs} to form Type A shore platforms. In the right-hand side area, no lowering of the platform surface occurs because of $f_{ws} < f_{rs}$, resulting in the formation of Type B shore platforms.

CHAPTER 9

SUMMARY AND CONCLUSIONS

Shore platforms which are major morphological features on rocky coasts are largely classified into two types (Fig. 1): (1) Type A shore platforms which have a slightly seaward-sloping surface without any topographic breaks, extending to the nearshore bottom; and (2) Type B shore platforms which have a nearly horizontal surface with marked topographic break at the seaward margin. In contrast to these landforms, plunging cliffs are found which continue beneath the sea level with no platform development. A review of previous studies showed that the degree of exposure to waves and the resistivity of rocks against wave force are crucial factors in the formation of these types of rocky coasts. However, the role of these factors were not fully explained because the previous studies failed to scrutinize this problem on a dynamic basis.

This study therefore attempted to quantitatively examine dynamical conditions demarcating these three landform types. With this purpose, twenty-five study sites were selected from various parts of Japanese coast (Fig. 6), and field investigations were

conducted. In the field, profile levelling was performed to obtain precise information on the subaerial and subaqueous topographic features. In an attempt to quantify the rock resisting force, various mechanical properties of rocks were examined. The wave assailing force was estimated from existing wave data.

Because wave-induced cliff recession results in shore platforms at the foot of the cliff, a formative condition for shore platforms and plunging cliffs should be equivalent to a critical condition whether cliff erosion occurs or not. The most important factors affecting cliff erosion are the assailing force of waves, f_w , and the resisting force of rocks against waves, f_r . A critical condition for shore platform initiation is given by $f_w = f_r$. These two quantities f_w and f_r are represented by wave pressure, p , and compressive strength of the rock body, S_C^* , respectively. Using these parameters, a dynamic condition for delimiting shore platforms and plunging cliffs is expressed by $p = 0.081S_C^*$ (Fig. 39). Shore platforms develop when $p > 0.081S_C^*$, whereas plunging cliffs form when $p < 0.081S_C^*$.

The most marked difference between Types A and B shore platforms is the existence or non-existence of a seaward bluff: Type B platforms have the bluff, whereas

Type A do not. A delimiting condition between Types A and B should be equivalent to a critical condition whether surface lowering of the platform once formed occurs or not, i.e., $f_{ws} = f_{rs}$ where f_{ws} is the wave assailing force which causes the surface lowering and f_{rs} is the rock resisting force against the lowering. By representing f and f by shear force, τ , and shear strength of the rock body, S_s^* , respectively, a dynamic condition for delimiting Type A and Type B shore platforms is expressed by the solid line in Fig. 40. This line is given by $\tau = 0.005S_s^*$. If the left-hand side of this equation is greater than the right-hand side, Type A shore platforms develop; otherwise Type B platforms form.

A necessary and sufficient condition for shore platform initiation is summarized in Table 7.

References

- Aramaki, M. (1978) Erosion of coastal cliff at Iwaki coast in Fukushima Prefecture, Japan: Bull. Assoc. Nat. Sci., Senshu Univ., vol. 11, pp. 5-36 (in Japanese with English abstract).
- Bartrum, J. A. (1926) "Abnormal" shore platform: Jour. Geol., vol. 34, pp. 793-807.
- Bartrum, J. A. (1938) Shore platforms: Jour. Geomorph., vol. 1, pp. 266-272.
- Bird, E. C. F., and Dent, O. F. (1966) Shore platforms on the south coast of New South Wales: Aust. Geogr., vol. 10, pp. 71-80.
- Coastal Engineering Research Center (1977) Shore protection manual: 3rd Ed., Fort Belvoir, U. S. A.
- Cotton, C. A. (1942) Geomorphology: Whitcombe & Tombs, London, 505 pp.
- Cotton, C. A. (1963) Levels of planation of marine benches: Zeit. Geomorph., vol. 7, pp. 97-111.
- Dana, J. D. (1849) Report of the United States exploration expedition 1838-1842, vol. 10, 442 pp. (in Bartrum, 1926)
- Edwards, A. B. (1941) Storm-wave platforms: Jour. Geomorph., vol. 4, pp. 223-236.
- Edwards, A. B. (1951) Wave action in shore platform

- formation: Geol. Mag., vol. 88, pp. 41-49.
- Emery, K. O., and Foster, H. L. (1956) Shoreline nips in tuff at Matsushima, Japan: Am. Jour. Sci., vol. 254, pp. 380-385.
- Flemming, N. C. (1965) Form and relation to present sea level of Pleistocene marine erosional features: Jour. Geol., vol. 73, pp. 799-811.
- Focke, J. W. (1978) Limestone cliff morphology on Curacao (Netherlands Antilles), with special attention to the origin of notches and vermetid/coralline algal surf benches ("cornices", "trottoirs"): Zeit. Geomorph., vol. 22, pp. 329-349.
- Gill, E. D. (1972a) The relationship of present shore platforms to past sea levels: Boreas, vol. 1, pp. 1-25.
- Gill, E. D. (1972b) Sanders's wave tank experiments and shore platform: Papers Proc. Royal Soc. Tasmania, vol. 106, pp. 17-20.
- Gill, E. D., and Lang, J. G. (1983) Micro-Erosion Meter measurements of rock wear on the Otway coast of southeast Australia: Marine Geol., vol. 52, pp. 141-156.
- Hansom, J. D. (1983) Shore-platform development in the south Shetland Islands, Antarctica: Marine Geol.,

- vol. 57, pp. 211-229.
- High, C., and Hanna, F. K. (1970) A method for the direct measurement of rock surfaces: Brit. Geomorph. Res. Gr., Tech. Bull., vol. 5, pp. 1-25.
- Hills, E. S. (1949) Shore platforms: Geol. Mag., vol. 86, pp. 137-152.
- Horikawa, K., and Sunamura, T. (1967) A study on erosion of coastal cliffs by using aerial photographs: Proc. 14th. Japan. Conf. Coast. Eng., pp. 315-324 (in Japanese).
- Horikawa, K., and Sunamura, T. (1968) An experimental study on erosion of coastal cliffs due to wave action: Proc. 15th. Japan. Conf. Coast. Eng., pp. 149-156 (in Japanese).
- Horikawa, K., and Sunamura, T. (1969) Erosion of coastal cliff at Byobugaura, Chiba Prefecture - study on erosion of coastal cliffs by using aerial photographs (report no. 2): Proc. 16th. Japan. Conf. Coast. Eng., pp. 137-145 (in Japanese).
- Horikawa, K., and Sunamura, T. (1970) Coastal cliff erosion at Byobugaura, Chiba Prefecture (2) - A study on erosion of coastal cliffs using aerial photographs (report no. 3): Proc. 17th. Japan. Conf. Coast. Eng., pp. 289-296 (in Japanese).
- Hujioka, K. (1958) Explanatory text of the geological

- map of Japan, scale 1: 50000, "Toga and Funakawa":
61pp. (in Japanese with English abstract).
- Ikebe, N. (1959) Stratigraphical and geographical
distribution of Fossil Elephants in Kinki District,
Central Japan: Quaternary research, vol.1, pp.109-
118 (in Japanese with English abstract).
- Inoue, E. (1962) Paleogene in the inferior region of
Misumi-machi, Uto Peninsula, Kumamoto Prefecture:
Bull. Geol. Survey, Japan, vol. 13, pp. 1053-1071
(in Japanese with Spanish abstract).
- Jaeger, J. C. (1972) Rock mechanics and engineering:
Cambridge Univ. Press, London, 417pp.
- Jaeger, J. C., and Cook, N. G. (1969) Fundamentals of
rock mechanics: Methuen & Co. Ltd., London, 513pp.
- Johannessen, C. L., and Feiereisen, J. J. (1982)
Weathering of ocean cliffs by salt expansion in
a mid-latitude coastal environment: Shore and
Beach, vol. 50, pp. 26-34.
- Johnson, D. W. (1919) Shore processes and shoreline
development: Hafner, New York, 584pp.
- Jutson, J. T. (1939) Shore platforms near Sydney, New
South Wales: Jour. Geomorph., vol. 2, pp. 237-250.
- Kaizuka, S. (1956) A study on the morphology of Tokachi
Plain: Geogr. Rev. Japan, vol. 29, pp. 232-239 (in
Japanese).

- Katsurahara, N. (1968) A study on the marine terraces and crustal movement in Oga Peninsula: Yokohama National Univ., Dept. Geogr., Graduation Thesis, (in Japanese) in Ota, Y., Kaizuka, S., Kikuchi, T., and Naito, H. (1968) Correlation between heights of younger and older shorelines for estimating rates and regional differences of crustal movements: Quat. Res., vol. 7, pp.171-181 (in Japanese with English abstract).
- Kirk, R. M. (1977) Rates and Forms of erosion on intertidal platforms at Kaikoura Peninsula, South Island, New Zealand: N. Z. Jour. Geol. Geophy., vol. 20, pp. 571-613.
- Kitazato, H. (1975) Geology and geochronology of the younger Cenozoic of Oga Peninsula: Contrib. Inst. Geol. Paleon., Tohoku Univ., no. 75, pp. 17-49 (in Japanese with English abstract).
- Kobayashi, R., and Okumura, K. (1971) Study on shear strength of rocks: Jour. Mining Metallurgical Inst. Japan, vol. 87, pp. 407-412 (in Japanese with English abstract).
- Kohno, F., Nagamatsu, K., and Kiyan, T. (1978) Field obserbation of wave transformation on a reef: Proc. 25th. Japan. Conf. Coast. Eng., pp. 146-150 (in Japanese).

- Komar, P. D. (1976) Beach processes and sedimentation: Prentice-Hall, Englewood Cliffs, New Zealand, 429 pp.
- Matsui, M., Satoh, H., Kosawa, T., Miyasaka, S., Sasajima, S., Akiba, C., Migiya, M., and Kasugai, A. (1973) Geology of Daiki District: quadrangle series, scale 1: 50000, Geol. Surv. Japan, 107 pp. (in Japanese with English abstract).
- Matsumoto, R., Katayama, T., and Iijima, A. (1985) Geology, igneous activity, and hydrothermal alteration in the Shimoda district, southern part of Izu Peninsula, central Japan: Jour. Geol. Soc. Japan, vol. 91, pp. 43-63 (in Japanese with English abstract).
- Miki, A. (1977) Late Cretaceous pollen and spore floras of northern Japan, composition and interpretation: Jour. Fac. Sci., Hokkaido Univ., ser. 4, vol. 17, pp. 399-436
- Mitsuyasu, H. (1962) Experimental study on wave force against a wall: Rep. Transport. Tech. Res. Inst., no. 47.
- Moritani, T. (1968) Geology of the Funakawa district: quadrangle series, scale 1: 50000, Geol. Surv. Japan, 57pp. (in Japanese with English abstract).
- Murakami, N. (1960) Cretaceous and Tertiary igneous

- activity in western Chugoku, Japan: Sci. Rep. Yamaguchi Univ., vol. 11, pp. 21-126 (in Japanese with English abstract).
- Nagahama, A., and Matsui, K. (1982) Geology of Haiki district: quadrangle series, scale 1: 50000, Geol. Surv. Japan, 50 pp. (in Japanese with English abstract).
- Nakajima, T., Makimoto, H., Hirayama, J., and Takahashi, S. (1981) Geology of Kamogawa district: quadrangle series, scale 1: 50000, Geol. Surv. Japan, 107 pp. (in Japanese with English abstract).
- Nakata, T., Iwaizumi, T., and Matsumoto, T. (1976) Late Quaternary tectonic movements on the Nishi-Tsugaru coast, with reference to seismic deformation: Sci. Rep. Tohoku Univ., 7th ser, vol. 26, pp.101-112.
- Newmann, A. C. (1966) Observations on the coastal erosion in Bermuda and measurements of the boring rate of the sponge, *Cliona Lampa*: Limnol. Oceanogr., vol. 11, pp. 92-108.
- Ozaki, H. (1958) Stratigraphical and Paleontological studies on the Neogene and Pleistocene Formations of the Tyoshi district: Bull. Nat. Sci. Mus. Tokyo, vol. 4, pp. 1-182.
- Ricketts, E. F., and Calvin, J. (1968) Between Pacific

- Tides: Stanford Univ. Press, Stanford, California, 614 pp.
- Robinson, L. A. (1977a) The morphology and development of the northeast Yorkshire shore platform: Mar. Geol., vol. 23, pp. 237-255.
- Robinson, L. A. (1977b) Marine erosive processes at the cliff foot: Mar. Geol., vol. 23, pp. 257-271.
- Ross, C. W. (1955) Laboratory study of shock pressure of breaking wave: Beach Erosion Board, Tech. Memo., no. 59, 22 pp.
- Sainflou, G. (1928) Essai sur les digues maritimes verticales: Ann. Ponts Chausses, vol. 98, pp. 5-48 (in CERC, 1977).
- Sanders, N. K. (1968) Wave tank experiments on the erosion of rocky coasts: Papers Proc., Royal Soc. Tasmania, vol. 102, pp. 11-16.
- Satoh, S., and Goda, Y. (1972) Coast and harbor: Shokokusha, Tokyo, Japan, 372 pp. (in Japanese).
- Sawamura, K., Sumi, K., and Moritani, T. (1969) Geology of the Shimoda district: quadrangle series, scale, 1: 50000, Geol. Surv. Japan, 41 pp. (in Japanese with English abstract).
- Shimazu, M., and Teraoka, Y. (1960) Explanatory map of Japan, scale 1: 50000, "Rikuchu-Noda": 53pp. (in Japanese with English abstract).

- Sumi, K. (1958) Explanatory map of Japan, scale 1: 50000, "Mikomotojima": 33 pp. (in Japanese).
- Sunamura, T. (1973) Coastal cliff erosion due to waves field investigations and laboratory experiments: Jour. Fac. Engng., Tokyo Univ., vol. 32, pp. 1-86.
- Sunamura, T. (1975) A laboratory study of wave-cut platform formation: Jour. Geol., vol. 83, pp. 389-397.
- Sunamura, T. (1976) Feedback relationship in wave erosion of laboratory rocky coast: Jour. Geol., vol. 84, pp. 427-437.
- Sunamura, T. (1977) A relationship between wave-induced cliff erosion and erosive force of waves: Jour. Geol., vol. 85, pp. 613-618.
- Sunamura, T. (1978a) Mechanism of shore platform formation on the southeastern coast of the Izu Peninsula, Japan: Jour. Geol., vol. 86, pp. 211-222.
- Sunamura, T. (1978b) A mathematical model of submarine platform development: Math. Geol., vol. 10, pp. 53-58.
- Sunamura, T. (1982) A wave tank experiment on the erosional mechanism at a cliff base: Earth Surface Processes Landforms, vol. 7, pp. 333-343.
- Sunamura, T. (1983) Processes of sea cliff and platform

- erosion: in Komar, P. D. Ed., CRC Handbook of coastal processes and erosion, pp. 233-265.
- Sunamura, T., and Tsujimoto, H. (1982) Long-term recession rate of Taitomisaki coastal cliff: Ann. Rep. Inst. Geosci., Univ. Tsukuba, no. 8, pp. 55-56.
- Suzuki, T. (1982) Rate of lateral planation by Iwaki River, Japan: Trans. Japan. Geomorph. Union, vol. 3, pp. 1-24.
- Suzuki, T., Takahashi, K., Sunamura, T., and Terada, M. (1970) Rock mechanics on the formation of washboard-like relief on wave-cut benches at Arasaki, Miura Peninsula, Japan: Geogr. Rev. Japan, vol. 43, pp. 211-221 (in Japanese with English abstract).
- Takahashi, K. (1975) Differential erosion originating washboard-like relief on wave-cut bench at Aoshima Island, Kyushu, Japan: Geogr. Rev. Japan, vol. 48, pp. 43-62 (in Japanese with English abstract).
- Takahashi, K. (1976) Differential erosion on wave-cut bench: Bull. Fac. Sci. Eng., Chuo Univ., vol. 19, pp.253-316 (in Japanese with English abstract).
- Takahashi, T. (1974) Distribution of shore platforms in southwestern Japan: Sci. Rep., Tohoku Univ., 7th ser. vol. 24, pp. 33-45.
- Takahashi, T., Hirose M., and Hashimoto N. (1982) Long-

- term statistical properties of waves in Japanese coasts: Proc. 29th. Japan. Conf. Coast. Eng., pp. 11-15 (in Japanese).
- Tanaka, N. (1980) The delimitation of coastal region in Japan from the viewpoint of the coastal engineering: Proc. 27th. Japan. Conf. Coast. Eng., pp. 211-215 (in Japanese).
- Tanaka, Y. (1970) On the measurement of the crack quantity in rocks by the elastic wave velocity: Eng. Geol., vol. 11, pp. 1-7 (in Japanese with English Abstract).
- Toyoshima, O. (1974) Sea cliff erosion and counter measures: Proc. Symp. Coast. Cliff Recession, Japan Soc. Civil Eng., Tokyo (in Japanese).
- Toyoshima, Y. (1967) A study on marine erosive features along San-in coast: Sci. Rep. Fac. Tottori Univ., vol. 18, pp. 1-34 (in Japanese).
- Toyoshima, Y. (1968) Abrasion platform and wave-cut bench at Kushimoto-machi, Wakayama Prefecture, : Sci. Rep. Fac. Educ., Tottori Univ., vol. 19, pp. 1-7 (in Japanese with English abstract).
- Toyoshima, Y. (1973) Coastal geomorphology - with special reference to coastal profiles and coastal changes: Oceanography (Kaiyo Kagaku), vol. 5, pp. 839-843 (in Japanese with English abstract).

- Trenhaile, A. S. (1978) The shore platforms of Gaspé, Quebec: *Ann. Assoc. Am. Geogr.*, vol. 4, pp. 95-114.
- Trenhaile, A. S. (1980) Shore platforms; a neglected coastal features: *Prog. Phys. Geogr.*, vol. 4, pp. 1-23.
- Trenhaile, A. S. (1983) The width of shore platforms; a theoretical approach: *Geogr. Ann.*, vol. 65A, pp. 147-158.
- Tricart, J. (1959) Problèmes géomorphologiques du littoral oriental du Brésil: *Cahiers Oceanogr.*, vol. 11, pp. 276-308.
- Trudgill, S. (1976) The marine erosion of limestones on Aldabra Atoll, Indian Ocean: *Zeit. Geomorph.*, vol. 26 (suppl. Bd.), pp. 164.
- Tsujimoto H. (1985) Types of rocky coasts and the resisting force of coastal rocks in the eastern part of Chiba Prefecture, Japan: *Geogr. Rev. Japan* (ser. A), vol. 58, pp. 180-192 (in Japanese with English abstract).
- Tsujimoto, H., and Sunamura, T. (1984) A wave tank experiment on the formation of shore platforms: *Bull. Envir. Res. Center, Tsukuba Univ.*, no. 8, pp. 45-48 (in Japanese).
- Wentworth, C. K. (1939) Marine bench-forming processes; (2) solution benching: *Jour. Geomorph.*, vol. 2,

pp. 3-25.

Yamaguchi, U., and Nishimatsu, Y. (1977) Introduction to rock mechanics: 2nd Ed., Univ. Tokyo Press, Tokyo, Japan, 266 pp. (in Japanese).

Yamamoto, H., and Minoda, K. (1973) Acid pyroclastic flow of Nojima Group (Miocene series) in the northwestern part of Nagasaki Prefecture: Jour. Geol. Collab. Japan, vol. 27, pp. 213-220 (in Japanese with English abstract).

Yoshikawa, T., Sugimura, A., Kaizuka, S., Ota, Y., and Sakaguchi, Y. (1973) Geomorphology of Japan, the New Edition: Univ. Tokyo Press, Tokyo, 415 pp. (in Japanese).

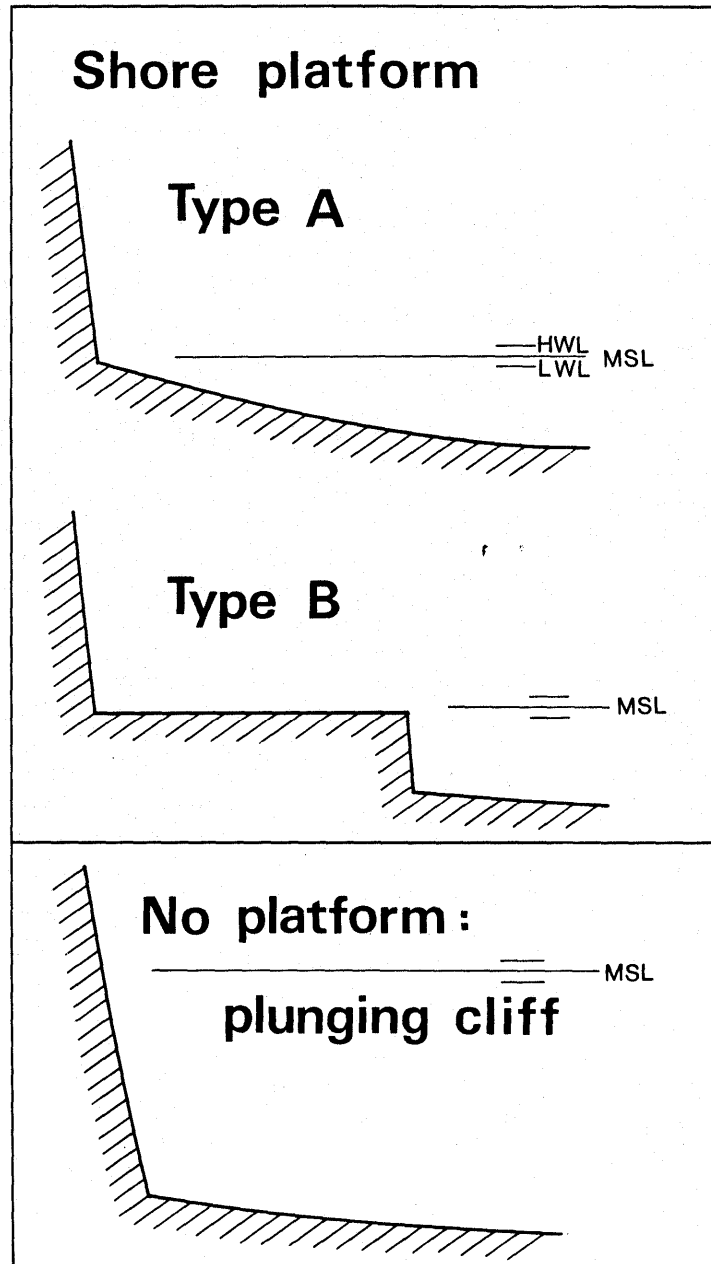


Figure 1. Three types of rocky coasts.

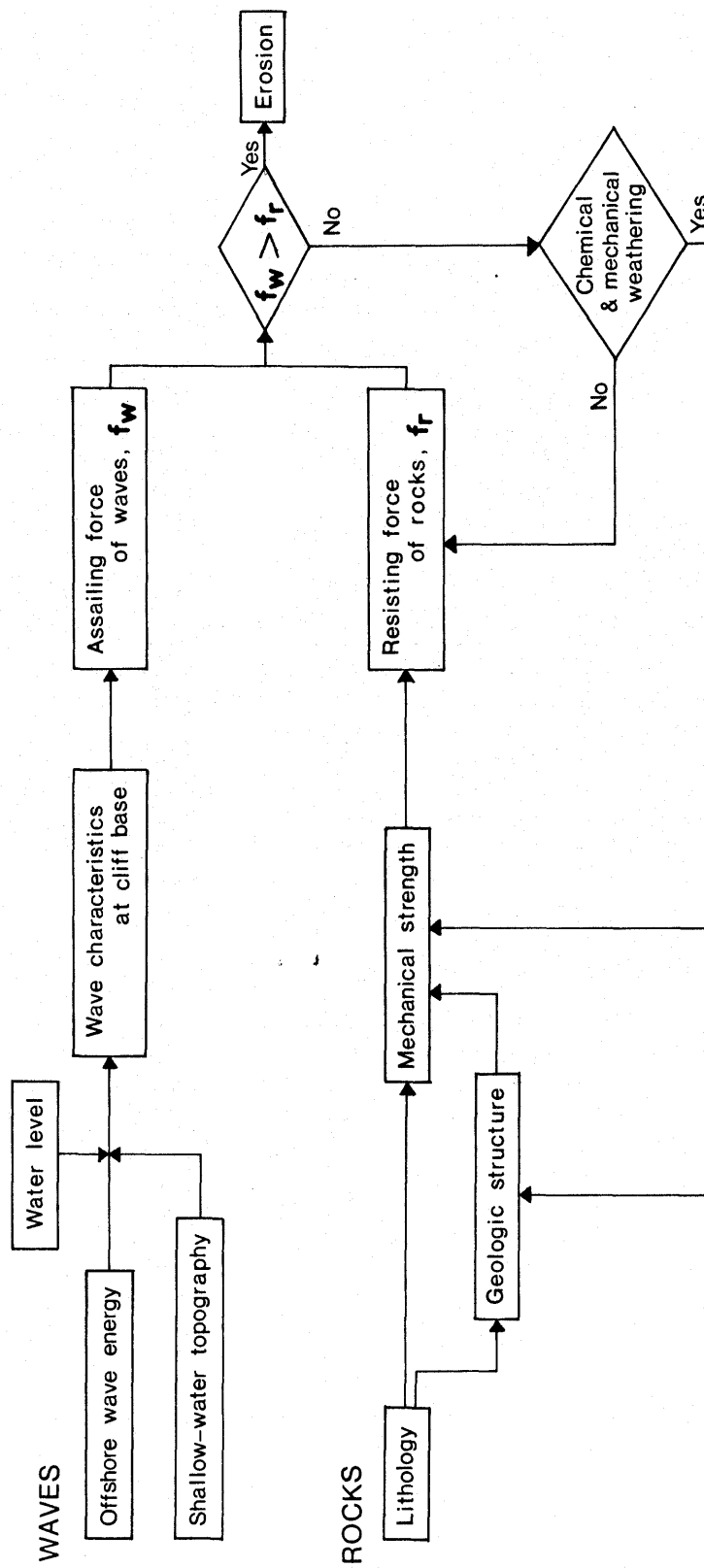


Figure 2. Factors affecting wave induced cliff erosion (simplified after Sunamura, 1983).

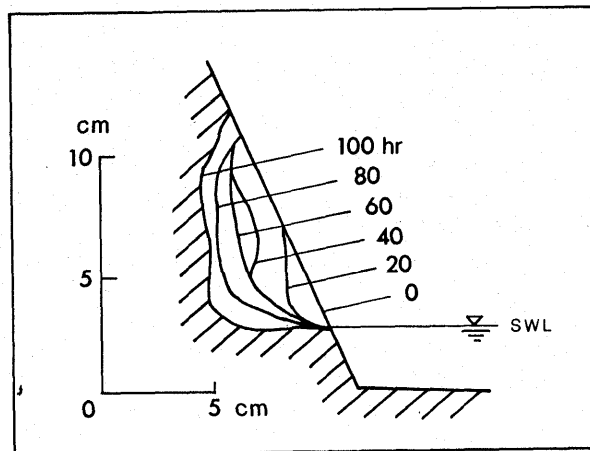


Figure 3. Profile change caused by breaking waves (after Sunamura, 1976).

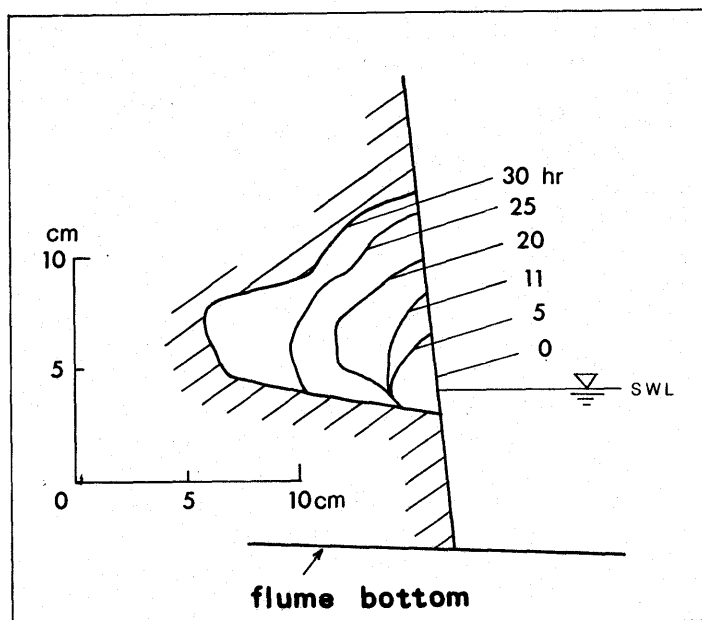


Figure 4. Profile change caused by breaking waves (after Tsujimoto and Sunamura, 1984).

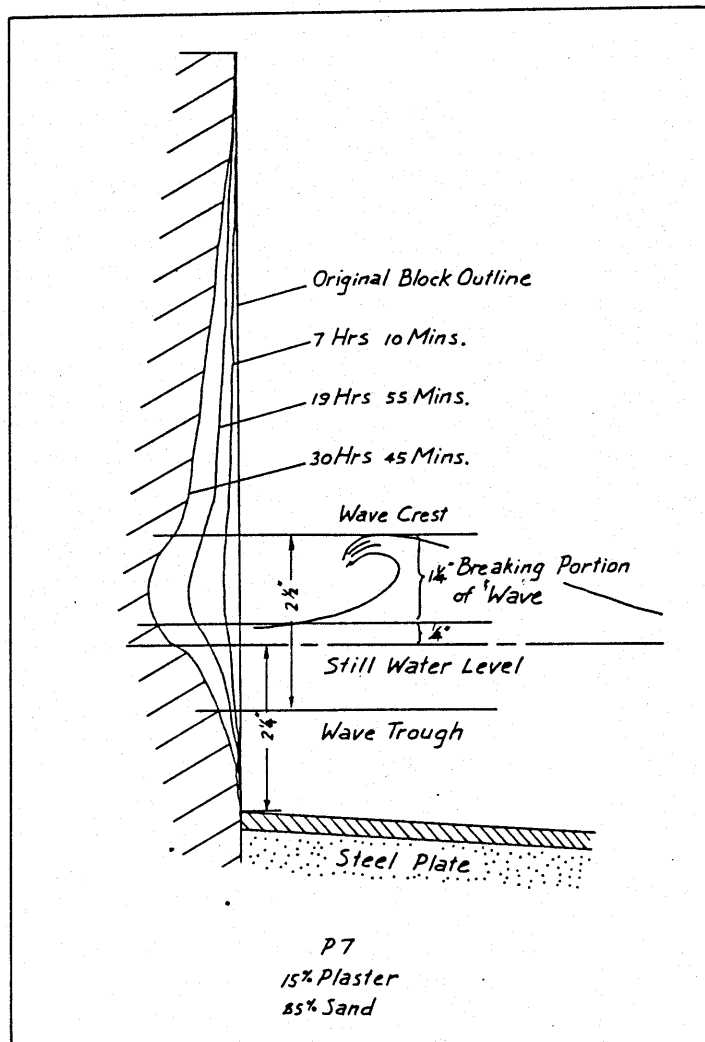


Figure 5. Profile change caused by breaking waves (after Sanders, 1968).

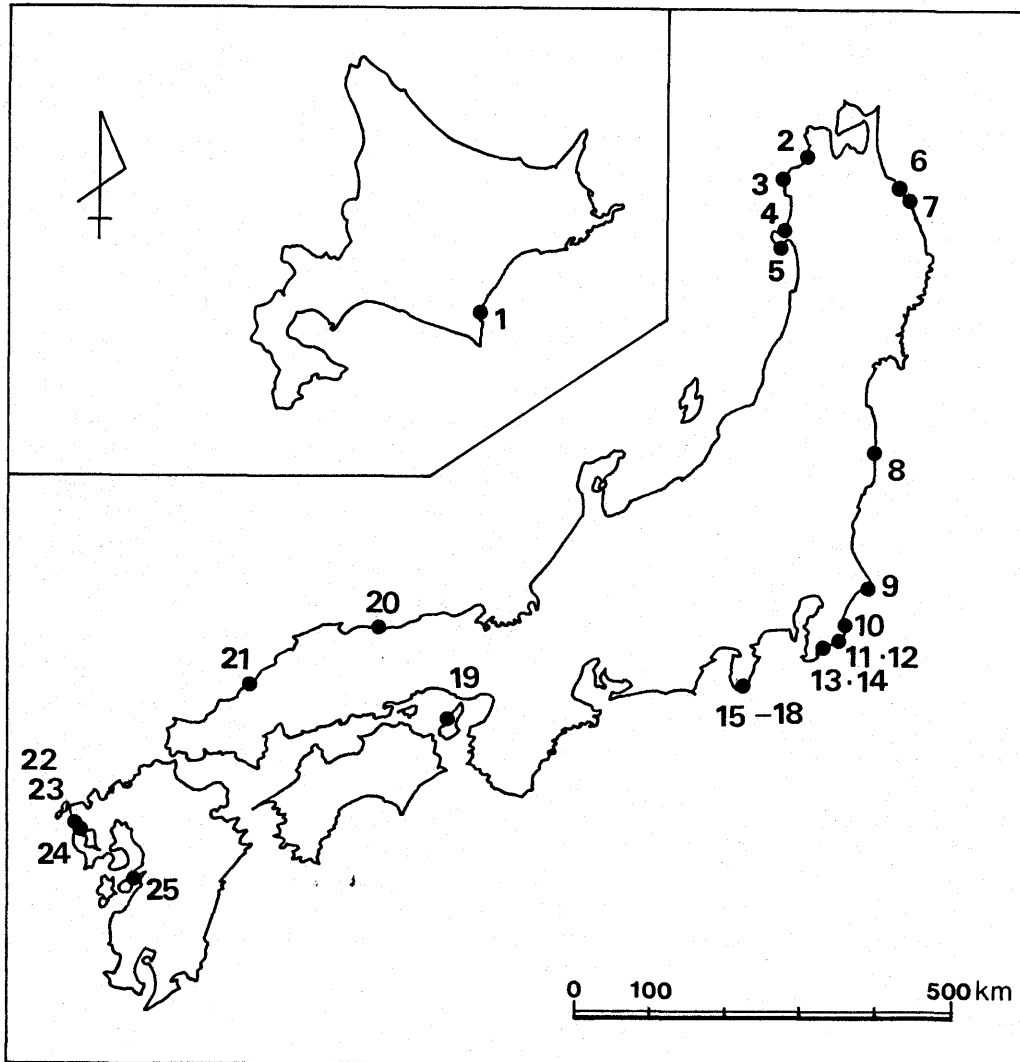
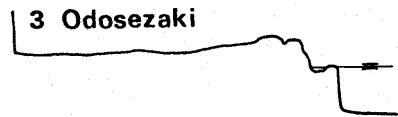
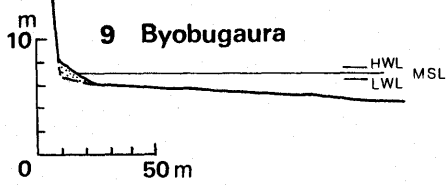


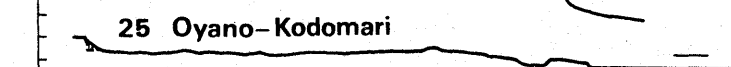
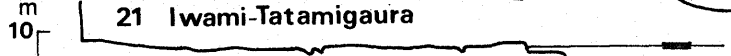
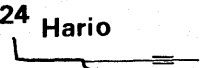
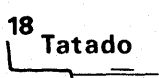
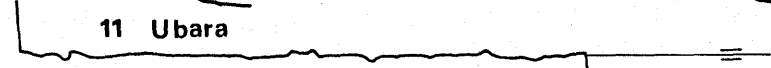
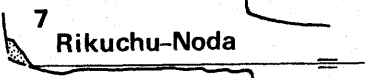
Figure 6. Location of study areas.

- 1 Notsuka, 2 Shichiri-Nagahama, 3 Odosezaki,
 4 Oga-Kitaura, 5 Unosaki, 6 Kuji, 7 Rikuchu-
 Noda, 8 Okuma, 9 Byobugaura, 10 Taito, 11 Ubara,
 12 Kominato, 13 Kamogawa-Bentenjima,
 14 Shinyashiki, 15 Shimoda-Ebisujima, 16 Shimoda-
 Kakizaki, 17 Shimoda-Akanejima, 18 Tatado,
 19 Tsushi-Tsunokawa, 20 Nagao-Bana, 21 Iwami-
 Tatamigaura, 22 Yadakemen, 23 Nagakushimen,
 24 Hario, 25 Oyano-Kodomari.

Type A shore platform



Type B shore platform



No platform

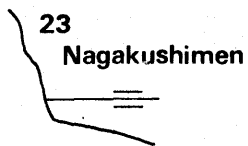
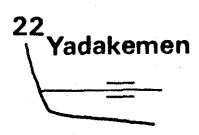
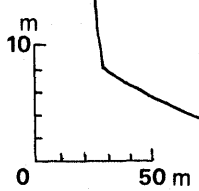
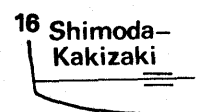
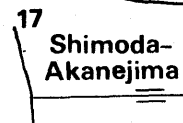
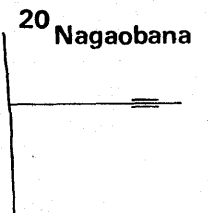
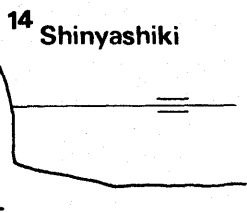
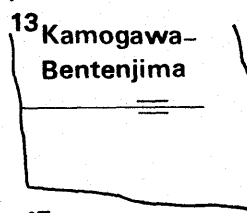


Figure 7. Coastal profiles of each study site.

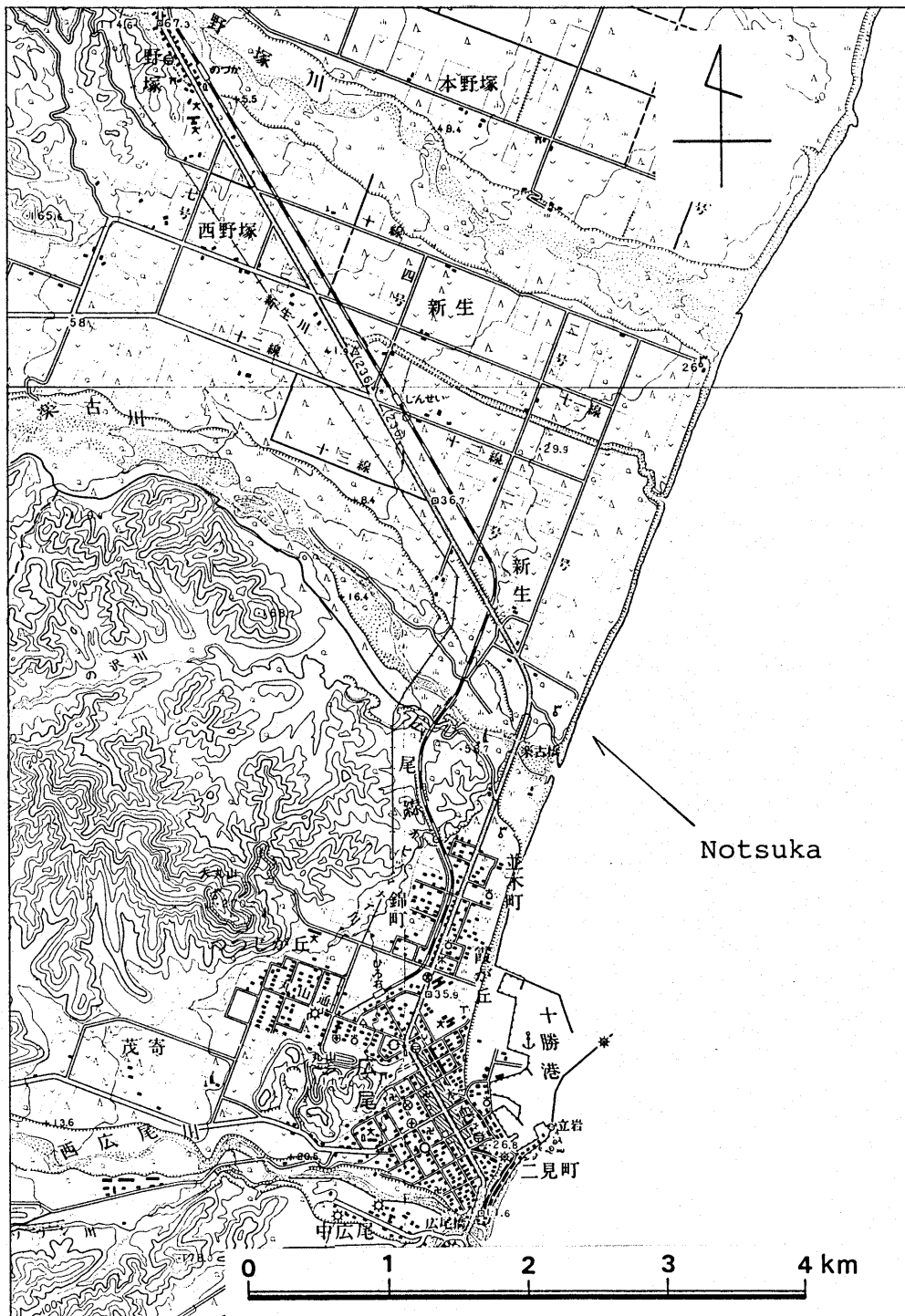


Figure 8. Study site of Notsuka.

Locality map is a part of topographic map published by Geographical Survey Institute of Japan (Hiroo and Taiki, with 1/50000 scale).

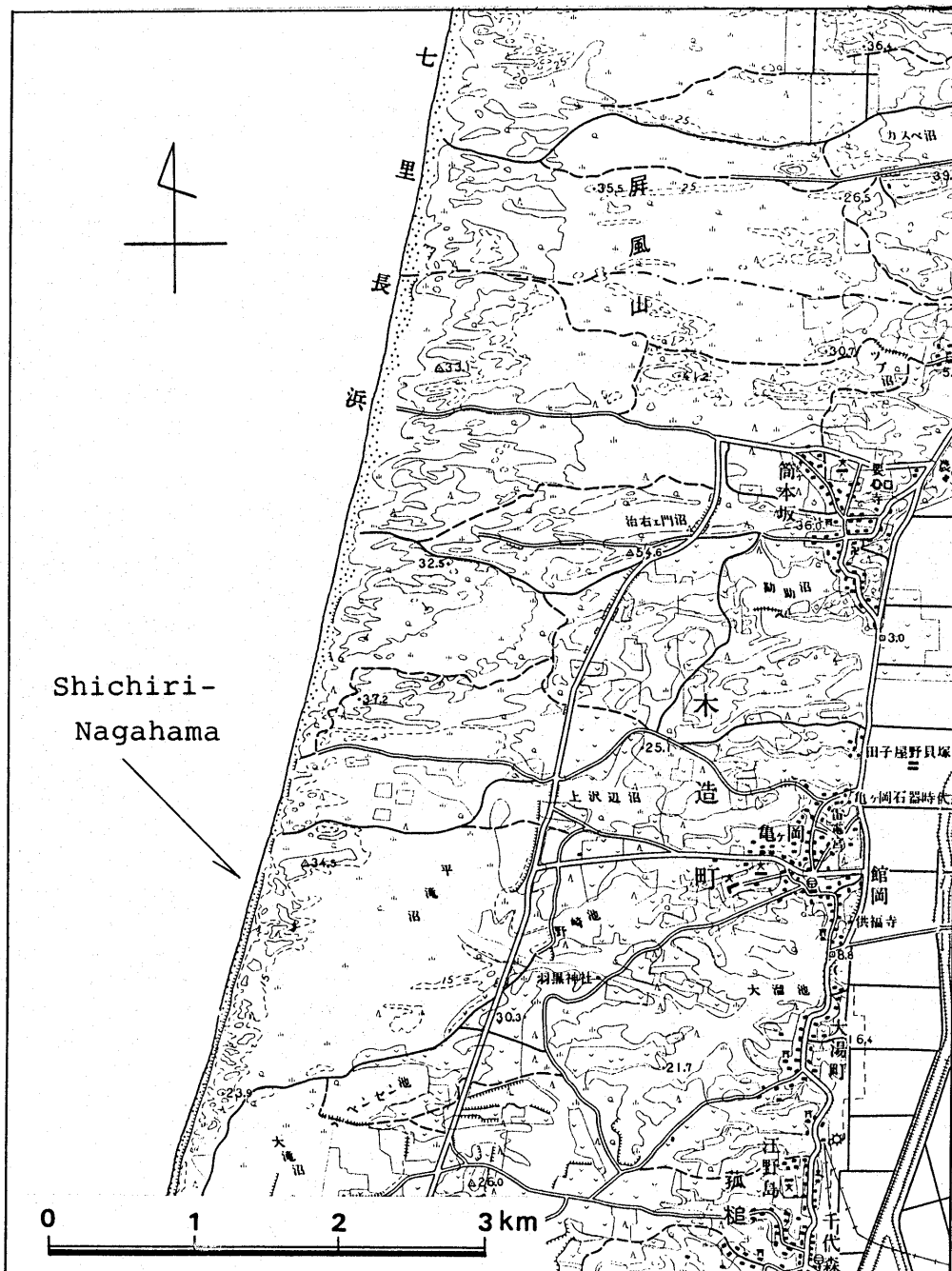


Figure 9. Study site of Shichiri-Nagahama.

Locality map is a part of topographic map published by Geographical Survey Institute of Japan (Kanagi, with 1/50,000 scale).

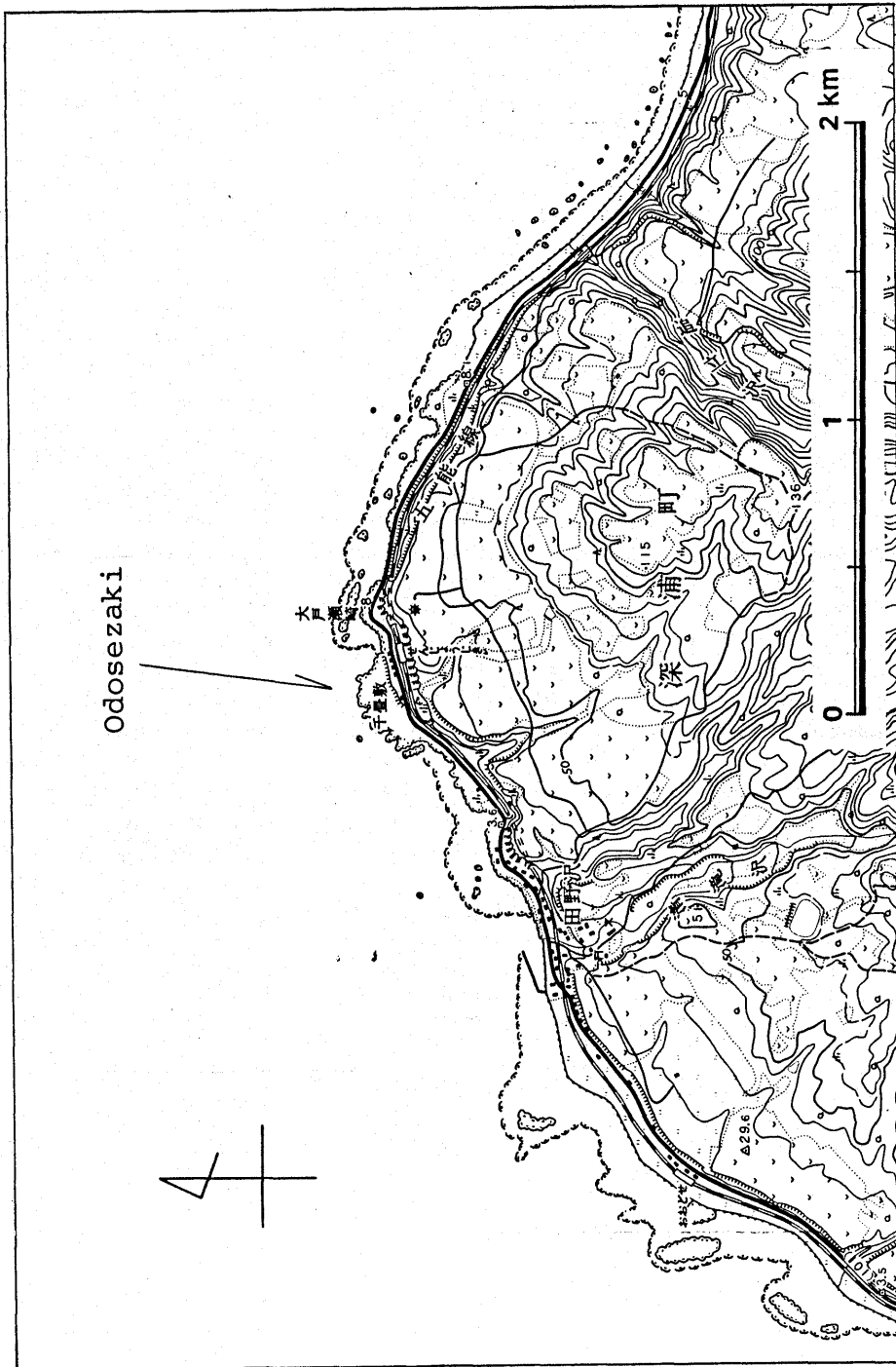


Figure 10. Study site of Odosezaki.

Locality map is a part of topographic map published by Geographical Survey Institute of Japan (Tanozawa, with 1/25,000 scale).

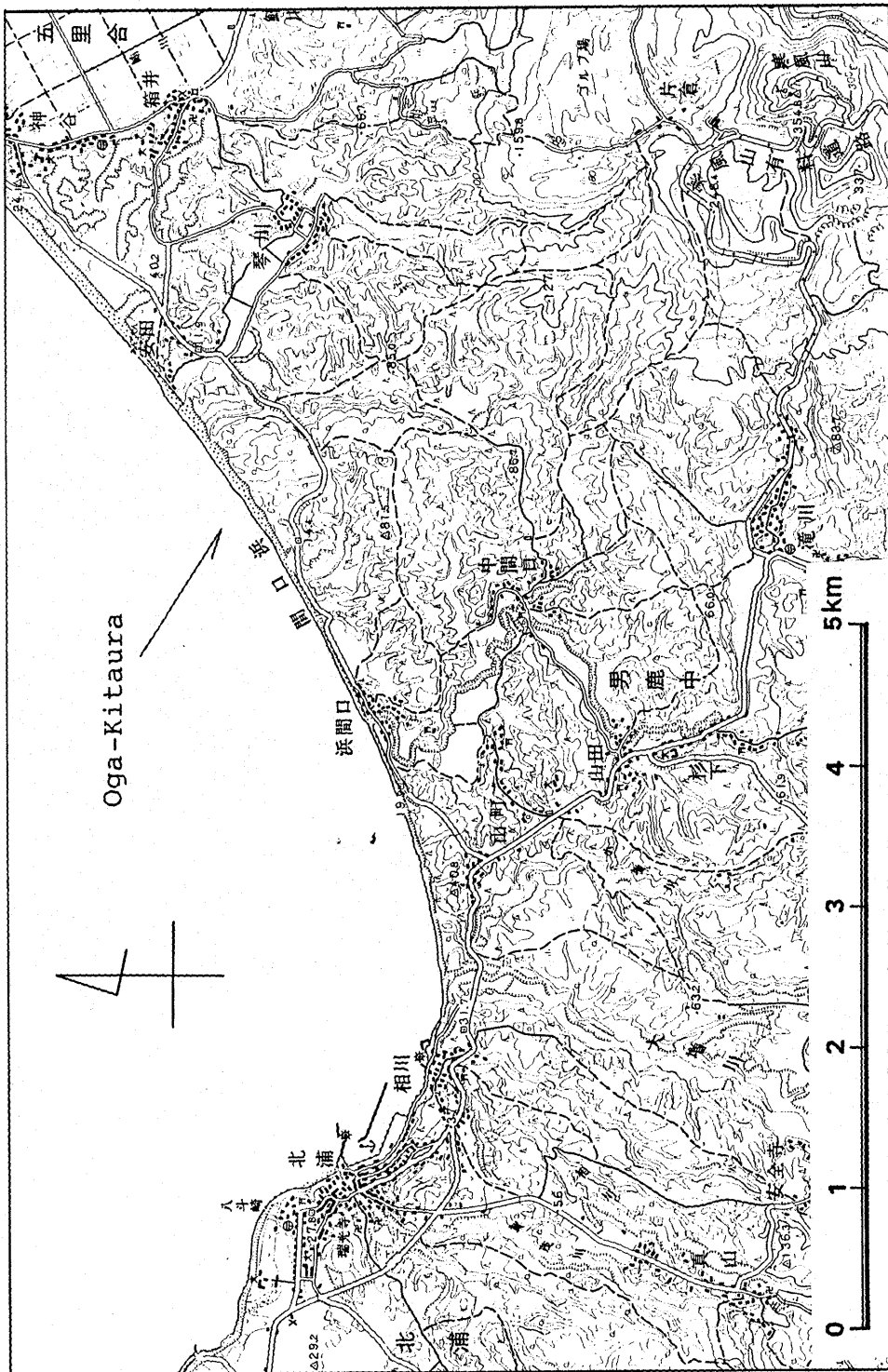


Figure 11. Study site of Oga-Kिताura.

Locality map is a part of topographic map published by Geographical Survey Institute of Japan (Funakawa, with 1/50,000 scale).

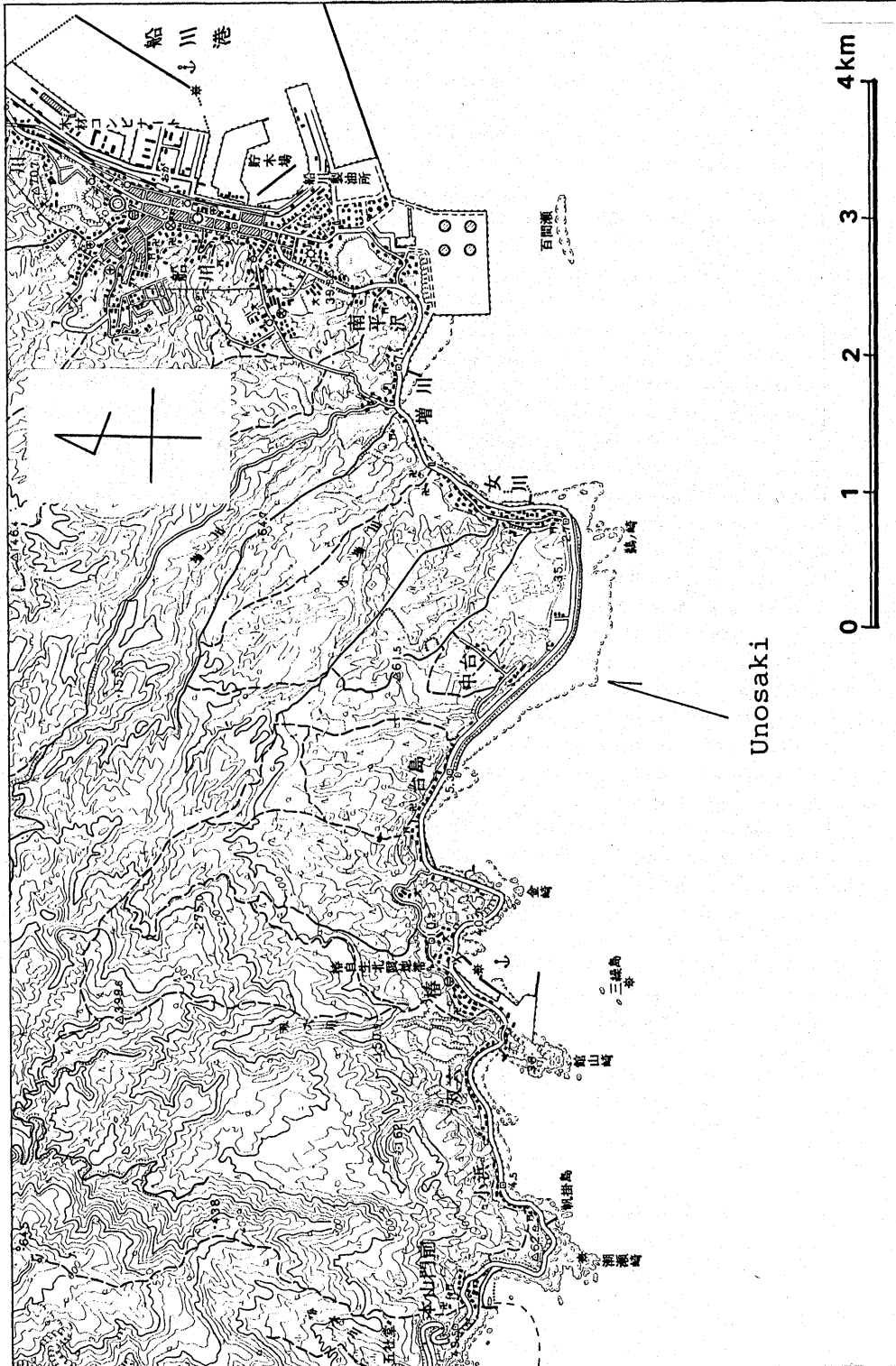


Figure 12. Study site of Unosaki.

Locality map is a part of topographic map published by Geographical Survey Institute of Japan (Funakawa, with 1/50,000 scale).

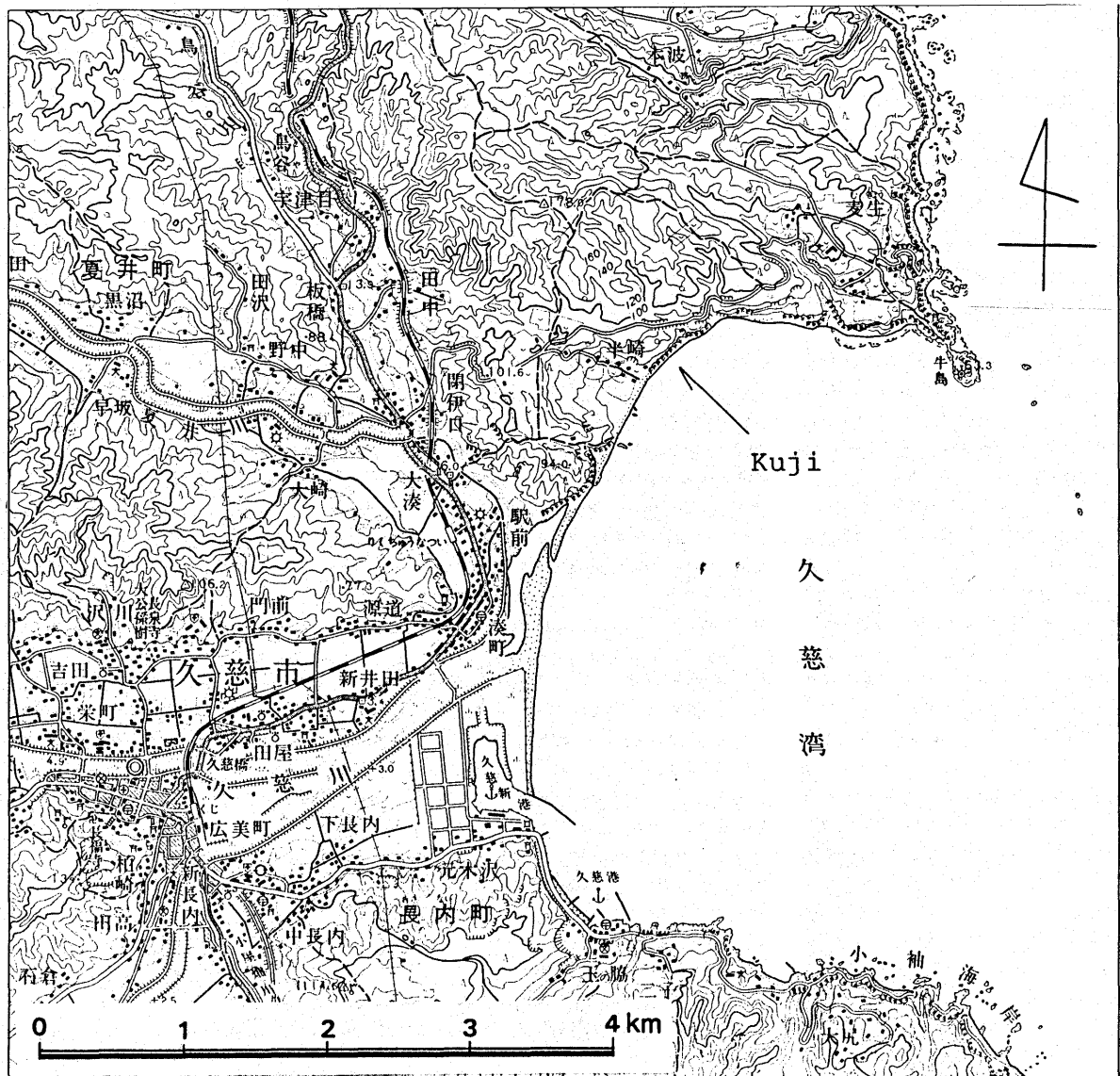


Figure 13. Study site of Kuji.

Locality map is a part of topographic map published by Geographical Survey Institute of Japan (Kuji, with 1/50,000 scale).

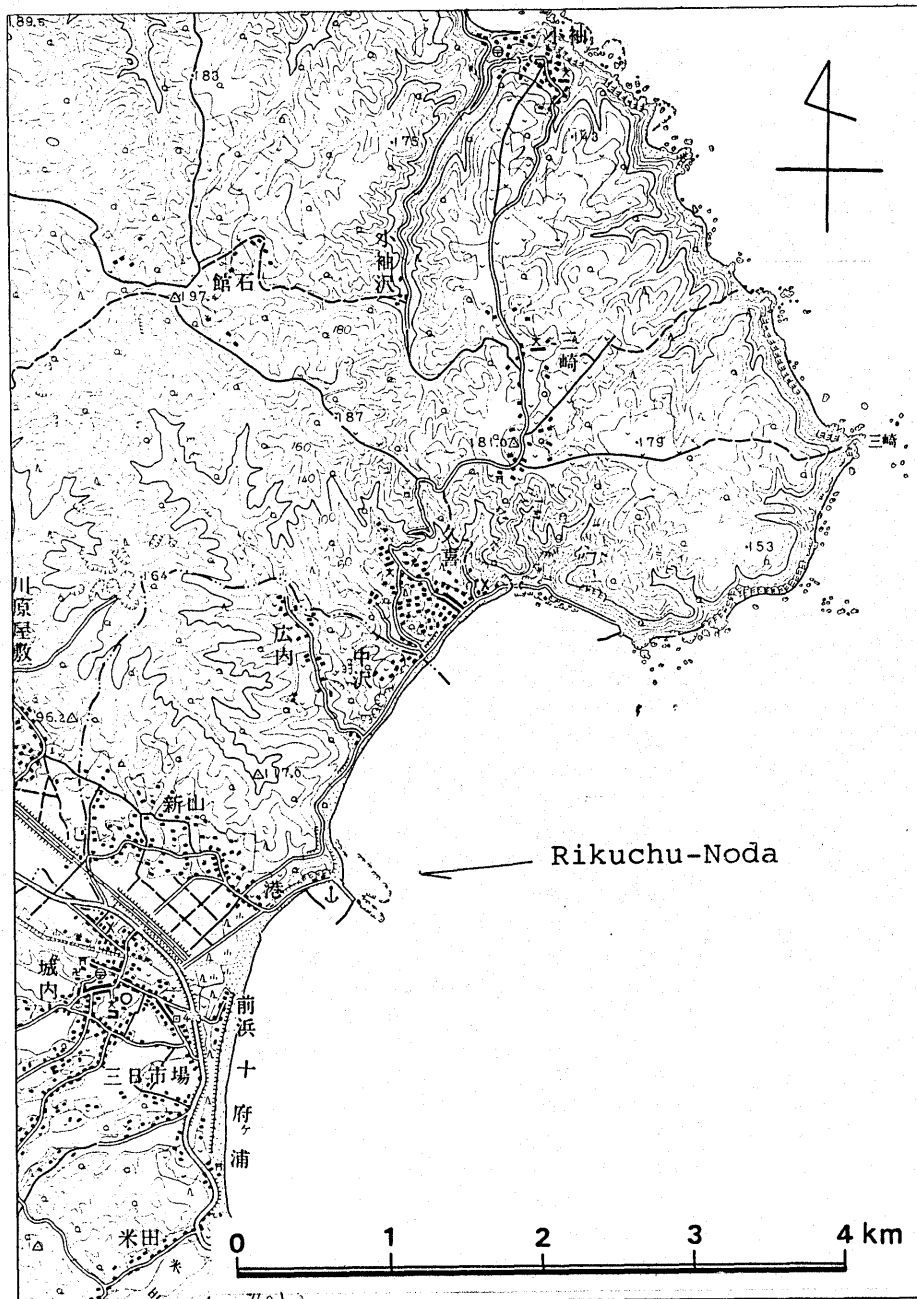


Figure 14. Study site of Rikuchū-Noda.

Locality map is a part of topographic map published by Geographical Survey Institute of Japan (Rikuchū-Noda, with 1/50,000 scale).

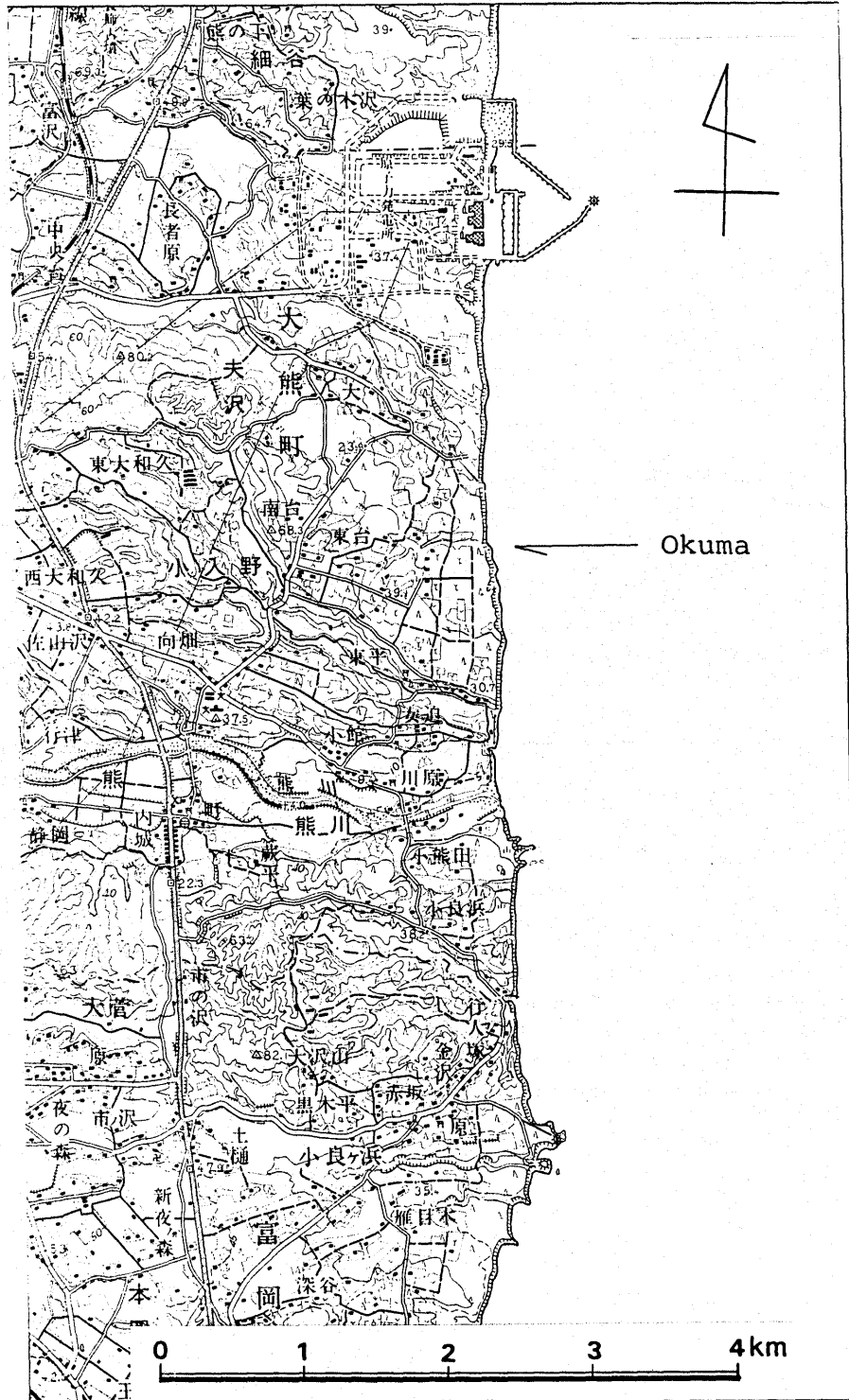


Figure 15. Study site of Okuma.

Locality map is a part of topographic map published by Geographical Survey Institute of Japan (Iwaki-Tomikawa, with 1/50,000 scale).

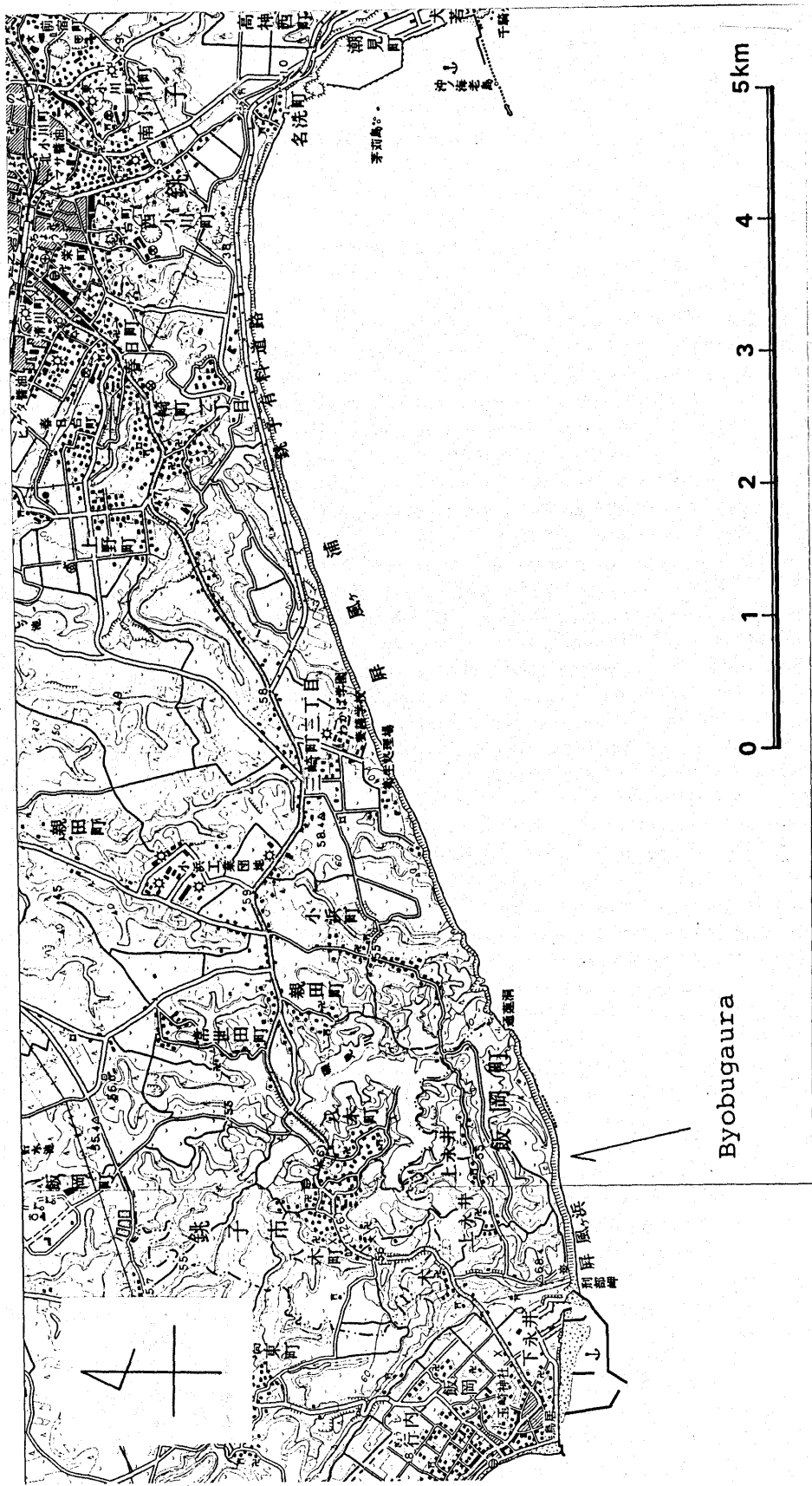


Figure 16. Study site of Byobugaura.

Locality map is a part of topographic map published by Geographical Survey Institute of Japan (Yoka-Ichiba and Choshi, with 1/50,000 scale).

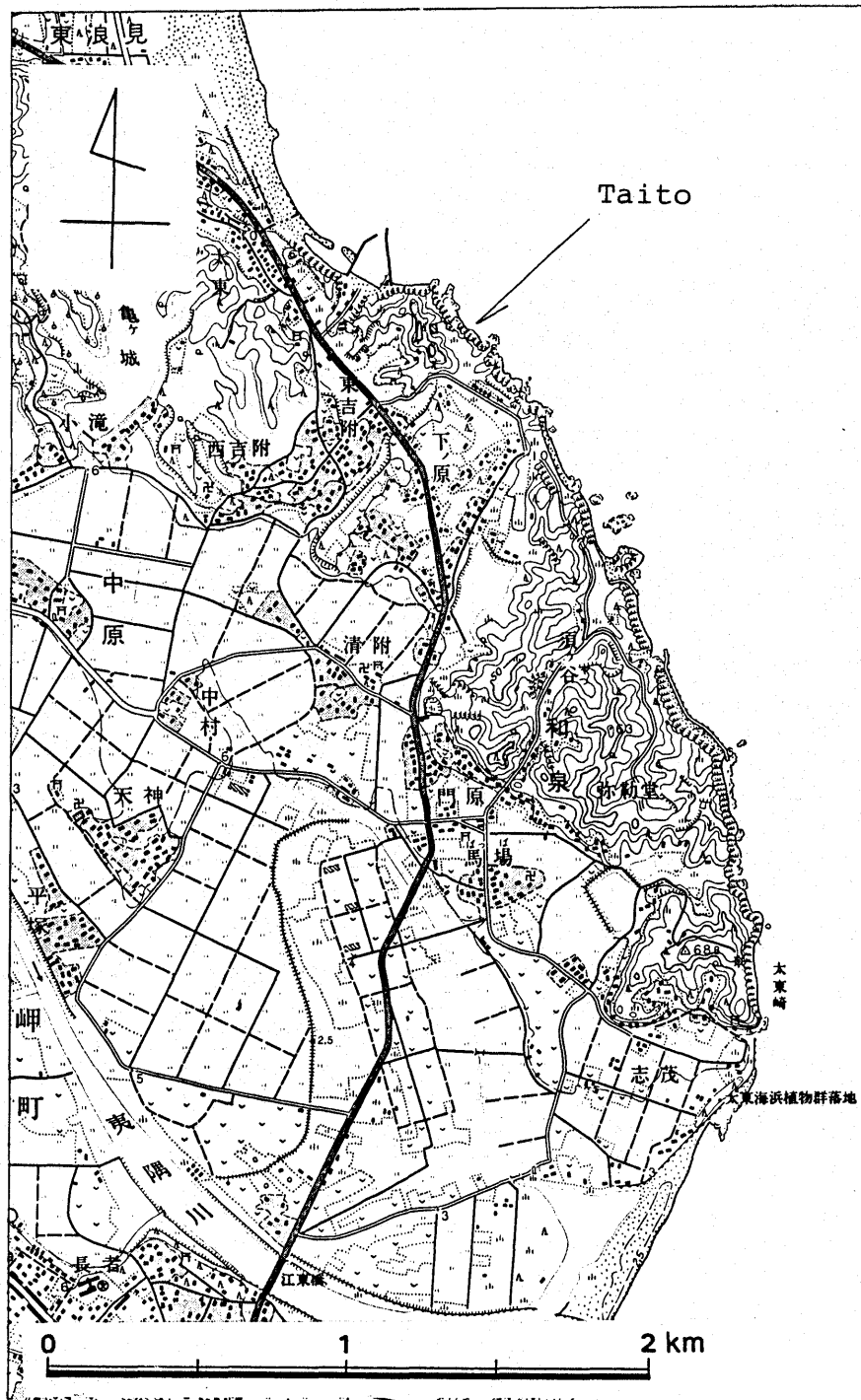


Figure 17. Study site of Taito.

Locality map is a part of topographic map published by Geographical Survey Institute of Japan (Kazusa-choja, with 1/25,000 scale).

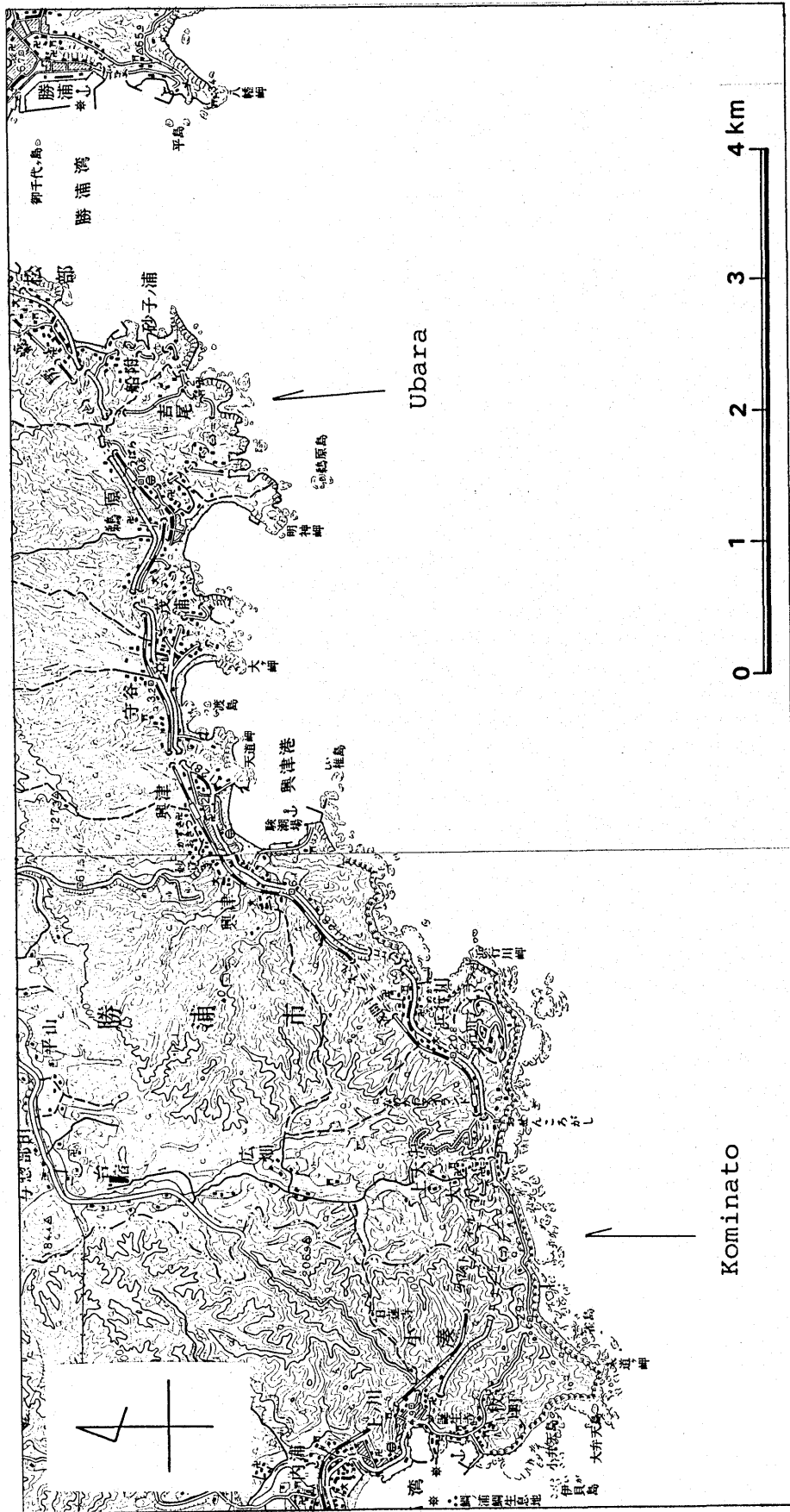


Figure 18. Study sites of Ubara and Kominato.

Locality map is a part of topographic map published by Geographical Survey Institute of Japan (Katsuura and Kamogawa, with 1/50,000 scale).

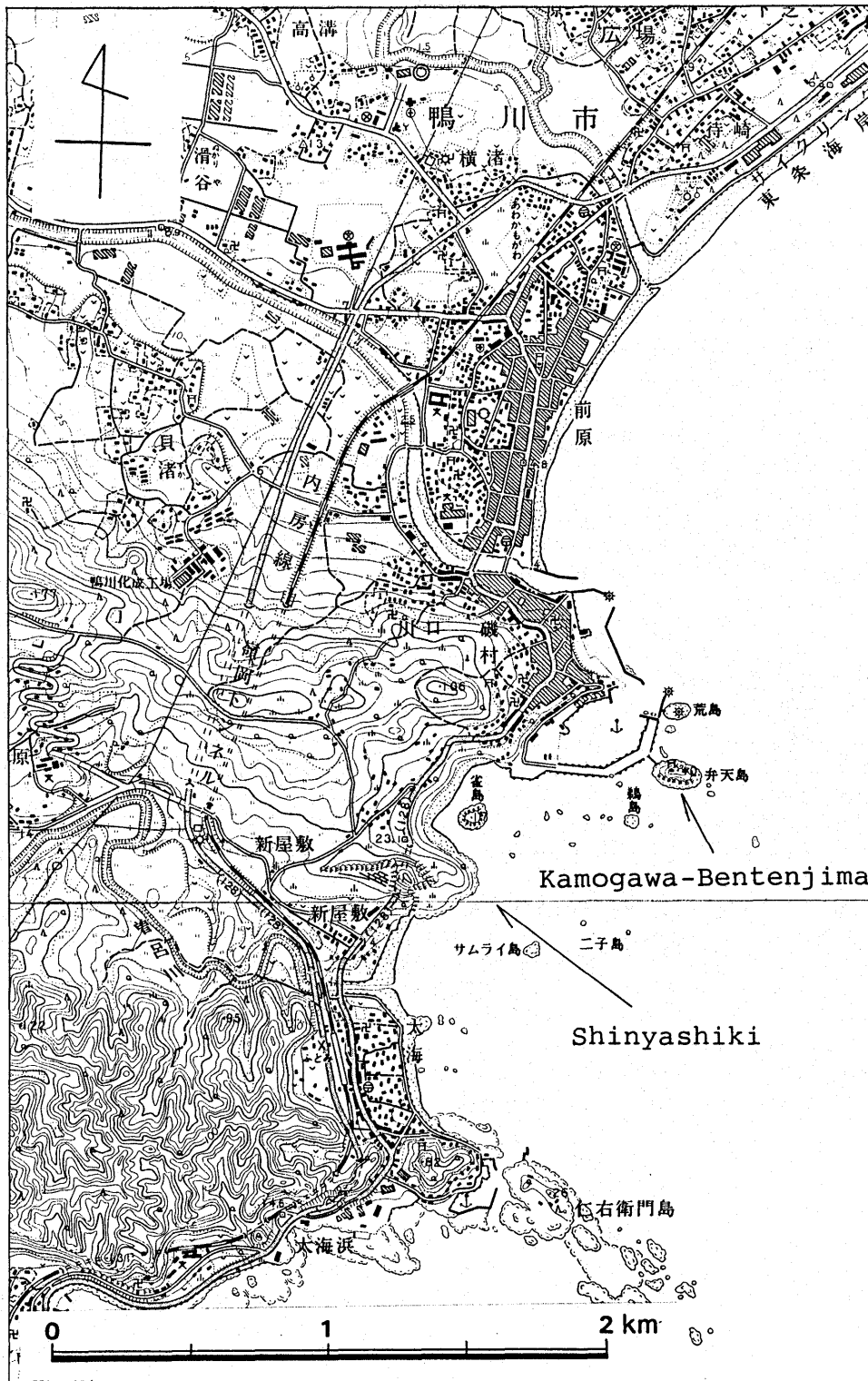


Figure 19. Study sites of Kamogawa-Bentenjima and Shinyashiki.

Locality map is a part of topographic map published by Geographical Survey Institute of Japan (Kamogawa and Awa-Furukawa, with 1/25,000 scale).

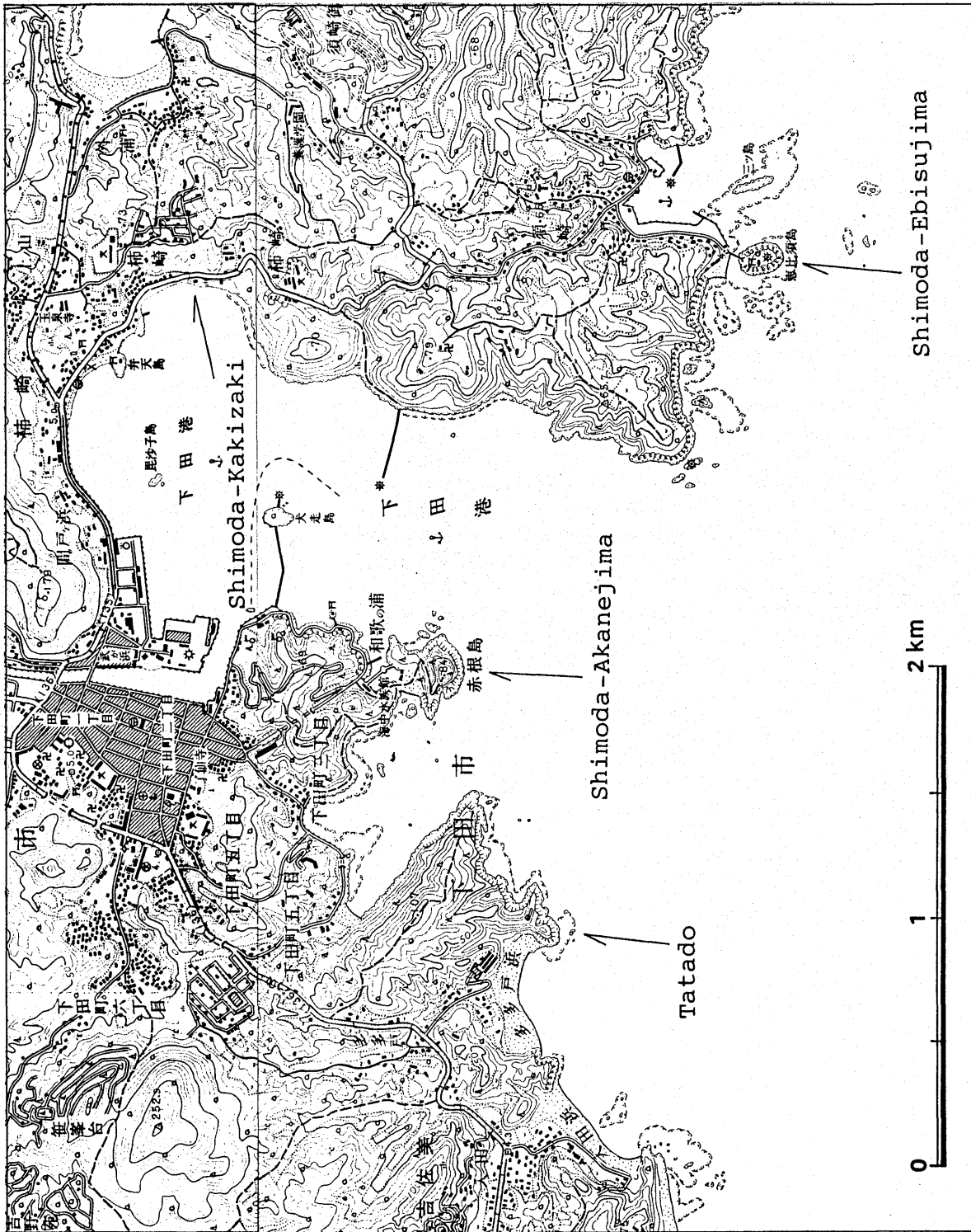


Figure 20. Study sites of Shimoda-Ebisujima, Kakizaki, Akanejima, and Tatado.

Locality map is a part of topographic map published by Geographical Survey Institute of Japan (Shimoda and Mikomotojima, with 1/25,000 scale)

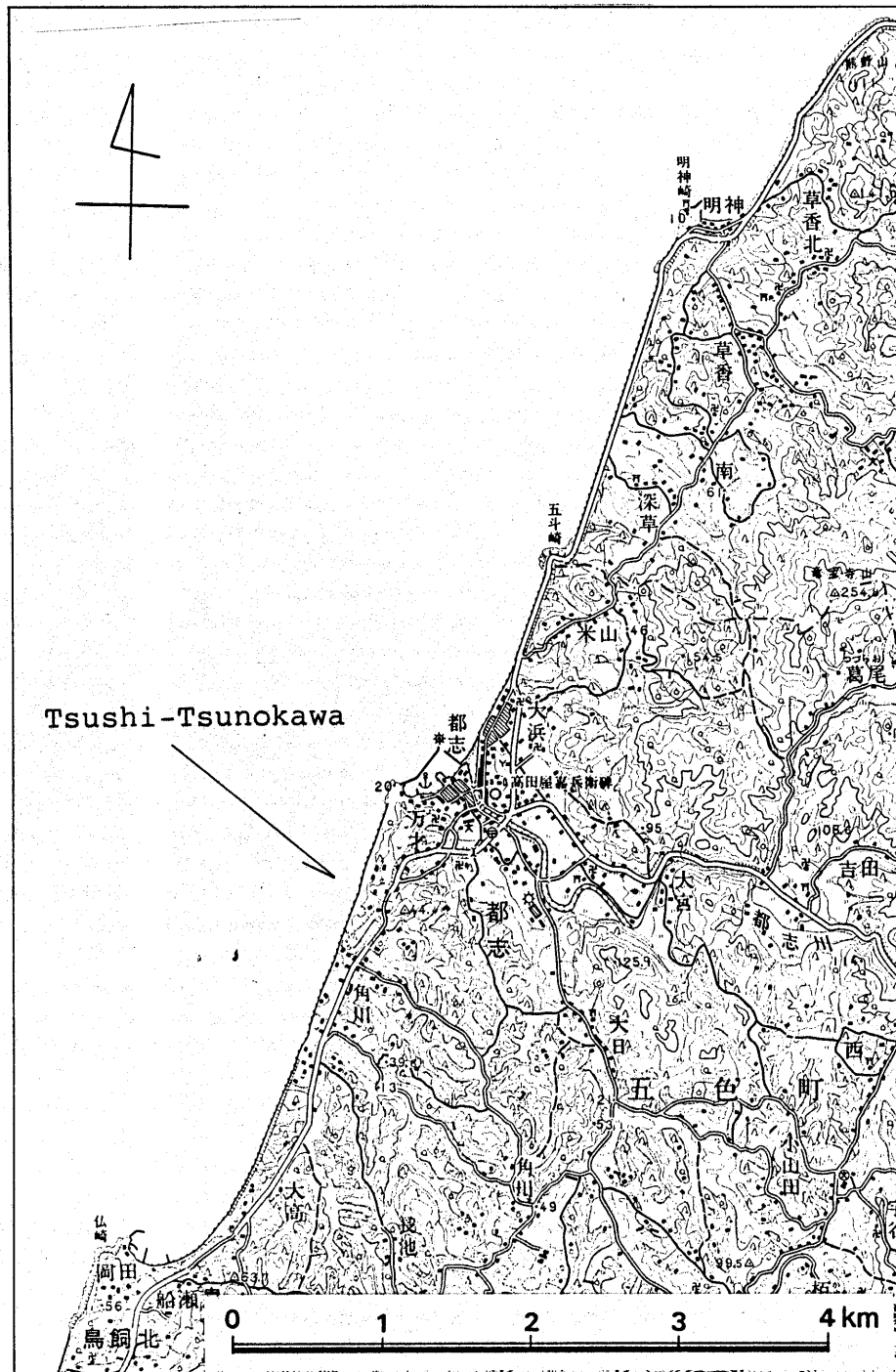


Figure 21. Study site of Tsushi-Tsunokawa.

Locality map is a part of topographic map published by Geographical Survey Institute of Japan (Sumoto, with 1/50,000 scale).

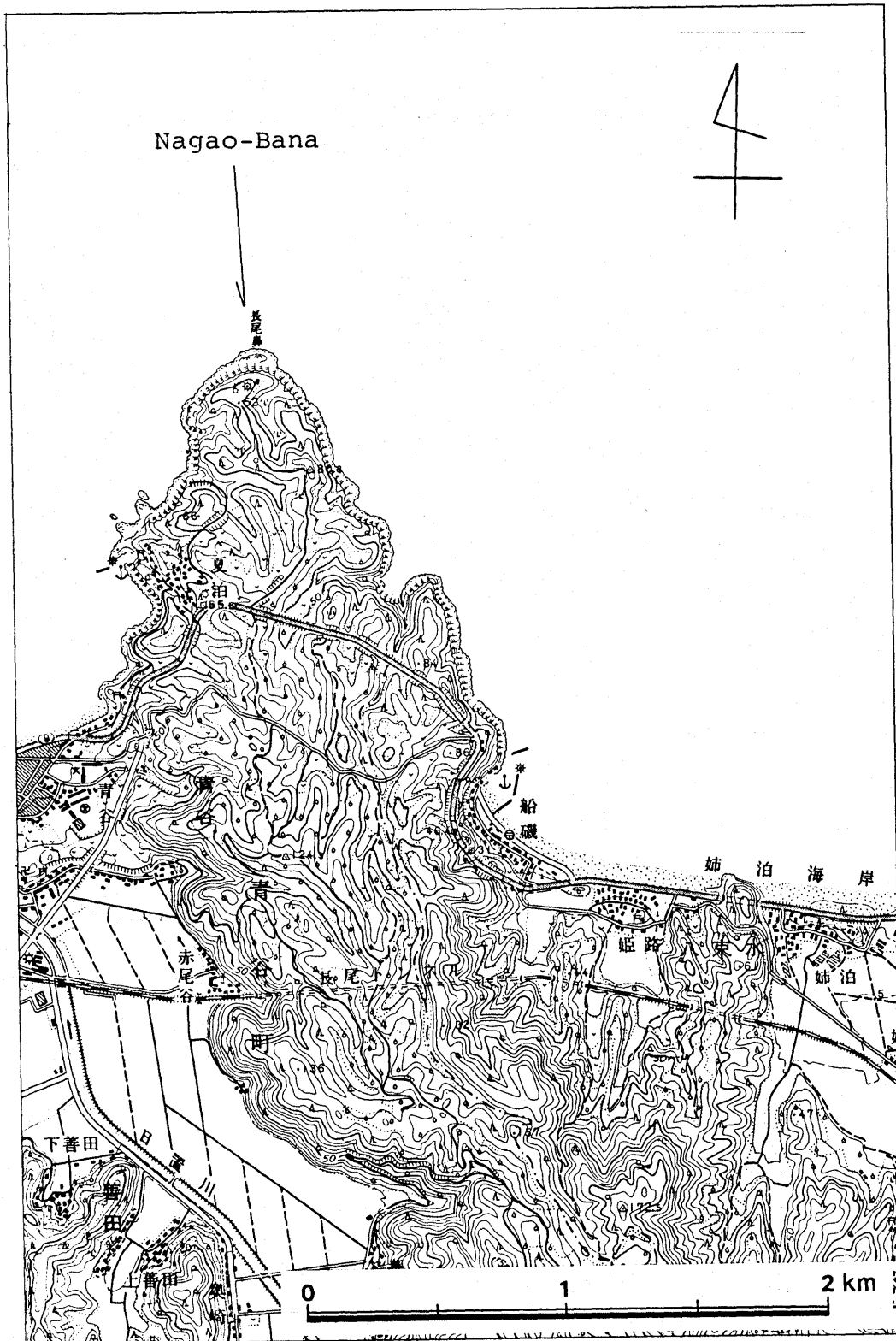


Figure 22. Study site of Nagao-Bana.

Locality map is a part of topographic map published by Geographical Survey Institute of Japan (Hamamura, with 25,000 scale).

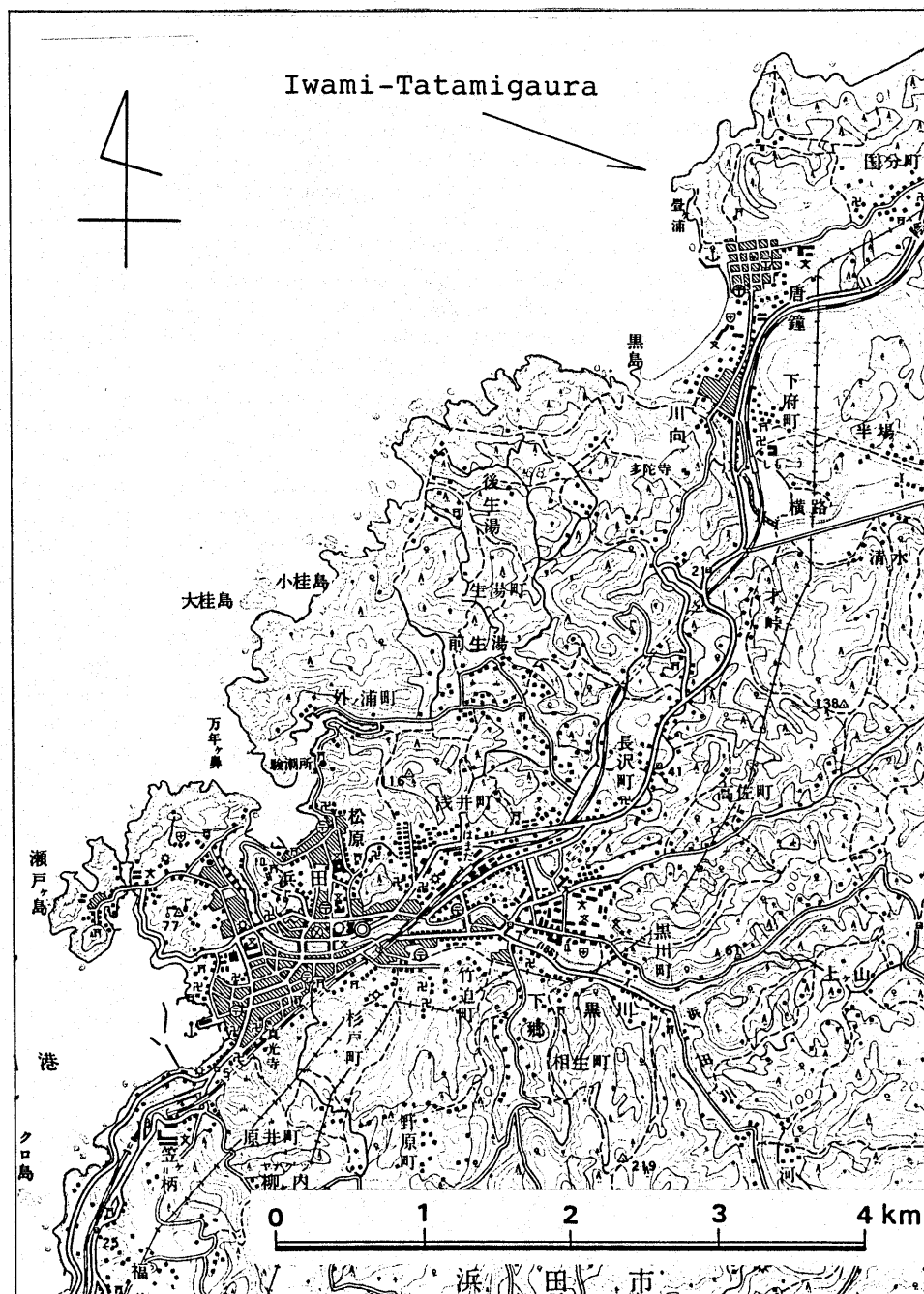


Figure 23. Study site of Iwami-Tatamigaura.

Locality map is a part of topographic map published by Geographical Survey Institute of Japan (Hamada, with 1/50,000 scale).

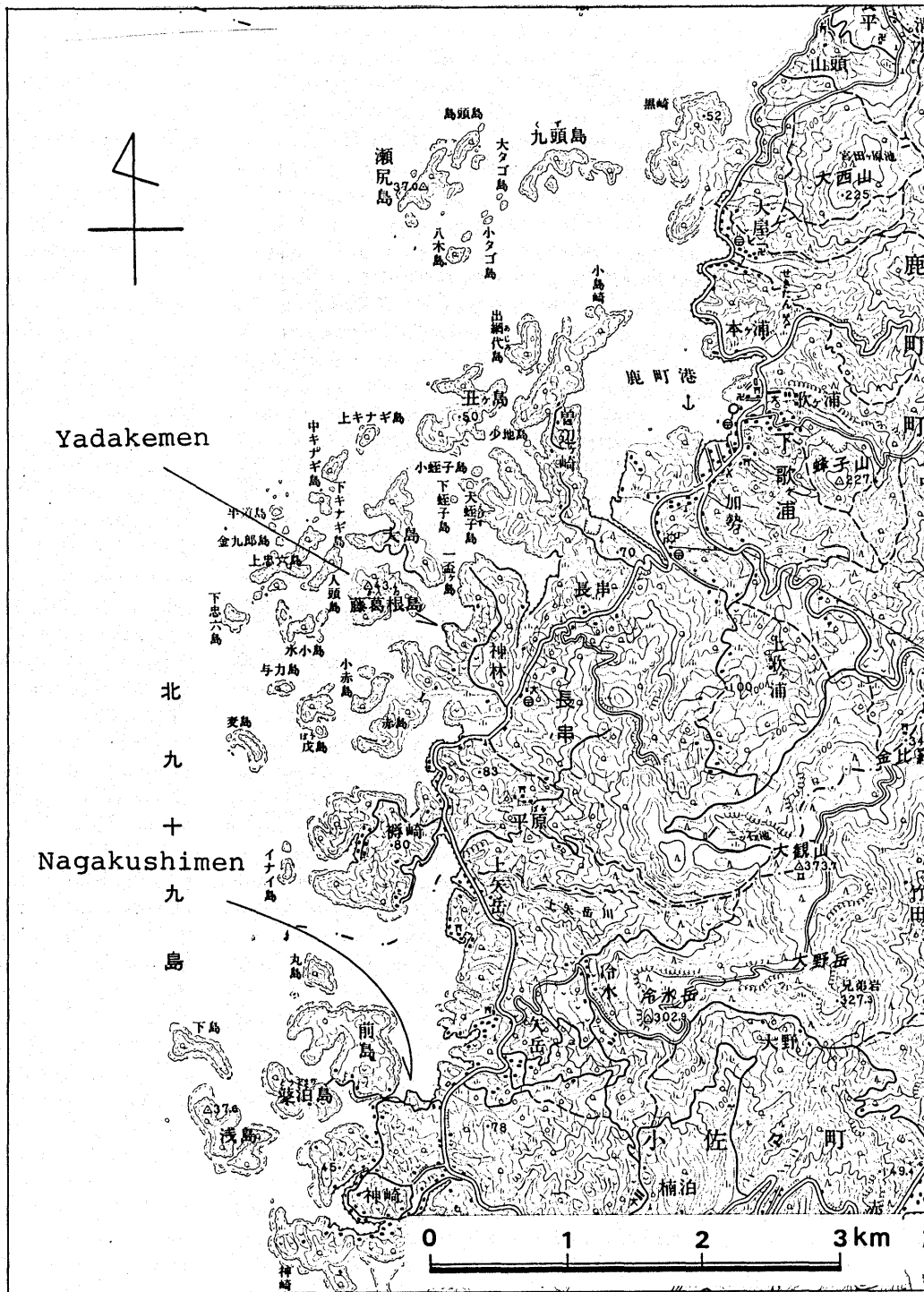


Figure 24. Study sites of Yadakemen and Nagakushimen.

Locality map is a part of topographic map published by Geographical Survey Institute of Japan (Sasebo, with 1/50,000 scale).

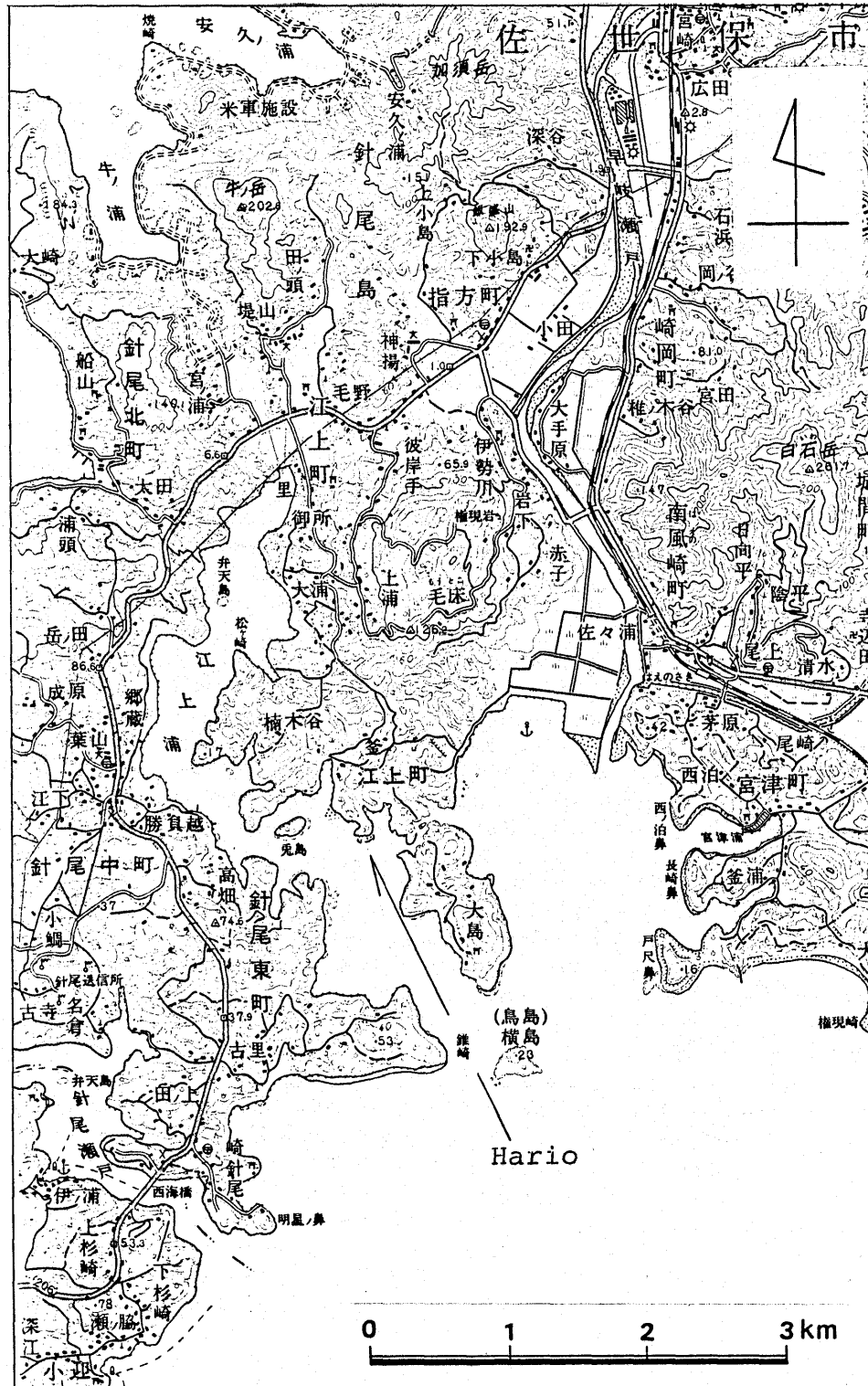


Figure 25. Study site of Hario.

Locality map is a part of topographic map published by Geographical Survey Institute of Japan (Haiki, with 1/50,000 scale).

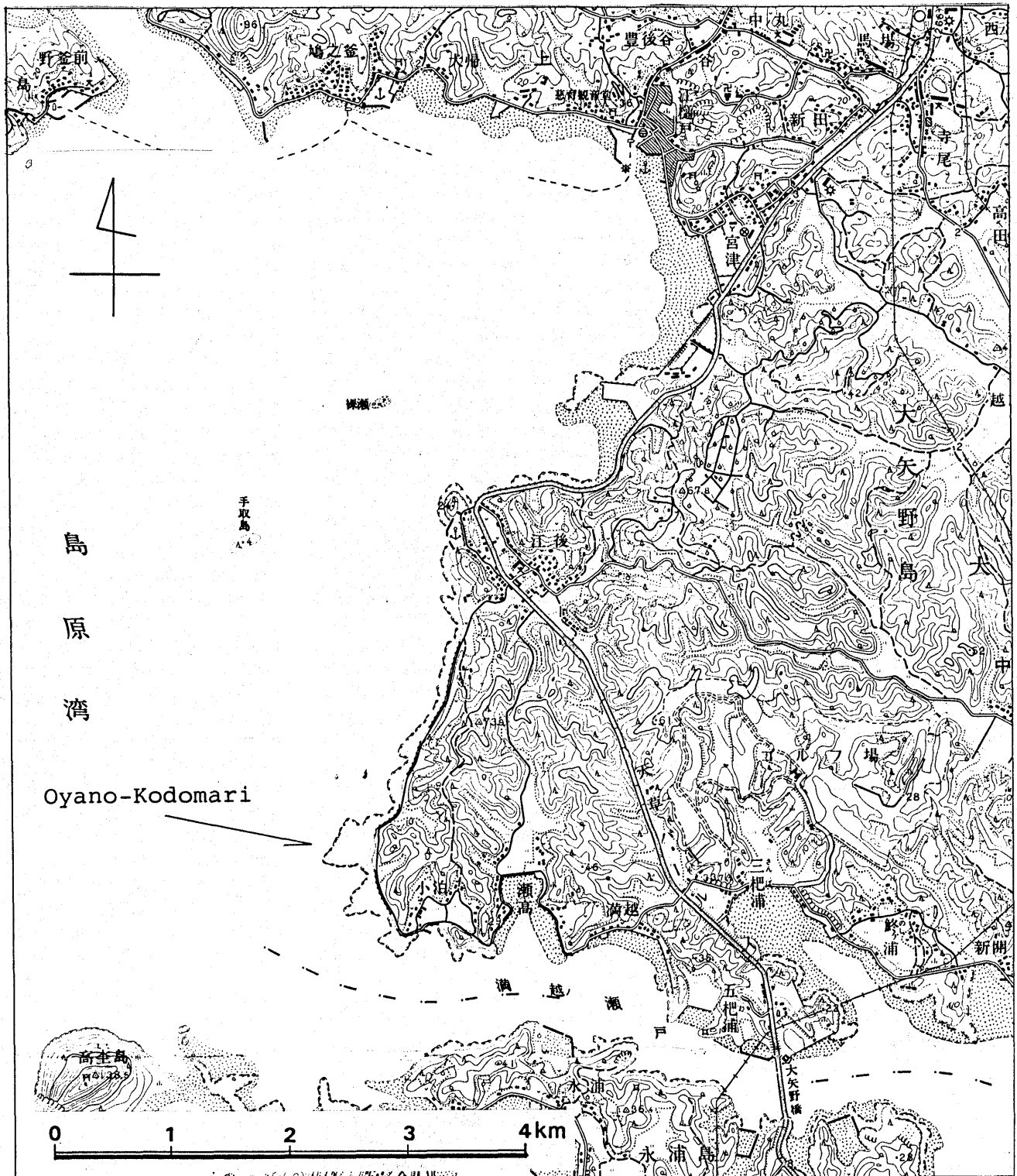


Figure 26. Study site of Oyano-Kodomari.

Locality map is a part of topographic map published by Geographical Survey Institute of Japan (Amakusa-Matsushima, with 1/25,000 scale).

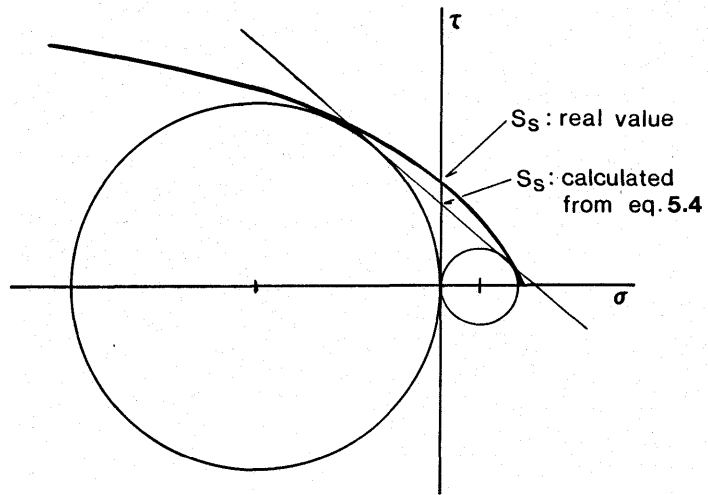


Figure 27. Definition of shear strength (after Yamaguchi and Nishimatsu, 1977). Real Mohr's envelope is plotted by a bold line and envelope assumed in equation (5.4) is plotted by a thin straight line.

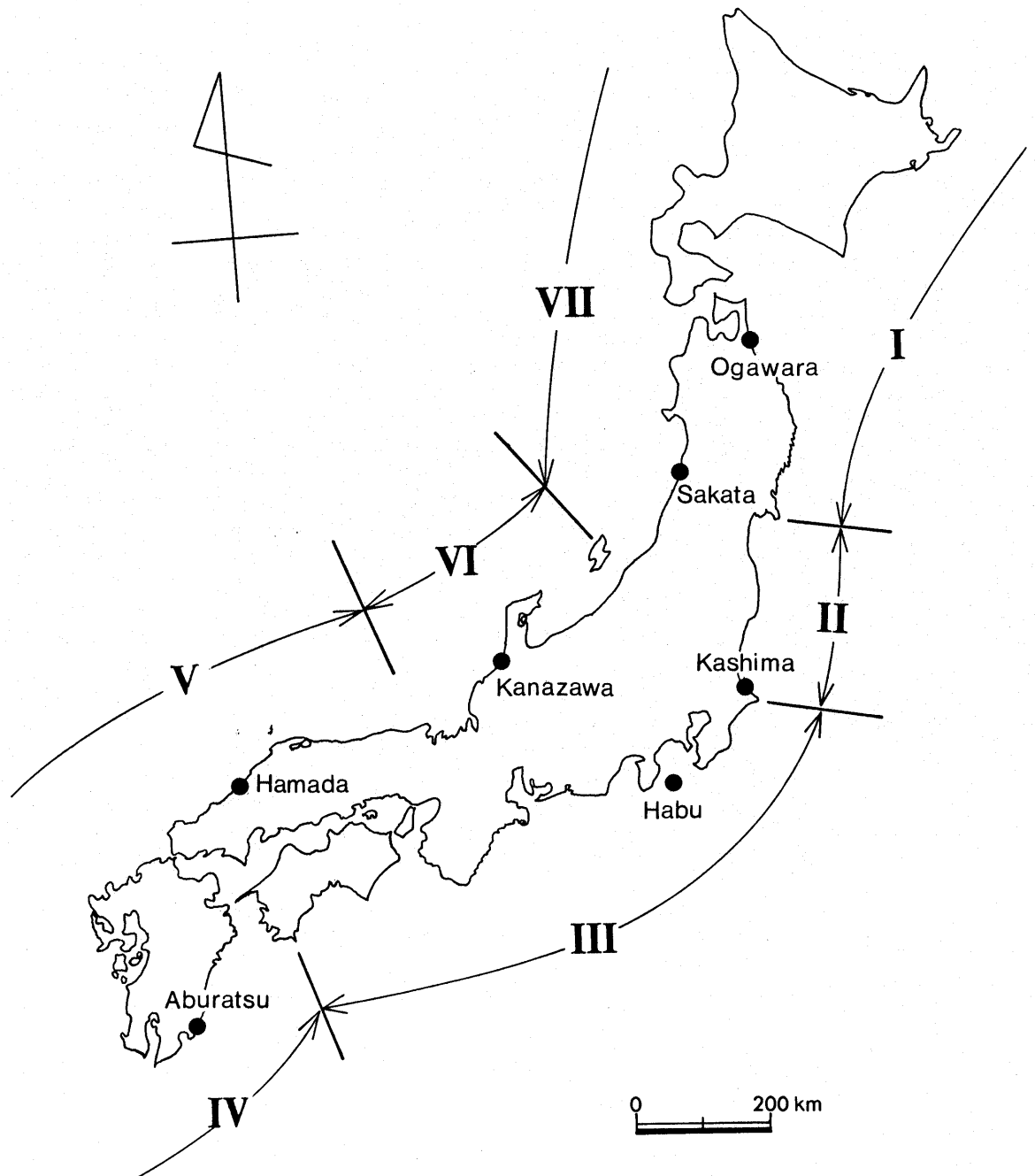


Figure 28. Seven coastal areas and representative stations.

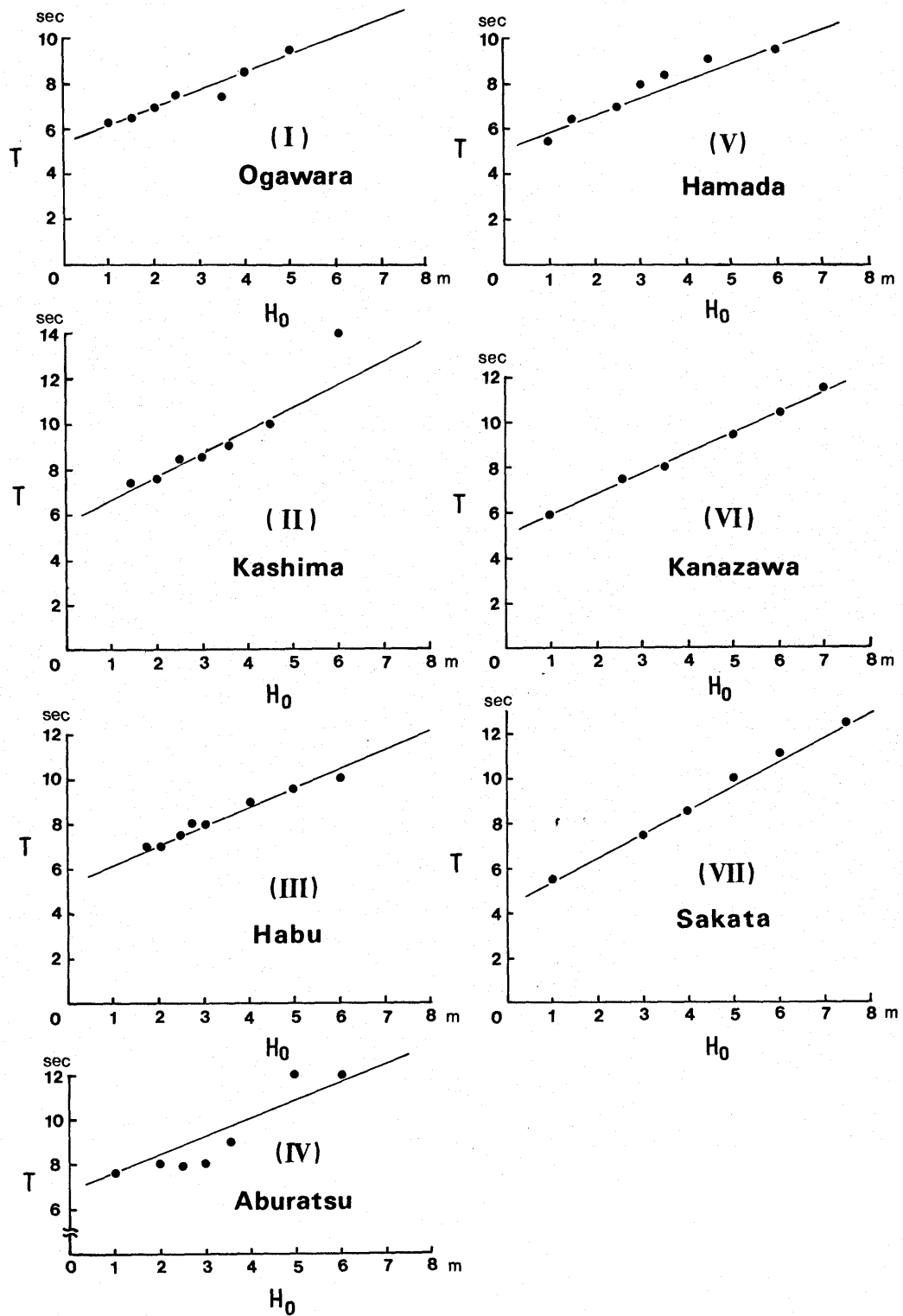


Figure 29. Wave climate (1): relationship between deep water wave height, H_0 , and wave period, T (after Tanaka, 1980).

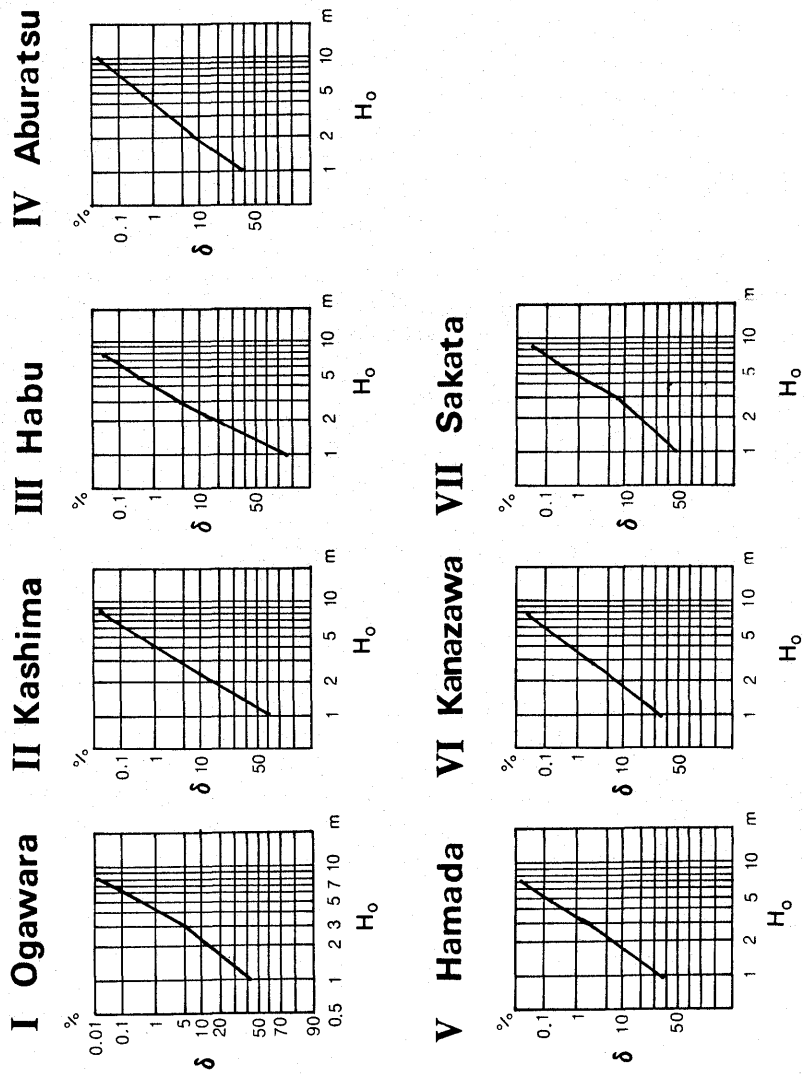


Figure 30. Wave climate (2): occurrence frequency of wave height (after Tanaka, 1980). δ means the occurrence frequency of waves which are larger than H_0 in deep-water wave height.

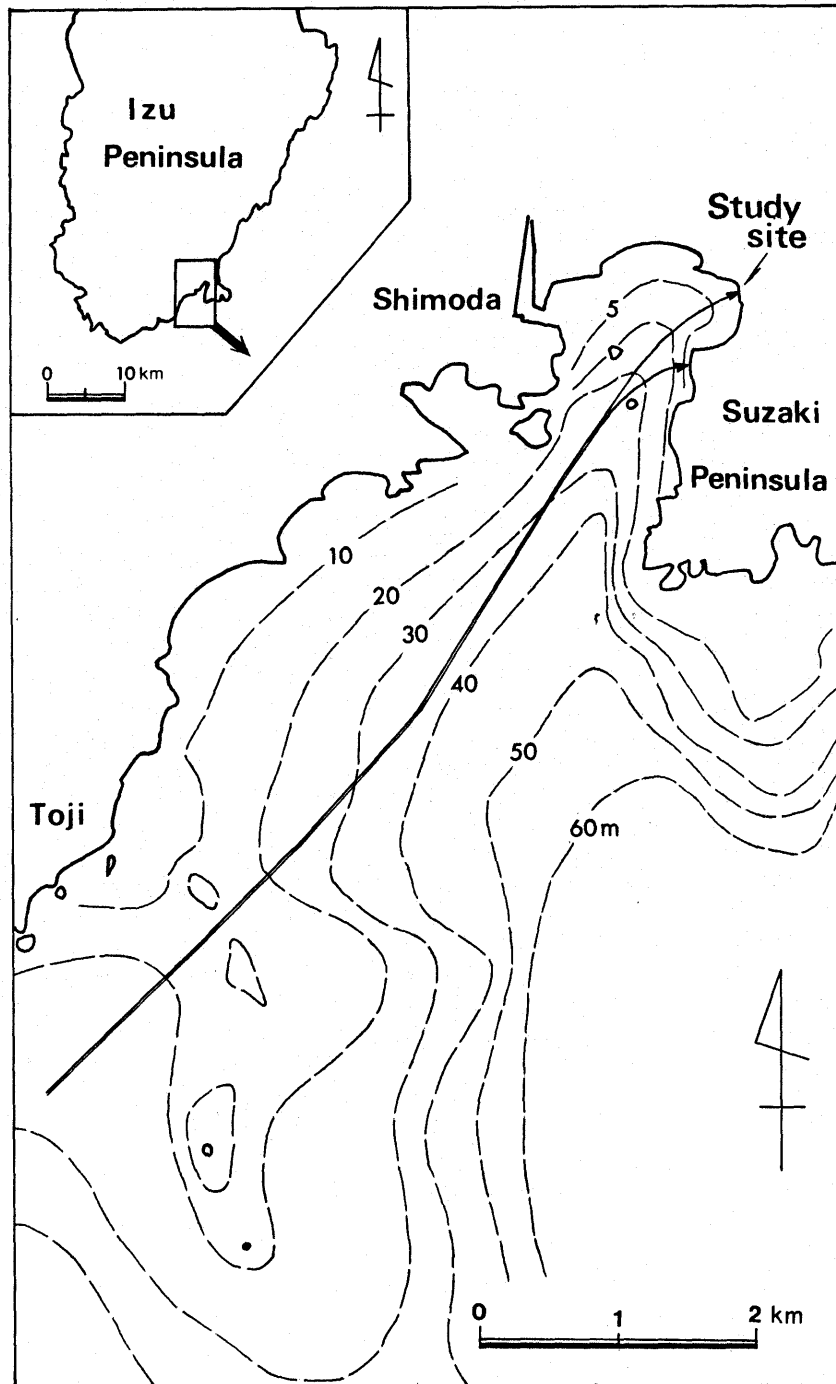


Figure 31. Wave refraction diagram at Kakizaki site. By the effect of wave refraction, spacing between the selected orthogonals in deep water increases fortyfold in shallow water.

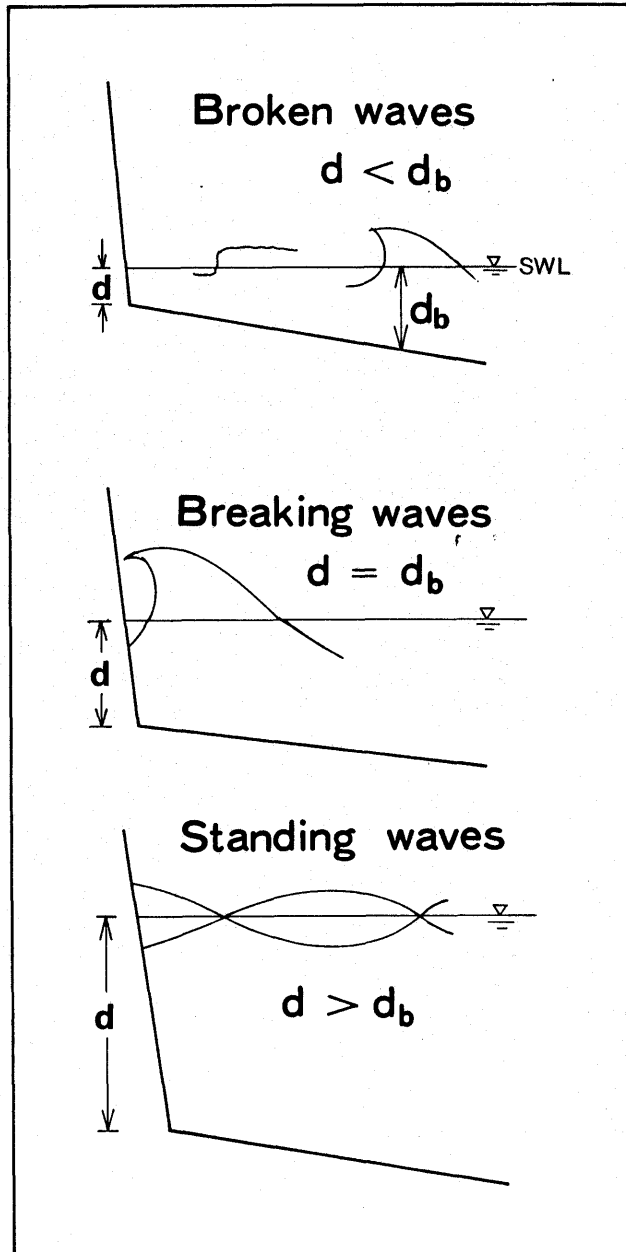


Figure 32. Wave types in front of the cliff. Standing waves occur when the water depth, d , is larger than wave breaking depth, d_b ; breaking waves occur when $d = d_b$; and broken waves occur when $d < d_b$.

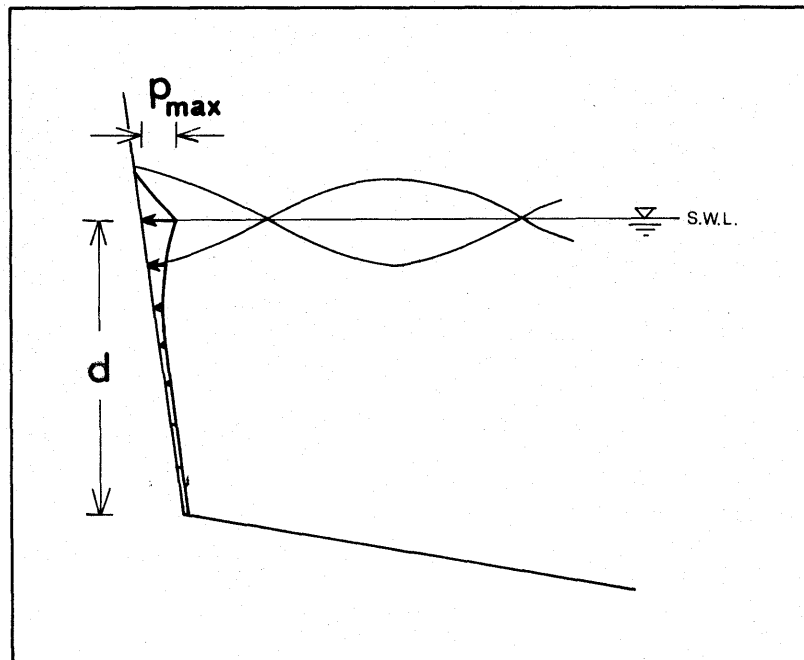


Figure 33. Vertical distribution of dynamic pressure caused by standing waves (after Sainflou, 1928).

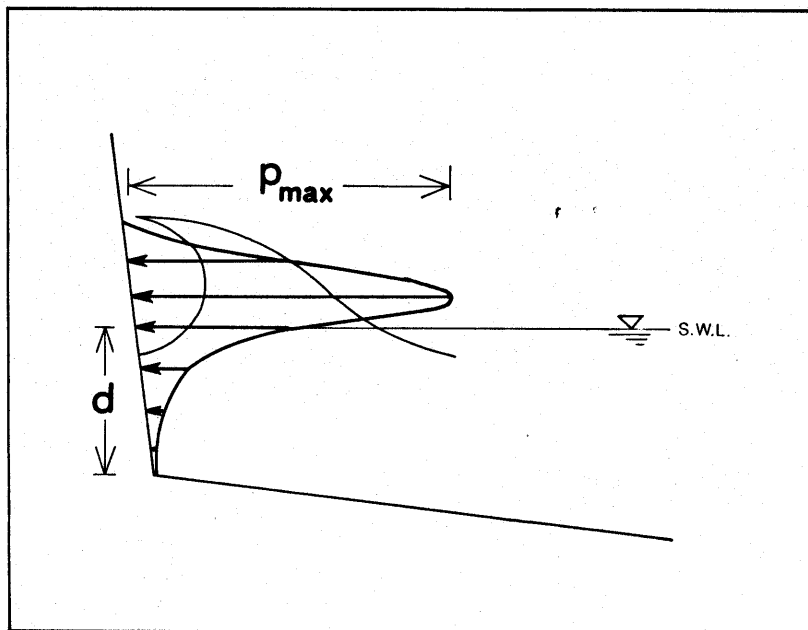


Figure 34. Vertical distribution of dynamic pressure caused by breaking waves (after Ross, 1955).

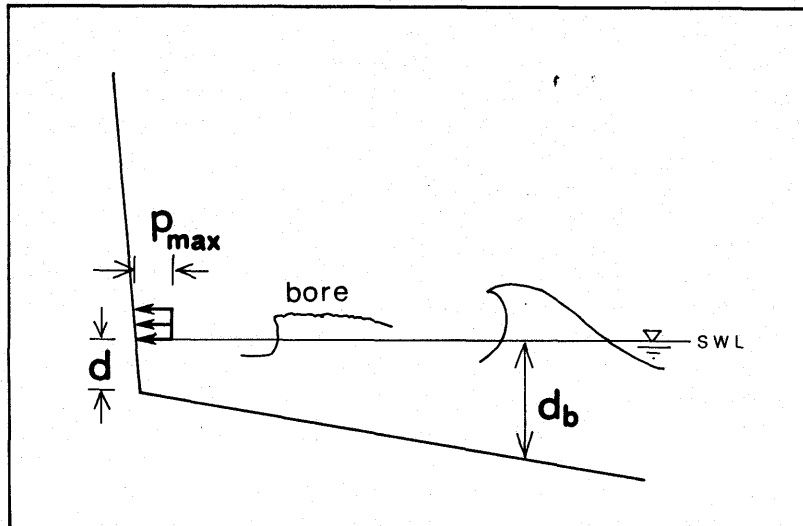


Figure 35. Vertical distribution of dynamic pressure caused by broken waves (after CERC, 1977).

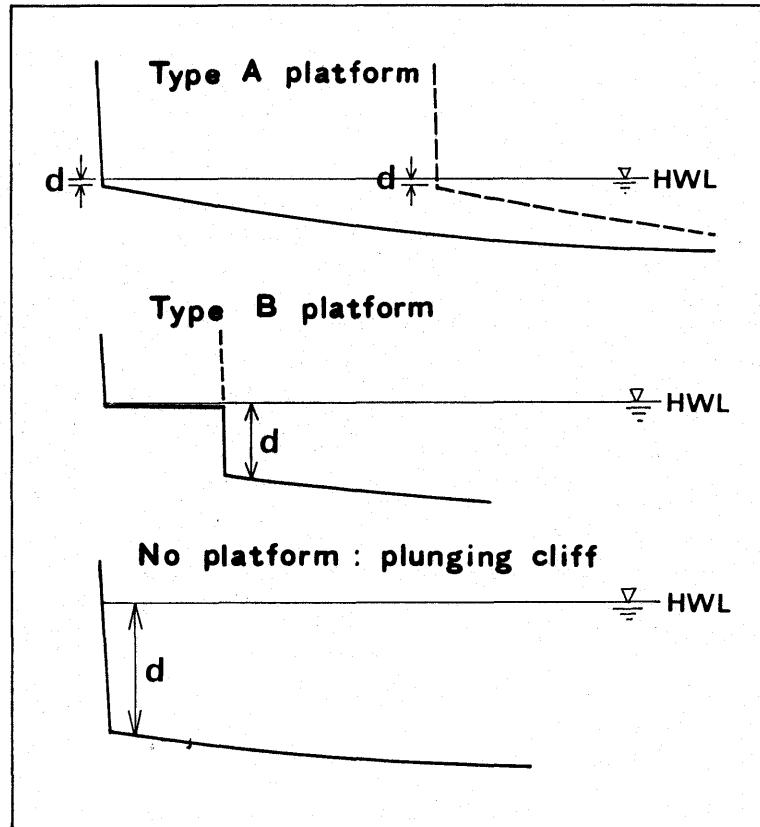


Figure 36. Determination of initial front depth.
Initial landform is plotted in a dashed line.

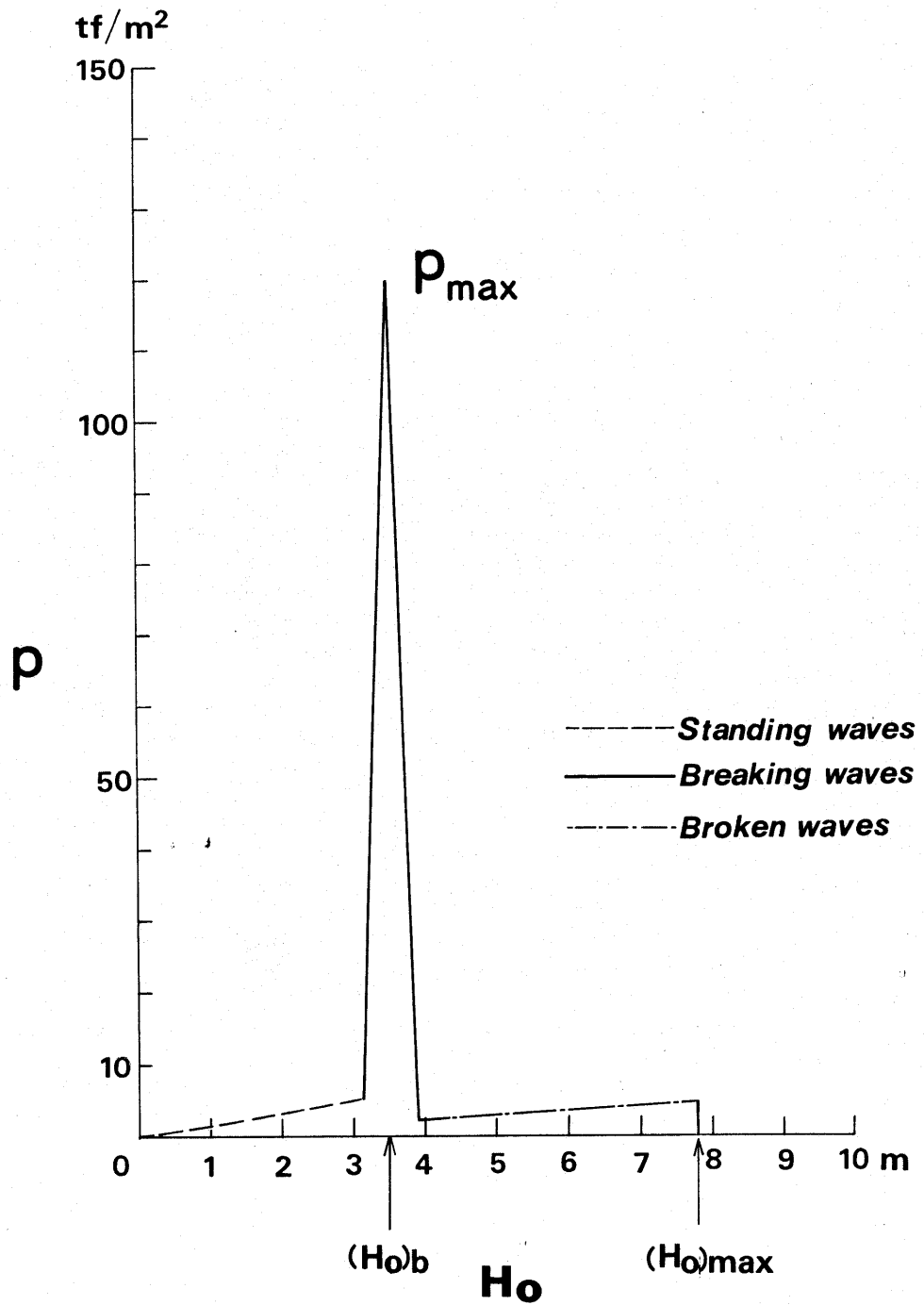


Figure 37. Result of wave pressure estimation. Maximum value of p , p_{\max} , is adopted as representative of wave assailing force.

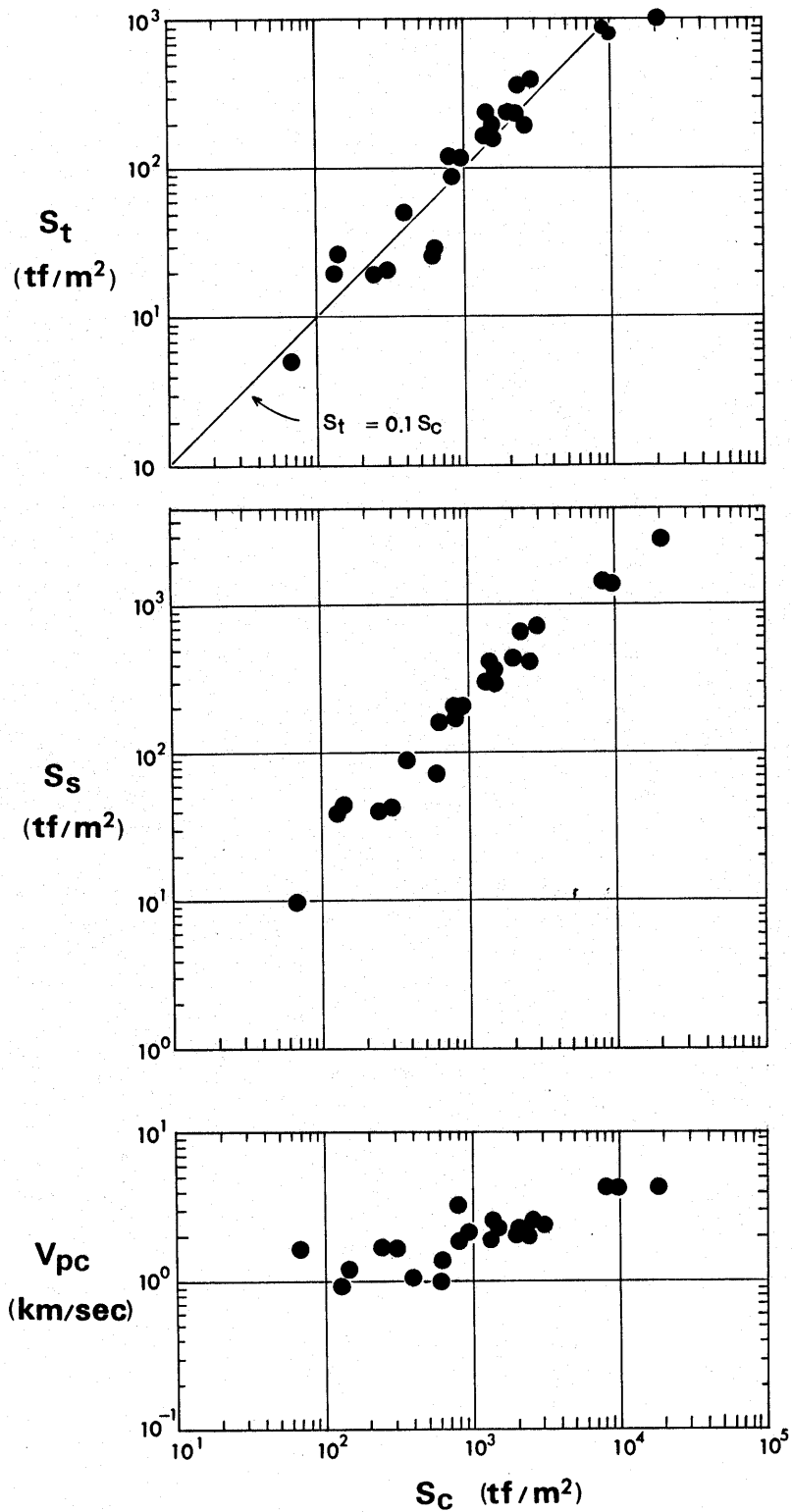


Figure 38. Relationship between compressive strength, S_C , and other indices. S_t , S_s , and V_{pc} are tensile strength, shear strength, and longitudinal wave velocity of rocks measured on the cylindrical specimen, respectively.

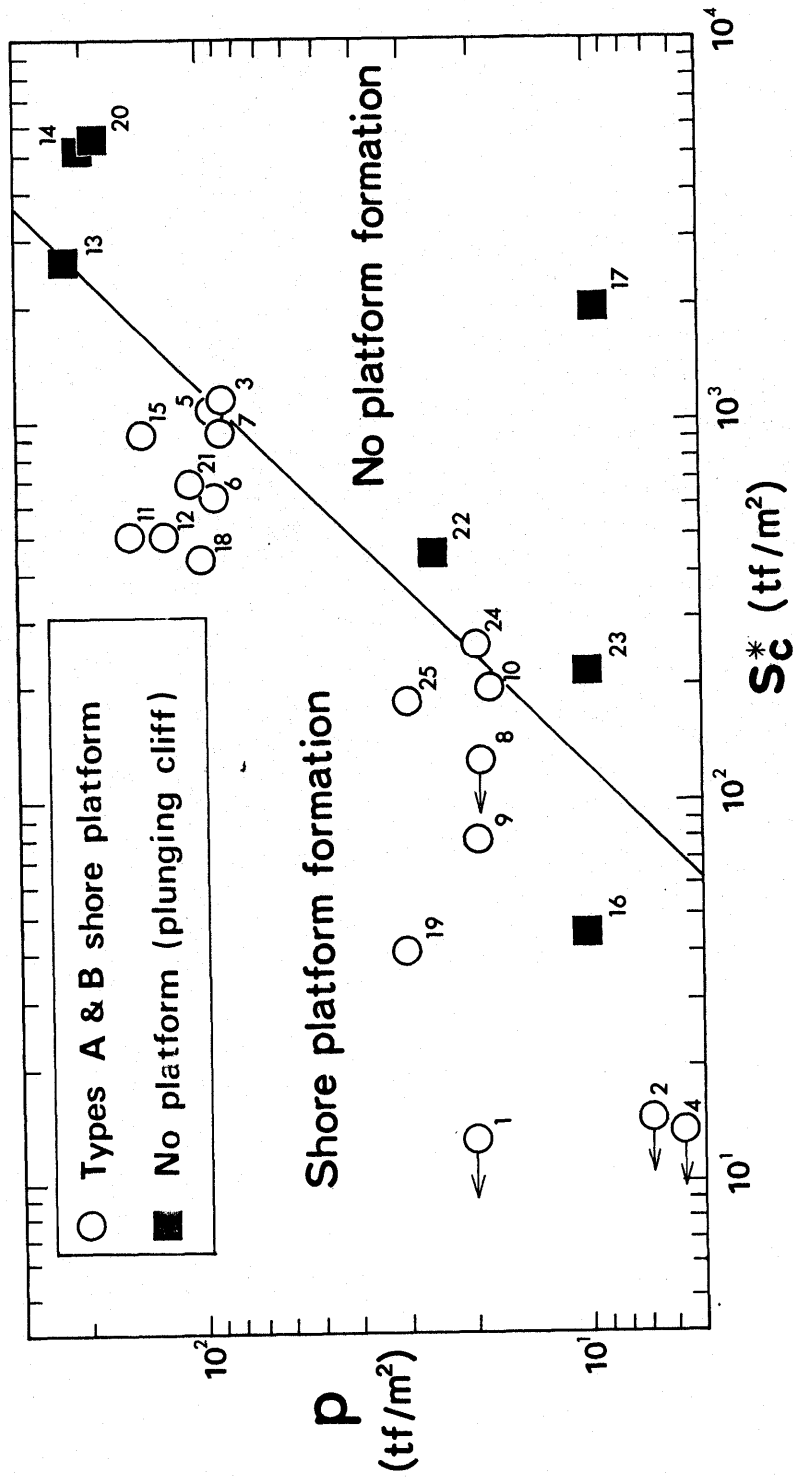


Figure 39. Demarcation between shore platforms and plunging cliffs. At the sites of 1, 2, 4, and 8, longitudinal wave velocity of rocks could not be measured, therefore the possibility of lower Sc^* value is expressed by an arrow.

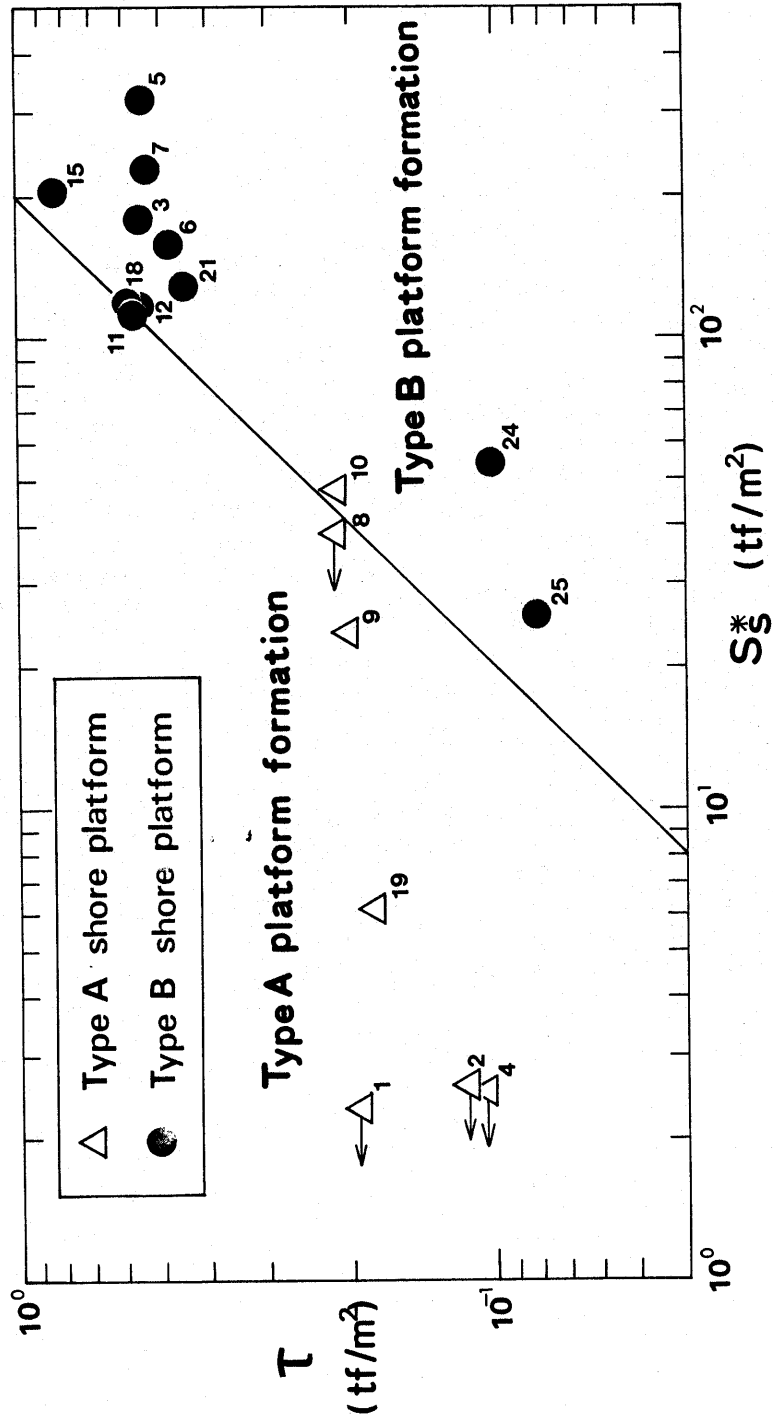


Figure 40. Demarcation between Type A and Type B shore platforms. Arrows denote the possibility of lower S_s^* value.

Table 1. Landform types

Location	Landform types	front depth erosion rate	
		(m)	(m/y)
1 Notsuka	Type A platform	0.7	1.3
2 Shichiri-Nagahama	Type A platform	0.2	0.9
3 Odosezaki	Type B platform	4.0	0.02*
4 Oga-Kitaura	Type A platform	0.2	0.5
5 Unosaki	Type B platform	4.0	0.05*
6 Kuji	Type B platform	3.0	0.01*
7 Rikuchu-Noda	Type B platform	3.5	0.02*
8 Okuma	Type A platform	0.7	0.1 - 2.1
9 Byobugaura	Type A platform	0.7	0.7 - 0.9
10 Taito	Type A platform	0.8	0.6 - 1.0
11 Ubara	Type B platform	4.0	0.04*
12 Kominato	Type B platform	4.0	0.04*
13 Kamogawa-Bentenjima	Plunging cliff	7.0	= 0 **
14 Shinyashiki	Plunging cliff	5.0	= 0 **
15 Shimoda-Ebisujima	Type B platform	6.0	0.01*
16 Shimoda-Kakizaki	Plunging cliff	1.1	= 0 **
17 Shimoda-Akanejima	Plunging cliff	14.0	= 0 **
18 Tatado	Type B platform	4.0	0.004*
19 Tsushi-Tsunokawa	Type A platform	0.8	0.2
20 Nagaobana	Plunging cliff	11.0	= 0 **
21 Iwami-Tatamigaura	Type B platform	4.0	0.03*
22 Yadakemen	Plunging cliff	1.8	= 0 **
23 Nagakushimen	Plunging cliff	2.0	= 0 **
24 Hario	Type B platform	1.3	0.004*
25 Oyano-Kodomari	Type B platform	1.5	0.04*

* Erosion rate was obtained by dividing the width of platforms by the time required for their formation (about 6000 years).

** No cliff recession occurs.

Table 2. Basic properties of rocks

Location	G_s	ρ_w (g/cm ³)	ρ_d (g/cm ³)	n (%)	w_{max} (%)
1 Notsuka	-	-	-	-	-
2 Shichiri-Nagahama	2.30	-	-	-	-
3 Odosezaki	2.57	2.21	1.98	23.0	10.8
4 Oga-Kitaura	2.63	-	-	-	-
5 Unosaki	2.58	2.12	1.82	29.5	15.9
6 Kuji	2.66	2.15	1.84	30.8	15.8
7 Rikuchu-Noda	2.54	2.01	1.67	34.3	19.7
8 Okuma	-	-	1.30	-	-
9 Byobugaura	2.67	1.68	1.08	59.5	54.9
10 Taito	2.62	1.82	1.32	49.5	37.6
11 Ubara	2.62	1.98	1.55	42.8	27.5
12 Kominato	2.63	2.05	1.68	36.6	21.9
13 Kamogawa-Bentenjima	2.97	2.83	2.77	5.9	2.1
14 Shinyashiki	2.94	2.87	2.82	5.2	1.9
15 Shimoda-Ebisujima	2.69	2.14	1.81	32.7	17.8
16 Shimoda-Kakizaki	2.55	1.52	0.85	66.7	66.8
17 Shimoda-Akanejima	2.69	2.36	2.16	19.7	8.7
18 Tatado	2.79	2.32	2.05	26.5	11.0
19 Tsushi-Tsunokawa	2.71	2.02	1.62	40.2	24.7
20 Nagao-Bana	2.73	2.58	2.49	8.8	3.0
21 Iwami-Tatamigaura	2.72	2.33	2.11	22.4	10.9
22 Yadakemen	2.83	2.37	2.12	25.1	9.8
23 Nagakushimen	2.69	2.40	2.23	17.1	6.9
24 Hario	2.65	2.33	2.13	19.6	9.0
25 Oyano-Kodomari	2.67	2.21	1.93	27.7	14.6

G_s = specific gravity, ρ_w = wet density,
 ρ_d = dry density, n = porosity,
 w_{max} = water content in saturated state.

Table 3. Mechaniocal properties of rocks.

Location	S_c (tf/m ²)	S_t (tf/m ²)	S_s (tf/ m ²)	V_{pc} (km/s)	V_{pf} (km/s)
1 Notsuka	13 (3)	1.3	2.3	-	-
2 Shichiri-Nagahama	15 (3)	1.5	2.6	-	-
3 Odosezaki	2600 (3)	200 (4)	410	2.5	1.1
4 Oga-Kitaura	14 (3)	1.4	2.5	-	-
5 Unosaki	2300 (3)	390 (3)	680	2.1	1.0
6 Kuji	630 (3)	30 (2)	160	1.4	1.4
7 Rikuchu-Noda	1500 (3)	210 (5)	370	2.1	1.3
8 Okuma	250	20	40	1.7	-
9 Byobugaura	130 (9)	20 (7)	40	0.9	0.6
10 Taito	390(10)	50 (5)	90	1.1	0.6
11 Ubara	1350(10)	170(12)	300	1.8	0.7
12 Kominato	2050(10)	240(12)	440	2.1	0.5
13 Kamogawa-Bentenjima	8600 (4)	900 (5)	1700	4.3	1.3
14 Shinyashiki	20000 (2)	1500 (2)	3100	4.2	1.1
15 Shimoda-Ebisujima	950 (3)	120 (3)	210	2.2	2.2
16 Shimoda-Kakizaki	140 (2)	26 (2)	45	1.2	0.4
17 Shimoda-Akanejima	3000 (2)	410 (3)	710	2.5	1.7
18 Tatado	800 (5)	120 (2)	210	3.4	2.0
19 Tsushi-Tsunokawa	68 (2)	5 (2)	10	1.8	1.1
20 Nagao-Bana	9400 (2)	830 (2)	1600	4.2	2.5
21 Iwami-Tatamigaura	1500 (2)	160 (3)	290	2.2	1.0
22 Yadakemen	610 (2)	29 (2)	72	1.0	0.7
23 Nagakushimen	1400 (3)	240 (2)	420	2.5	0.4
24 Hario	820 (3)	91 (2)	170	2.0	0.6
25 Oyano-Kodomari	310 (2)	20 (2)	44	1.7	1.0

S_c = compressive strength (no. of specimen is shown in parenthesis), S_t = tensile strength (no. of specimen), S_s = shear strength, V_{pc} = P. wave velocity for specimen, V_{pf} = P. wave velocity in situ.

Table 4. Oceanographical conditions of study areas.

Location	Sea area	Tidal range (m)	(H _o)max (m)
1 Notsuka	Open coast	1.4	7.0
2 Shichiri-Nagahama	Open coast	0.4	9.4
3 Odosezaki	Open coast	0.4	9.4
4 Oga-Kitaura	Open coast	0.4	9.4
5 Unosaki	Open coast	0.4	9.4
6 Kuji	Open coast	1.4	7.0
7 Rikuchu-Noda	Open coast	1.4	7.0
8 Okuma	Open coast	1.4	8.3
9 Byobugaura	Open coast	1.4	7.8
10 Taito	Open coast	1.5	7.8
11 Ubara	Open coast	1.5	7.8
12 Kominato	Open coast	1.5	7.8
13 Kamogawa-Bentenjima	Open coast	1.5	7.8
14 Shinyashiki	Open coast	1.5	7.8
15 Shimoda-Ebisujima	Open coast	1.5	7.8
16 Shimoda-Kakizaki	Embayment	1.5	1.9
17 Shimoda-Akanejima	Open coast	1.5	7.8
18 Tatado	Open coast	1.5	7.8
19 Tsushi-Tsunokawa	Sheltered	1.5	1.3
20 Nagao-Bana	Open coast	0.5	7.7
21 Iwami-Tatamigaura	Open coast	0.6	7.7
22 Yadakemen	Sheltered	2.6	0.5
23 Nagakushimen	Sheltered	2.6	0.3
24 Hario	Sheltered	1.0	0.8
25 Oyano-Kodomari	Sheltered	4.0	0.7

Table 5. Estimation of p and S_c^*

Location	$(H_o)_{max}$ (m)	d (m)	$(H_o)_b$ (m)	p (tf/m ²)	V_{pf} (km/s)	V_{pc} (km/s)	S_c (tf/m ²)	S_c^* (tf/m ²)
1 Notsuka	7.0	1.4	0.6	20	*	*	13	< 13
2 Shichiri-Nagahama	9.4	0.4	0.2	6.7	*	*	15	< 15
3 Odosezaki	9.4	4.2	2.5	86	1.1	2.5	2600	1100
4 Oga-Kitaura	9.4	0.4	0.2	5.8	*	*	14	< 14
5 Unosaki	9.4	4.2	2.7	96	1.0	2.1	2300	1100
6 Kuji	7.0	3.7	2.4	84	1.4	1.4	630	630
7 Rikuchu-Noda	7.0	4.2	2.5	88	1.3	2.1	1500	930
8 Okuma	8.3	1.4	0.5	19	*	1.7	250	< 250
9 Byobugaura	7.8	1.4	0.5	19	0.6	0.9	130	87
10 Taito	7.8	1.5	0.5	18	0.6	1.1	390	210
11 Ubara	7.8	4.7	4.3	150	0.7	1.8	1400	540
12 Kominato	7.8	4.7	3.5	120	0.5	2.1	2100	500
13 Kamogawa-Bentenjima	7.8	7.7	6.3	220	1.3	4.3	8600	2600
14 Shinyashiki	7.8	5.7	5.7	200	1.1	4.2	20000	5100
15 Shimoda-Ebisujima	7.8	6.7	4.0	140	2.2	2.2	950	950
16 Shimoda-Kakizaki	7.8	1.8	0.3	9.8	0.4	1.2	140	47
17 Shimoda-Akanejima	7.8	14.7	**	9.4	1.7	2.5	3000	2000
18 Tatado	7.8	4.7	2.9	100	2.0	3.4	800	440
19 Tsushi-Tsunokawa	1.3	1.5	0.9	30	1.1	1.8	68	41
20 Nagao-Bana	7.7	11.2	5.3	190	2.5	4.2	9400	5600
21 Iwami-Tatamigaura	7.7	4.2	3.1	110	1.0	2.2	1500	670
22 Yadakemen	0.5	3.1	0.5	25	0.7	1.0	820	450
23 Nagakushimen	0.3	3.3	0.3	10	0.4	2.5	1400	220
24 Hario	0.8	1.8	0.5	19	0.6	2.0	820	260
25 Oyano-Kodomari	0.7	3.5	0.7	29	1.0	1.7	310	190

$(H_o)_{max}$ = the largest height of waves, d = front depth measured at H.W.L., $(H_o)_b$ = the height of deep water waves which break just in front of the cliff, p = wave pressure, V_{pc} = P. wave velocity measured on the specimen, V_{pf} = P. wave velocity on the bedrock, S_c = compressive strength, S_c^* = compressive strength of rock body.

* Samples are so weak that P. wave velocity could not be measured.

** Waves do not break.

Table 6. Estimation of τ and S_s^*

Location	τ (tf/m ²)	H_b (m)	S_s (tf/m ²)	S_s^* (tf/m ²)
1 Notsuka	0.19	1.3	2.3	< 2.3
2 Shichiri-Nagahama	0.11	0.7	2.6	< 2.6
3 Odosezaki	0.56	3.6	410	180
4 Oga-Kitaura	0.11	0.7	2.5	< 2.5
5 Unosaki	0.55	3.6	680	320
6 Kuji	0.47	3.1	160	160
7 Rikuchu-Noda	0.53	3.5	370	230
8 Okuma	0.22	1.4	40	< 40
9 Byobugaura	0.21	1.4	36	24
10 Taito	0.21	1.4	90	49
11 Ubara	0.59	3.8	300	120
12 Kominato	0.58	3.8	440	110
15 Shimoda-Ebisujima	0.81	5.3	210	210
18 Tatado	0.59	3.8	210	120
19 Tsushi-Tsunokawa	0.18	1.2	10	6.1
21 Iwami-Tatamigaura	0.46	3.0	290	130
24 Hario	0.10	0.7	170	54
25 Oyano-Kodomari	0.08	0.5	44	26

τ = shear force, H_b = the height of breaking waves,
 S_s = shear strength, S_s^* = shear strength of rock body.

Table 7. Conditions for shore platform initiation.

Type A platforms	Type B platforms	plunging cliffs
$p > 0.081S_C^*$	$p > 0.081S_C^*$	$p < 0.081S_C^*$
$\tau > 0.005S_S^*$	$\tau < 0.005S_S^*$	—————